Aalto University
School of Engineering

Matti Randelin

The use of self-clinching inserts in busbar joints of a frequency converter

Thesis submitted for examination for the degree of Master of Science in Technology.
Espoo 04.04.2013
Thesis supervisor: Professor Petri Kuosmanen
Thesis instructor: Risto Laurila, Master of Science (Technology)

Aalto University
School of Engineering

AALTO UNIVERSITY SCHOOL OF ENGINEERING PO Box 11000, FI-00076 AALTO http://www.aalto.fi	ABSTRACT OF THE MASTER'S THESIS

Author: Matti Randelin

Title: The use of self-clinching inserts in busbar joints of a frequency converter

School: School of Engineering

Department: Department of Engineering Design and Production

Professorship: Machine Design	Code: Kon-41

Supervisor: Professor Petri Kuosmanen

Instructor: Risto Laurila, Master of Science (Technology)

The purpose of this thesis was to analyze the suitability of self-clinching inserts in high power busbar joints. Self-clinching inserts are planned to use in busbar joints for getting the joint smaller and easing the assembly of busbar line. There was searched suitable inserts from the markets and their features were analyzed in busbar joint use. Also ABB's own design of self-clinching nut was analyzed.

There was carried out a short literature review to describe the operating conditions of busbar joint. The mechanical, thermal and electrical special features shall be taken into account, when designing busbar joint. The needed additional calculations of these special features were added to the VDI 2230 calculation.

The analysis was made based on calculations and experimental tests. Calculations were carried out using the VDI 2230 design guideline for bolted joints as a basis. There was compared PEM®-, KALEI®- and ABB self-clinching nuts in the experimental tests. The torque out and joint tests were performed to find out the performance of self-clinching nut and to analyze the behavior of the joint.

The suitability of VDI 2230 design guideline for self-clinching inserts was verified in this thesis. The comparison between calculation results and the measured values describe the reliability of the calculation. The comparison gave also additional information from the initial values that shall be used in the calculation.

The results of experimental tests pointed out self-clinching nuts can be used in busbar joints when the design is made correctly. The strength of nut is adequate in busbar joint use but high surface pressure may cause problems in high power joints.

Date: 04.04.2013	Language: English	Number of pages: 94

Keywords: bolted joints, busbar joints, self-clinching insert, VDI 2230, torque out

Foreword

This thesis is made to clear the use of self-clinching inserts in high power busbar joints in products at ABB Drives. The proper design guideline for the use of self-clinching insert is lacking and the results of this thesis shall give the basis of new design guideline. This thesis shall also provide the wider understanding about the supply of self-clinching inserts on the markets.

I would like to thank Risto Laurila, the instructor of this thesis, for the support and opportunities given in this thesis and in previous assignments. Special thanks also to Pirkka Myllykoski and Klaus Kangas for the help with the determination of testing samples and the analysis with the methods of design of experiments.

Espoo 04.04.2013

Matti Randelin

Index

Symbols

A	area general [mm^2]
A_c	true contact surface area [mm^2]
A_{d3}	cross section of thread at minor diameter [mm^2]
A_i	area of contact spot [mm^2]
A_N	nominal cross section [mm^2]
$A_{p\,min}$	minimum bearing area under the screw head, nut or washer [mm^2]
A_S	stress cross section of the screw, average of the cross section of pitch diameter d_2 and the minimum cross section of the screw A_0 [mm^2]
A_{surf}	surface area of the piece [mm^2]
A_0	minimum cross-sectional area of the screw [mm^2]
C_i	auxiliary variable
$D_{A'}$	outside diameter of the joint (width of the joint) [mm]
D_A	outside diameter of the basic solid at the interface [mm]
$D_{A,Gr}$	limiting outside diameter [mm]
D_B	diameter of the assembly hole or the hole diameter of the washer, which is smaller [mm]
D_{km}	effective diameter for friction moment at the bearing area [mm]
D_1	inner diameter of a nut thread [mm]
D_2	pitch diameter of a nut thread [mm]
D_{2max}	pitch diameter of the nut at upper tolerance limit [mm]
E_M	Young's modulus of the nut or tapped thread region [MPa]
E_P	Young's modulus of clamped parts [MPa]
E_{PRT}	Young's modulus of the clamped parts at the room temperature [MPa]
E_{PT}	Young's modulus of the clamped parts at temperature different from room temperature [MPa]
E_S	Young's modulus of the screw material [MPa]
E_{SRT}	Young's modulus of the screw material at room temperature [MPa]
E_{ST}	Young's modulus of the screw material at temperature different from room temperature [MPa]
F_{EM}	electromagnetic force [N]
F_M	assembly preload (clamping force) [N]
F_V	corrected assembly preload [N]
F_{VRT}	preload in room temperature [N]
F_X	test variable of F-deviation [N]
F_Z	preload loss due to embedding and relaxation [N]
H	hardness of material [MPa]
M_A	tightening moment of the joint [Nm]
M_G	thread friction torque [Nm]
M_K	friction torque under bolt head or nut [Nm]
P	pitch of the thread [mm]
P_f	plating factor
R_m	tensile strength of the screw [MPa]
$R_{p0,2}$	0,2 % proof stress [MPa]
Rq	root mean square value of surface roughness [µm]
SSE	residual sum of squares
SST	sum of squares for all observations
SSX	sum of squares for factor X

T	sum of all observation values
T_s	surface temperature [°C]
T_∞	ambient temperature [°C]
W_p	polar moment of resistance of a screw cross section [mm^4]
X	factor general
a	distance between busbar centerlines [mm]
a_c	contact spot radius [mm]
b	width general [mm]
d	screw nominal diameter [mm]
d_h	hole diameter of clamped parts [mm]
d_{min}	outer diameter of the screw at lower tolerance limit [mm]
d_w	diameter of bearing surface of the screw [mm]
d_{wa}	diameter of bearing surface [mm]
d_0	diameter at the smallest cross section of the screw [mm]
d_1	inner diameter of a screw thread [mm]
d_2	pitch diameter of a screw thread [mm]
f_Z	amount of embedding [µm]
f_T	linear deformation of part due to thermal expansion [m]
i	current general [A]
k	number of factors
l	length general [mm]
l_i	length of part i [mm]
l_k	clamping length [mm]
l_{Gew}	length of the unengaged loaded thread [mm]
m_{eff_min}	minimum thread length [mm]
n	quantity general
p_M	surface pressure [MPa]
s	width across flats [mm]
y	diameter ratio
$\bar{y}$	average of values
$\hat{y}$	linear response surface model
α_{conv}	convective heat transfer coefficient [W/m^2K]
α_P	coefficient of linear thermal expansion of the clamped parts [1/°C]
α_S	coefficient of linear thermal expansion of the screw [1/°C]
α_T	coefficient of thermal expansion [1/°C]
β_L	dimensional ratio
δ_i	elastic resilience of the section I [mm/N]
δ_{Gew}	elastic resilience of the unengaged loaded thread [mm/N]
δ_{GM}	elastic resilience of the engaged thread and of the nut or tapped thread region [mm/N]
δ_p	elastic resilience of the clamped parts [mm/N]
δ_S	elastic resilience of the screw [mm/N]
δ_{SK}	elastic resilience of the screw head [mm/N]
ε	emissivity of material
ε_e	error term
η	empirical coefficient of contact resistance
λ	conductivity of material [W/mK]
μ_G	friction coefficient in the thread
μ_K	friction coefficient in the bearing area
μ_0	permeability of the medium [Vs/Am]
ρ	resistivity of material [Ωm]

ρ_p	resistivity of plating [Ωm]
σ	Stefan-Boltzmann's coefficient ($5{,}67*10^{-8}$ W/m^{2}K^4)
σ'	combined surface roughness [µm]
σ_{red}	comparative stress [MPa]
σ_M	tension stress [MPa]
τ_{BM}	shearing strength of the nut [MPa]
τ_{BS}	shearing strength of the screw [MPa]
τ_M	torsional stress [MPa]
υ	utilization factor
φ	angle between the screw axis and the deformation cone [°]
ΔF_{Vth}	preload change due to temperature change [N]
ΔT	temperature difference general [°C]
ΔT_P	temperature difference of the clamped parts from room temperature [°C]
ΔT_S	temperature difference of the screw from room temperature [°C]
Φ_{cond}	conduction heat transfer power [W]
Φ_{conv}	convection heat transfer power [W]
Φ_{rad}	radiation heat transfer power [W]

1 Introduction

A frequency converter is an electronic device, which converts frequency of alternating current and voltage from one to another depending on the need of an application. Frequency converters are used for example to control the rotating speed or torque of an electric motor. Because the control is continuous, the frequency converter drives save energy, productivity is better and the production process is better controllable. The most usual frequency converter applications are industrial pump and fan drives. Also conveyor and crane drives are common.

1.1 Background

This thesis deals with busbar joining methods of a frequency converter and especially joints with self-clinching inserts. The insert can be a self-clinching nut or threaded stud, later called self-clinching screw. The busbar is the transmission line of electricity between different operational units of the frequency converter and it is made of copper or aluminum bars. There is presented one example busbar assembly in figure 1. Busbars are usually assembled by bolted joints, but there are also some quick joining methods. Depending on the size of the frequency converter the busbars can be long and, because of high through going current, thick. The busbar lines are normally made of copper, which is heavy material and it is quite expensive material nowadays. Because of these two reasons, aluminum busbars have become more common. The problem with aluminum is the electrical conductivity of aluminum is less than the conductivity of copper, which demands the busbar to be even thicker for getting the same current through the busbar with same resistance. There is very little space in the tightly packed device cabinet for thicker busbars so there is a need for to compact the busbar line. The cabinet must meet the requirements about clearance and creepage distances, which are the major restrictions for use of space. Clearance and creepage distances secure, there will not occur electric discharge between components, which are in different voltages. Normally the problems occur in positions, where the thickness of the busbar line changes. The thickest part of a busbar line is the joint of two busbars and this part has been tried to do in a more compact way.

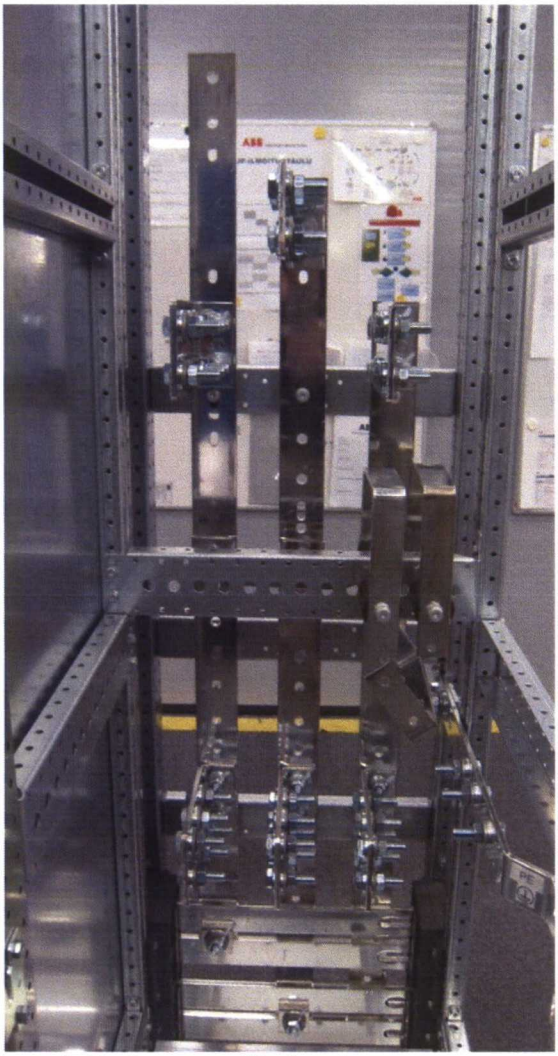

Figure 1. Busbar assembly in a frequency converter cabinet.

A bolted joint is strong, but quite bulky joint for busbar joints. It has been tried to improve by developing self-clinching inserts, which are partly pressed straight into the busbar. When the self-clinching insert is in place, the projection above the busbar surface is only a few millimeters. The target of using the self-clinching inserts is to replace regular nut-washer or bolt-washer combination in a bolted joint and that way get the space requirement of the joint as small as possible. The differences between regular screw-nut joint and self-clinching nut joint is seen in figure 2. Self-clinching inserts also ease component assembly in difficult positions, where is not possible to access the busbar from both sides. When there is a nut or screw already in the busbar, the next component can be assembled from one side.

Despite the benefits of the self-clinching insert joints, there is a need for study, how reliable these joints are before extensive use in production. The busbar joints shall meet certain mechanical, electrical and thermal requirements, like vibration resistance, joint conductivity and different operational temperatures. If these requirements are not fulfilled, the joint may come loose, which leads to warming of the joint or complete joint failure with electric discharge.

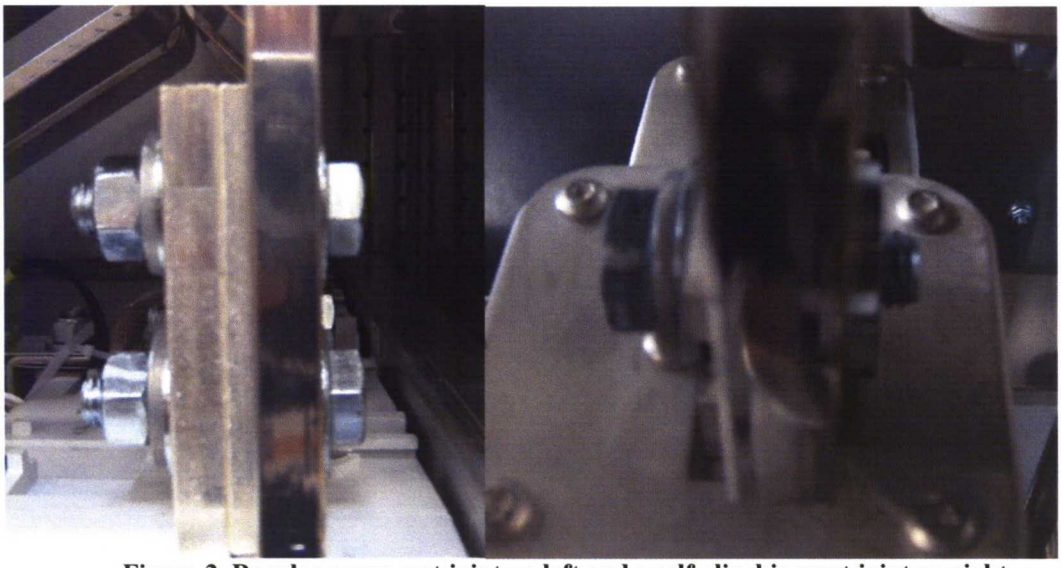

Figure 2. Regular screw-nut joint on left and a self-clinching nut joint on right.

The purpose of this thesis was to study bolted joints with self-clinching inserts as a joining method of electrical busbar joints in frequency converters. There had been used self-clinching nuts in busbar joints in some products, but the fundamental understanding of joint behavior was defective. There had been some problems with the self-clinching nut joints, which pointed out that the joint with self-clinching nut did not withstand as high tightening torques as the regular through bolted joint. The use of self-clinching screw has been low. The target of this work is to study the requirements of busbar joints and find information about joining methods with self-clinching inserts from literature. Finally, the purpose is to compare the joint features of self-clinching insert joints to normal screw-nut joint by measuring preload and torque from example joints. Based on the measuring recommendations are given to design a self-clinching insert joint at the end of this work.

1.2 Aim of the work

The aim of this work is to examine the suitability of self-clinching inserts in busbar joints. This work shall clear up the common usable self-clinching insert types and their possible limitations of use. The ABB's own self-clinching nut is analyzed more accurately to understand its behavior during tightening. The suitability of VDI 2230 designing guidelines of bolted joints is verified for self-clinching insert joints.

1.3 Scope

Bolted joints are the most common way to join busbar to another busbar or operation unit. Bolt size in these busbar joints can be from M8 to M16 depending the current that goes through the joint. This work concentrates to self-clinching inserts generally and in experimental part to self-clinching nuts of sizes M10 and M12, because these are the most used screw sizes in busbar joints. There are numerous manufacturers for these self-clinching nuts, but there are only a few different nut designs, because some insert types are standardized and some are protected by patents. This work concentrates mainly on the ABB's own self-clinching nut design, but there are also taken two regular self-clinching nut types from the market. The self-clinching screws are dealt with generally, but experiments are not carried out, because of the extent subject.

This work deals with the regular bolted busbar joints, where the busbar material is copper or aluminum. To improve electrical contact between busbars and ease the assembly work both materials are usually tin plated in the ABB's production and that is taken into account in this work. The joints dealt with in this work were as close production design as possible. This way the results corresponds the mechanics of frequency converter.

In the experimental part, there are carried out the design calculation according to the theory and the actual measuring of joints. The target was to verify the calculation results with measurements. If the measurements point out that the calculations are at least close to the measuring results, it can be concluded the designing calculations give reliable results. When the results are reliable, it can be assumed the theory is correct also for other bolt sizes.

1.4 Methods

There is a short literary review about bolted joints, self-clinching inserts and busbar joints in the beginning of this work. The purpose was to find out what kind of self-clinching inserts there were available on sale and how the manufacturer determines the strength of the insert. There was not available a general guideline for calculating the strength of a self-clinching insert joint. For that reason, there is an experimental part in this work to measure the actual joint preload on certain tightening torque.

This work deals also with the theory of bolted joints and the requirements of busbar joints of a frequency converter to understand the mechanics of bolted joints and the special requirements of the frequency converter. The basis of the theory is VDI 2230 - standard, but also other standards and suitable references were searched and then applied for understanding the behavior of the self-clinching nut joint. Based on the theory and the measuring, the purpose was to form guidelines for designing self-clinching insert joints.

The measuring was done with a special bolt tightening device, which has a force and torque measuring. The test joint was assembled in the device and the joint was tightened. The device tightened the joint evenly to the determined tightening torque and measured the preload force and torque at the same time. The measuring device had already been built for other purpose, but it had not the force measuring. For this work the force measuring was applied and the torque sensor was switched to another sensor for higher torques. After these changes, it was possible to measure the torque and the force at the same time and it was easy to see how the preload has formed during tightening.

2 Bolted joints

2.1 Screw and its mechanics

Screw is a very old invention and it is widely used in different applications. Bolted joints are commonly used in mechanical assemblies as a detachable joint. Bolted joints have some significant benefits:

- Easy to assemble
- Standard parts
- Costs are low
- Usable in different operation conditions

The reliability of a bolted joint is good when it is designed correctly, but the operation conditions may cause unexpected problems. The main problem about bolted joints is that there is many discontinuities in the joint, where are high stress concentrations. [1, p1-3][2, p161-162]

Depending on the application, the screw may have a different thread profile. Fastening screws have usually sharp profile, where the profile is formed from isosceles triangle with cut tip. This type is easy to produce by cutting or cold forming, which improves processibility. Other benefits are easy clearance control by moving the profile, good force distribution in threads and high friction in threads, which protects against self-loosening. In this work is concentrated to metric ISO-thread screws, which thread is introduced in figure 3. The symbols in figure 3 are D is the outer diameter of a nut thread, d is the outer diameter of a screw thread, D_2 is the pitch diameter of a nut thread, d_2 is the pitch diameter of a screw thread, D_1 is the inner diameter of a nut thread, d_1 is the inner diameter of a screw thread, P is the pitch of a thread and H is the height of fundamental triangle. [2, p163-164][3]

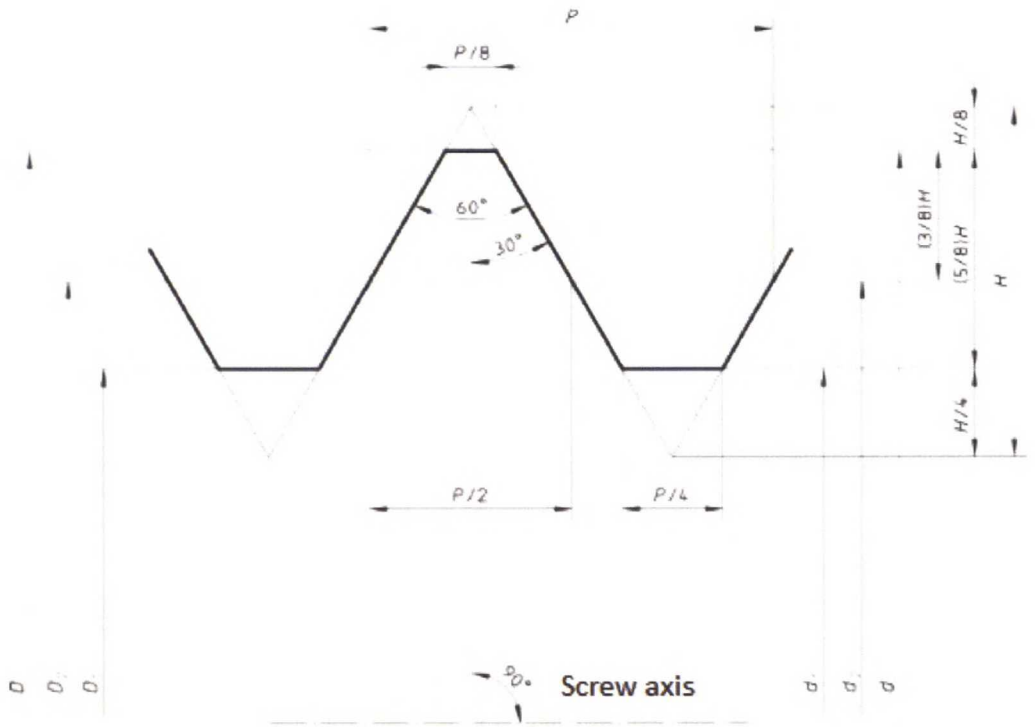

Figure 3. Metric ISO-thread. [3]

Screws and other threaded fasteners are well standardized and hence it is possible to purchase same type of fasteners from different supplier. There are standards for different types of screws, nuts, washers and inserts. Hexagon bolts and nuts and different sets of washers are commonly used in busbar joints. These fastener types are introduced more deeply later.

The material properties of a screw and nut determine how high maximum tightening torque can be used in the joint and also how high the preload force is. Screws and nuts are usually made of low-carbon steel and the different strength grades of the screw are formed by different heat-treatments like annealing. The strength grade is announced with two numbers separated with a dot. The first number describes the 1/100 of the ultimate strength and the second number describes the relation between the yield strength and the ultimate strength multiplied by 10. [2, p180][1, p49] The most used strength grades are 4.8, 8.8, 10.9 and 12.9. Screws of strength grade 8.8 and also some 12.9 are used in busbar joints, but in this work are only 8.8 screws dealt with.

The coating of a screw or nut is important to prevent corrosion, but it has also an effect to the friction of threads and the joint reliability. The most important coating methods are electroplated zinc coating and hot-dip zinc coating. Electroplated zinc coating is suitable indoor conditions, but it can be strengthen by chromating so it is possible to use in mild outdoor conditions. Hot-dip zinc coating is thick, which shall take into account in manufacturing, but it is suitable in severe conditions. Both coatings have susceptibility to hydrogen embrittlement. [2, p183-184]

2.2 Joint mechanics

The main purpose of fastening screws is to attach two or more structural parts or other components together. Bolted joints are normally observed as a part of a machine structure. Hence, only the elastic deformations are allowed in the strength calculations of the joint. The reliability of a bolted joint is better under control when there are not plastic deformations in the joint. [2, p161]

A bolted joint carries transverse loads in two ways. If the preload is high enough, the friction between clamped parts transmits the transverse loads from one part to another. Hence, the transverse loads of a screw are low. If the preload is not high enough, clamped parts can slip and a screw transmits the transverse loads between parts. It is difficult to predict the displacements of this kind of joint and hence the reliability of the joint is lower. Normally, the bolted joint is not designed so that the screw carries transverse loads, but in some structures displacements and plastic deformations are allowed. For this kind of joints, there are Eurocode 3 standards, which give the guidelines for designing. Busbar joints are supported so there are not external loads in the joint. In practice, there are loads caused by operating conditions and it is safer to calculate the joint strength during non-slip method. The most used strength calculating guideline for non-slip joint is VDI 2230. [2, p225][4][5]

When using non-slip joints, it shall be ensured the preload is high enough. If the preload force is not adequate, it may cause slipping of clamped parts, joint loosening under vibration, jointed surface separation under axial loading and fatigue of screw. Excessively high preload force is also harmful, hence it can cause static overload of a

screw under external load, joint loosening after plastic deformations of a screw and screw breakage during tightening. The tightening shall be done accurately, when the optimal joint is wanted. The more accurate tightening is, the lighter joint can be made. The equipment for accurate tightening is expensive so economic optimization is needed to determine adequate accuracy level. [2, p228]

2.3 Joint types

This paragraph deals with joint types that are used in busbar joints. There are also several joint types, which are used in other structural or machine building applications.

2.3.1 Through bolted joint with a nut

The most common busbar joining method is a regular through bolted joint with a nut. Hence, the busbars are copper or aluminum, which are quite soft materials, the joint shall be equipped with washers. The purpose of washers is to expand the affected area of screw load and that way reduces the contact pressure under nut or screw head. If relaxation and embedding of a joint is a significant issue, a spring washer is also used in the joint. A spring washer maintains the preload of the joint and increases the elasticity of the joint. There is introduced a regular busbar joint in figure 4.

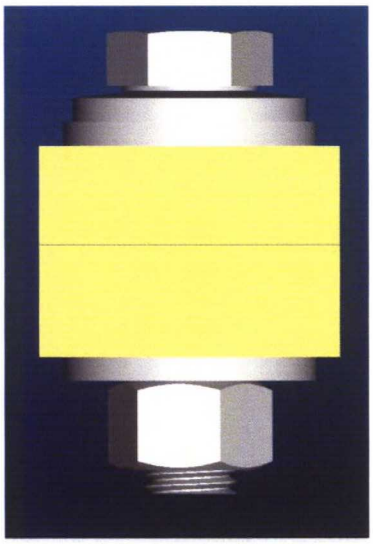

Figure 4. A regular through bolted busbar joint used in ABB Drives.

A through bolted joint with a nut is easy and cheap method to join busbars together. The problems of this method are large size, need of access from both sides of the joint and the large number of fastening parts. The regular through bolted joint contains a hexagon screw and nut, two plain washers and a spring washer. The used fastening parts are standard parts. The screw is hexagon screw in accordance with standard ISO 4017. This screw is the regular hexagon screw. The used nut is like in standard ISO 4032 defined nut. Plain washers are DIN 9021 type washers, because these washers provide large contact area, which decreases contact pressure. The spring washers are SFS 3737 spring washers for electronic applications. The SFS 3737 spring washers provide larger spring force than regular spring washers, which is benefit in busbar joints where the preload shall be large. [6][7][8][9]

2.3.2 Through bolted joint with self-clinching inserts

A through bolted joint with a self-clinching insert is an improved joint type from previous joint. The original purpose of a self-clinching insert was in sheet metal use, where it was designed to replace threaded drawholes and studs. Hence, a self-clinching insert has better thread quality and stronger structure the joints can be made more reliable than with a drawhole. The use in busbar joints is quite similar, but the thickness of sheet is greater. In busbar joints a regular nut and washer can be replaced with self-clinching nut or a screw and washer with self-clinching screw. [10]

A self-clinching insert is assembled by pressing it to a mounting hole of a work piece. When the insert is pressed into a ductile metal, it displaces material around the mounting hole. The displaced material is guided to the designed grooves of the insert so the insert is locked to its place. The pressure shall be even and accurately perpendicular against the work piece to ensure good material flow in the grooves of the insert. The assembly of self-clinching insert is shown in figure 5. [10]

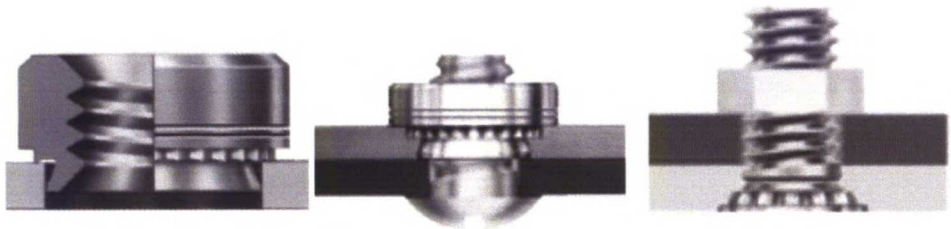

Figure 5. Left: Self-clinching nut before assembly Center: Self-clinching nut assembled Right: Self-clinching screw assembled. [10]

The joint is possible to make smaller with self-clinching insert and also reduce the number of fastening parts. Hence, the self-clinching insert is fixed in busbar the joint is needed to access only from one side, which eases the joint assembly. A through bolted busbar joint with a self-clinching nut is introduced in figure 6.

Figure 6. A through bolted busbar joint with a self-clinching nut.

ABB Drives has made its own design from a self-clinching nut, which is used in busbar joints. The reason behind the new design is the commercial self-clinching nut designs have some problems, when used in busbar joints. The main problem is small bearing area under the nut. The busbars are copper or aluminum, which have lower limiting surface pressure level then steel, and hence there occur plastic deformations under the nut, when using high tightening torques. In ABB design, the bearing surface is increased by increasing the outer diameter of the nut.

There are two different designs of self-clinching nuts in ABB's production. The two designs can be seen in figure 7. The difference between designs is the length of the collar. The longer nut is for thick busbars, but the reason to increase the length is not completely known. The purpose to increase the length of the nut is possibly to increase the contact length of the collar against the busbar and increase the strength of the nut. The serrated area is made on the collar of nut to prevent the nut rotating during tightening. The longer nut has also large groove for displaced material in the base of the collar. When the groove is full of material, it prevents the nut to come off the busbar in axial loading. The shorter nut does not have the groove so the detachment is prevented only by friction from squeezed material.

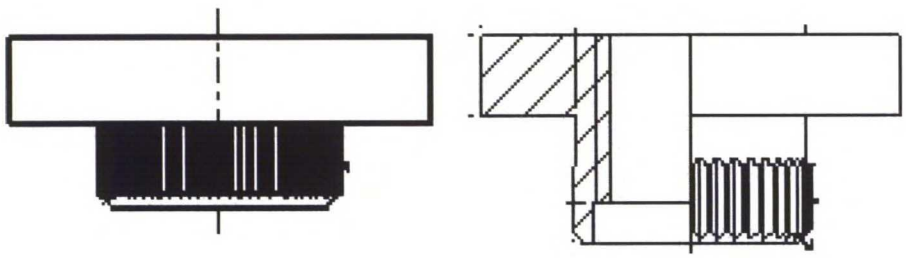

Figure 7. ABB design self-clinching nuts.

There are different designs of self-clinching inserts on the markets. One of the oldest self-clinching insert manufacturers is PennEngineering. PennEngineering has an extensive collection of different types of self-clinching inserts. The PEM®-series might be usable in busbar joints and this series is dealt with in this work. The shape of PEM®-nuts is complicated and it has many features. There is a serrated part at the end of the collar, which prevents the rotation of the nut. The large groove in the middle of the collar is for displaced material and it prevents the nut to come off the work piece. The PEM®-nuts are available from size M2 to M12. In figure 8 are introduced the parts of PEM®-nut assembly. [10]

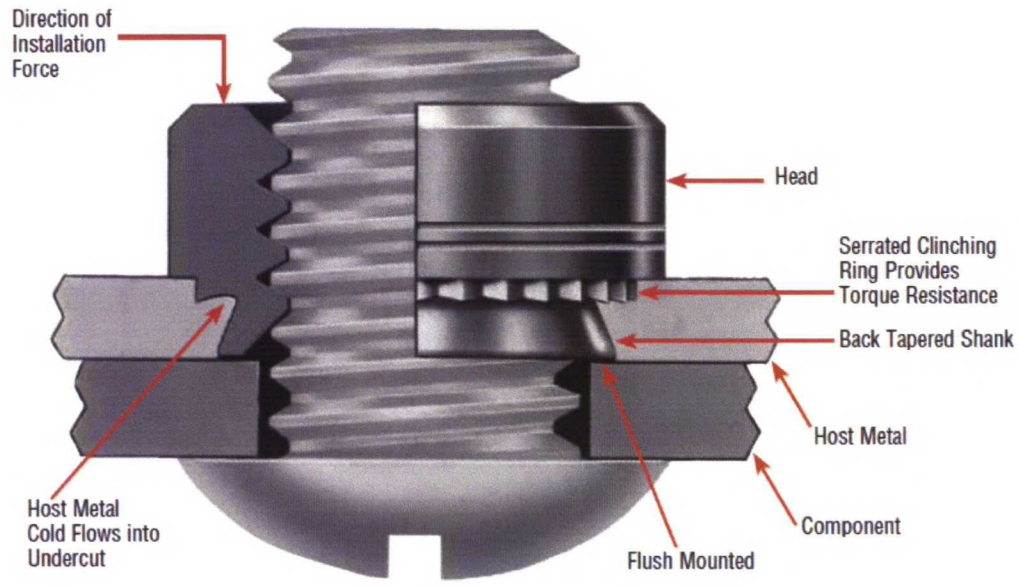

Figure 8. PEM®-nut assembly. [10]

The adhesion of the PEM®-nuts in common materials is usually tested by manufacturer and the tested values are announced in the datasheet. There are two tests for self-clinching inserts: torque out test and push out test. These tests ease the selection of fastener in the design. The reliability of insert is good, when the designed loading of insert is lower than the torque and push out values. The push out value is normally not so important, because that value limits the joint loading only when the joint is loose. The torque out value is more useful, because that value predict when the insert starts to rotate during tightening. [11]

The torque out test is performed to define the torque, which the insert can resist before it comes off. The torque out test is carried out with the test setup showed in figure 9. There is inserted a screw in the nut in the test and the screw is tightened until the nut has come off. The torque when nut comes off is measured. There shall be used a washer between screw and nut to prevent the screw neck from contacting threads. [11]

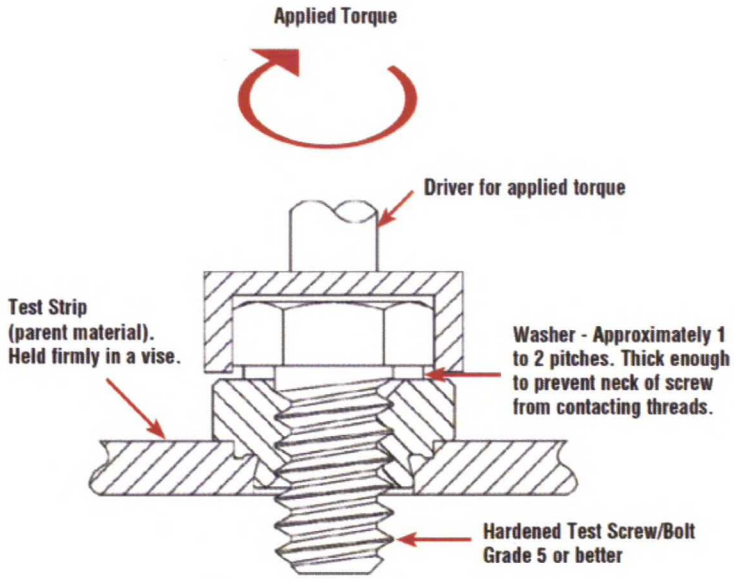

Figure 9. Torque out test. [11]

The push out test is carried out to define the force, which is needed to push the insert out of the material. The screw is inserted in the nut in the test and axial load is directed to the screw head. The force is measured when the insert comes off. The push out force is usually 5-10 % of the used assembly force. [11]

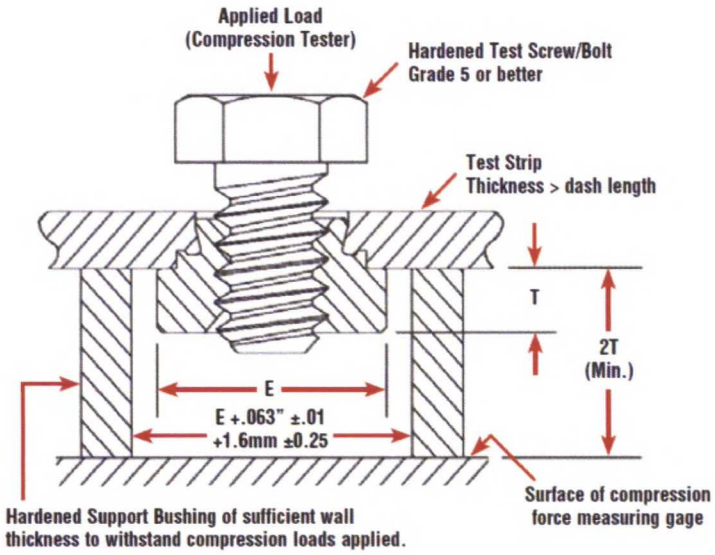

Figure 10. Push out test. [11]

The other significant self-clinching insert manufacturers are PSM International and Würth Elektronik, which have the same kind of self-clinching inserts as PennEngineering. PSM International offers P-S and P-CLS nuts, which are almost the same self-clinching nut design as PennEngineering, but the shape of the collar of the nut is slightly different. The design of Würth Elektronik's self-clinching nut is a bit more different, especially the outer diameter of the nut is smaller, and the nut is not suitable in busbar joints. [12][13]

One kind of a self-clinching nut is KALEI®-nut, which is introduced in figure 11. It is used in busbar joints, where is not needed high preload force. The shape of KALEI®-nut is like normal hexagonal nut, but it has a serrated part at the other end of the nut [13]. The serrated part is used to clinch the nut into busbar and it prevents the rotation during the tightening. The incline serration prevents also the nut come off the work piece. The bearing surface of KALEI®-nut is small and hence the maximum preload force is low. KALEI®-nuts are available from size M2 to M20.

Figure 11. KALEI®-nut. [13]

PennEngineering offers also different types self-clinching screws. There are heavy duty HFE-studs in FH-series, which are self-clinching screws in applications, where large bearing surface is needed. The HFE-screw has larger bearing area of the screw head than regular self-clinching screw. The HFE-screw is designed for thin sheets, but it is also usable for thicker pieces, which require low surface pressure. The sizes of HFE-screws are from M5 to M8. HFH-screw is other type of self-clinching screw that PennEngineering offers for thin sheet and electrical applications. The HFH-screw has smaller bearing surface of screw head than HFE-screw, but still larger than regular self-clinching screw. The HFH-screw has more sizes than HFE-screw providing the selection from M5 to M10. When looking other manufacturers, PSM International has P-HFH-screw and Würth Elektronik has WEHFH-screw, which are identical screws and almost the same design as PennEngineering's HFH-screw. Würth offers their self-clinching screw from size M4 to M10 and PSM from M5 to M10. [14][12][13]

Figure 12. PennEngineering's HFE-screw on left and HFH-screw on right. [14]

The above-mentioned self-clinching screws are possible to use in busbar joints, when estimated in the point of views surface pressure and single tightened joints. The actual performance and reliability shall be verified with tests. The reliability in operation conditions and the adhesion of the screw during re-tightening are the most significant features to find out.

2.3.3 Other types of through bolted joints

There are some variations of through bolted joints that are used in busbar joints in the production. The most common joint types are joints, where a carriage bolt is assembled instead of hexagon bolt, and joint, where the hexagon nut is replaced with a lock nut.

The carriage bolt is standard bolt according to DIN 603. The carriage bolt is used, when there is not access to both sides of joint. The carriage bolt requires a groove or square hole in the busbar, where the square neck of bolt can be set. The square neck prevents the bolt to rotate during tightening of the nut. In figure 13 is seen a typical through bolted joint, where is used carriage bolt. [15]

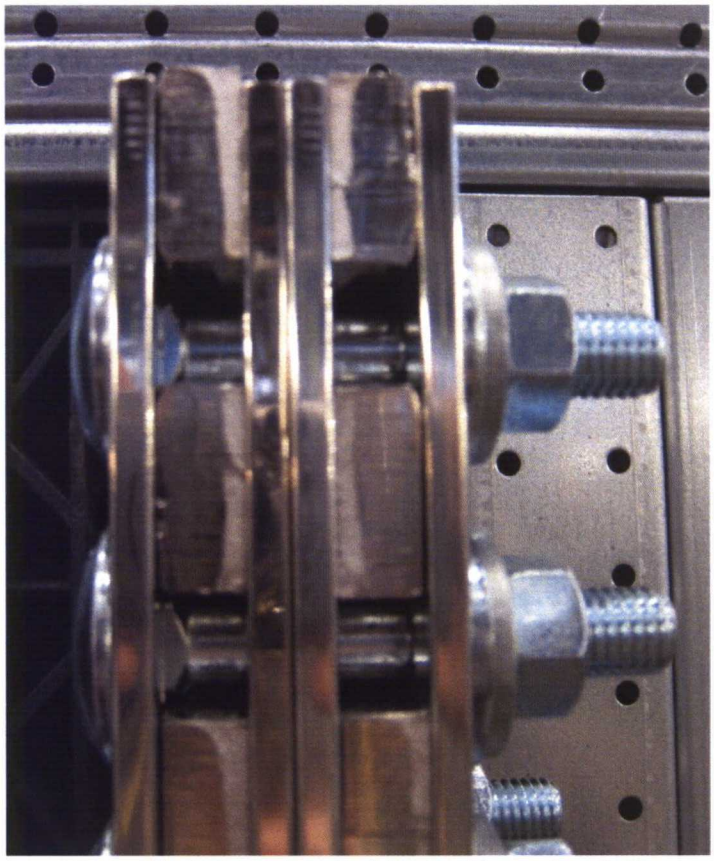

Figure 13. A through bolted joint with carriage bolt.

The used lock nut type in ABB is with conical spring washer as seen in figure 14. It is used in joints where the preload is low and the flexibility of the joint is needed. The preload is lower than regular through bolted joint with spring washer because the spring washer integrated in the lock nut has lower spring constant. The tightening is difficult, because the nut is used without plain washer under it. The soft busbar material can cause the spring washer sink into the busbar instead of flattening the washer and the preload remains low. Every joint with this nut shall be checked after assembly. Because of difficult tightening, ABB is abandoning the use of the lock nut in busbar joints. [16][17, p23-24]

Figure 14. Lock nut.

2.4 Designing theory

This paragraph deals with the designing theory of bolted joints according to VDI 2230. This guideline is used also for busbar joints because it is based on theory, which does not allow slip in the joint. When these guidelines are followed, the joint is reliable and different operating conditions are taken into account. The VDI 2230 guidelines provide the systematic and reliable way to calculate the strength of a joint. The VDI 2230 is divided in two parts. The part 1 deals with single bolted joints and the part 2 multibolted joints. The part 1 is normally adequate for multibolted joints if the construction is simple, because the structure can be divided into single bolted joints. Mostly busbar joints are single bolted joints or very simple multibolted joints so it is used the guidelines of VDI 2230 part 1 to calculate these joints. [5, p4-5]

It is important to remember that VDI 2230 calculation does not give exact result. Result is only an approximation, because the calculation model is always an idealization from the actual conditions. The calculations can handle also multiaxial cases for example tension, bending and transverse loading at the same time. The calculation is based on elastic behavior of the joint and hence, if it is known there are plastic deformations in the joint, the calculations are not reliable. The possible small plastic deformations on the contact surfaces of clamped parts can be taken into account in preload loss calculation. [5, p8-10]

The calculating process is iterative when following the VDI 2230 guidelines step by step. There is selected preliminary selection for the screw size of the joint and the joint type and then the required strength calculations are made. If the verification is not successful the selections are changed and the calculations are repeated. The calculations do not do away experimental or numerical tests for verifying the results in complex joints.

The VDI 2230 contains following calculations: [5, p4]

- Assembly stress verification
- Working stress verification
- Alternating stress verification
- Preload changes due to temperature and embedding
- Tightening torque verification
- Thread strength verification
- Surface pressure verification
- Affect of tightening method

ABB has made an assembly guideline, where the tightening torques for regular through bolted busbar joints are defined with the help of VDI 2230. Now, it is interested to know if this guideline is valid for joints with self-clinching nut. This point of view demand to use reversible way the VDI 2230 thus the tightening torque is known and the joint properties have to find out. These calculations are introduced next. All calculations are made with assumption that the joint is concentrically clamped single bolted joint.

2.4.1 Clamping force in the joint

The tightening torque used in joint contains two torques. The other torque is the torque from the threads which is formed from the pitch angle and the friction of the threads and the other is the friction moment under nut or bolt head. According to VDI 2230 the tightening torque is [5, p66]

$$M_A = M_G + M_K, \tag{1}$$

where M_G is the thread torque and M_K is the friction moment under nut or bolt head.

When using metric screws with flank angle 60°, the thread torque M_G can be written as [5, p67]

$$M_G = \frac{1}{2} d_2 \cdot F_M \left(1.155\mu_G + \frac{P}{\pi \cdot d_2}\right) \tag{2}$$

Correspondingly the friction torque at the bearing area under the nut or screw head is [2, p230][5, p67]

$$M_K = \frac{1}{2} \mu_K \cdot D_{km} \cdot F_M \tag{3}$$

where

d_2	is the pitch diameter of the screw
F_M	is the assembly preload (clamping force)
μ_G	is the friction coefficient in the thread
μ_K	is the friction coefficient in the bearing area
P	is the pitch of the thread
D_{km}	is the effective diameter for friction moment at the bearing area

The effective diameter for friction moment can be expressed [2, p231][5, p67]

$$D_{km} = \frac{d_w + D_B}{2} \tag{4}$$

where d_w is the diameter of bearing surface of the screw and D_B is the diameter of the assembly hole or the hole diameter of the washer, which is smaller.

When M_G and M_K are substituted in equation 1 with equations 2 and 3, the tightening torque is [5, p67]

$$M_A = \frac{1}{2} F_M (1.155\mu_G \cdot d_2 + \mu_K \cdot D_{km} + \frac{P}{\pi}) \tag{5}$$

The interested parameter is the clamping force of the joint thus F_M is solved from equation 5: [2, p231][5, p67]

$$F_M = \frac{2M_A}{1.155\mu_G \cdot d_2 + \mu_K \cdot D_{km} + \frac{P}{\pi}} \tag{6}$$

When the tightening torque is known and the dimensions of screw are taken from screw data sheet, the friction coefficients shall be estimated before getting the clamping force. Some friction coefficients are introduced in table 1.

Table 1. Friction coefficients for certain material pairs. [5, p114]

	Static friction coefficient in the state	
Material combination	**Dry**	**Lubricated**
Steel-Steel/cast steel	0.1-0.23	0.07-0.12
Steel-Gray cast iron	0.12-0.24	0.06-0.1
Steel-Copper alloy	0.07	
Steel-Aluminum alloy	0.1-0.28	0.05-0.018
Aluminum-Aluminum	0.21	

The calculated thread torque is also interesting value for self-clinching inserts. The self-clinching inserts have normally the torque out value and now that value is important. The thread torque resists the rotation of screw during tightening and that torque transmits to the interface between busbar and the insert. In other words the torque out value limits the possible thread torque in the joint. If the thread torque during tightening is higher than the torque out value, the insert starts to rotate and the joint fails.

2.4.2 Assembly stress of the joint during tightening

The first check after finding out the assembly preload is that the stresses in the screw are on allowable level. If the stress level is too high, the screw can yield or even break under loading. The VDI 2230 recommends the maximum assembly stress shall be under 90 % of the yield strength of the screw. [5, p74]

The maximum possible stress in the screw consists of simultaneously acting tension σ_M and torsional τ_M stresses. These two stresses are reduced by means of the deformation energy theory to an equivalent uniaxial stress state. Comparative stress is [5, p74]

$$\sigma_{red} = \sqrt{\sigma_M^2 + 3\tau_M^2} \tag{7}$$

The tension stress can be expressed [5, p74]

$$\sigma_M = \frac{F_M}{A_0} \tag{8}$$

where A_0 is the minimum cross-sectional area of the screw.

The torsional stress can be expressed [5, p74]

$$\tau_M = \frac{M_G}{W_p} \tag{9}$$

where W_p is the polar moment of resistance of a screw cross section.

The polar moment of resistance of a screw cross section is according to VDI 2230: [5, p74]

$$W_p = \frac{\pi d_0^3}{12} \tag{10}$$

where d_0 is the diameter of the smallest cross section of the screw.

When equations 8, 9 and 10 are substituted in equation 7 follows [5, p75]

$$\sigma_{red} = \sigma_M \sqrt{1 + \left(\frac{\tau_M}{\sigma_M}\right)^2} = \frac{F_M}{A_0} \sqrt{1 + 3\left[\frac{3}{2} \cdot \frac{d_2}{d_0}\left(\frac{P}{\pi d_2} + 1.155\mu_G\right)\right]^2} \tag{11}$$

The comparative stress can also be expressed with the 0.2 % proof stress of the screw $R_{p0.2}$ and the utilization factor υ. [5, p75]

$$\sigma_{red} = \vartheta \cdot R_{p0.2} \tag{12}$$

Now, the utilization factor can be calculated by substituting equation 12 to equation 11

$$\vartheta = \frac{\frac{F_M}{A_0}\sqrt{1+3\left[\frac{3}{2}\cdot\frac{d_2}{d_0}\left(\frac{P}{\pi d_2}+1.155\mu_G\right)\right]^2}}{R_{p0.2}} \tag{13}$$

If the utilization factor is smaller than 0.9, the joint is safe.

2.4.3 Preload changes in the joint

When the assembly preload is known and the assembly stress is checked, it is important to know, how much clamping force is left after the joint has settled and how the clamping force changes under different operating conditions. Hence, the preload change calculation shall be carried out to ensure the reliability of the joint.

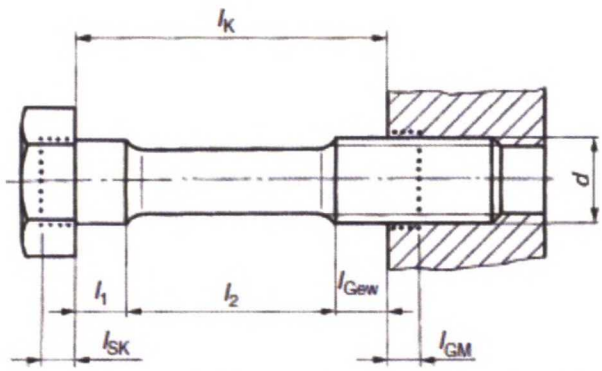

Figure 15. Regions of the screw for calculation. [5, p28]

First, it shall be calculated the axial resiliences of the all joint members. In the calculations is assumed that all deformations are elastic and reversible. Plastic deformations are not allowed because they cause irreversible preload loss, which weaken the joint. The elastic resilience of the screw can be expressed [5, p28]

$$\delta_S = \delta_{SK} + \delta_1 + \delta_2 + \cdots + \delta_i + \delta_{Gew} + \delta_{GM} \tag{14}$$

where

δ_{SK}	is the elastic resilience of the screw head
δ_i	is the elastic resilience of any section i=1,2,3… of the screw
δ_{Gew}	is the elastic resilience of the unengaged loaded thread
δ_{GM}	is the elastic resilience of the engaged thread and of the nut or tapped thread region

The regions of screw are explained in figure 15.

The elastic resilience of the engaged thread and the nut can be calculated from equation [5, p28]

$$\delta_{GM} = \frac{0.5d}{E_S \cdot A_{d3}} + \frac{0.4d}{E_M \cdot A_N} \tag{15}$$

where

d	is the nominal diameter of the screw
E_S	is the Young's modulus of the screw material
A_{d3}	is the cross section area of thread at minor diameter
E_M	is the Young's modulus of the nut or tapped thread region
A_N	is the nominal cross section area

The equation 15 is for through bolted joint. If it is wanted to calculate tapped thread joint, the factor 0.4 in the second term shall be replaced with factor 0.33. [5, p29]

Similarly, the elastic resilience of the unengaged loaded thread can be calculated [5, p29]

$$\delta_{Gew} = \frac{l_{Gew}}{E_S \cdot A_{d3}} \tag{16}$$

where l_{Gew} is the length of the unengaged loaded thread.

The elastic resilience of the screw head for hexagon head bolt is calculated [5, p29]

$$\delta_{SK} = \frac{0.5d}{E_S \cdot A_N} \tag{17}$$

And finally the elastic resilience of the other sections of the screw is calculated [5, p29]

$$\delta_i = \frac{l_i}{E_S \cdot A_{d3}} \tag{18}$$

where l_i is the length of part i.

The elastic resilience of clamped parts is more difficult to calculate. The preload affects axially right under the screw head, but it decreases rapidly, when moving out of the bearing area of screw head. Hence, the clamped part is only deformed near the screw so the calculation, where the preload is assumed to be uniform at the whole surface of clamped part, will not work. The VDI 2230 calculation model has a region in the joint, where the preload affects. That region is called the deformation cone. The actual calculated elastic resilience of clamped parts is the elastic resilience of this deformation cone. The calculation model is introduced in figure 16. If the joint is thick and narrow, the deformation cone meets the outer edges of the joint earlier than the contact surface between clamped parts. In that case the rest of joint between the deformation cone and the contact surface is modeled as a sleeve and added to the deformation cone. [5, p30-32]

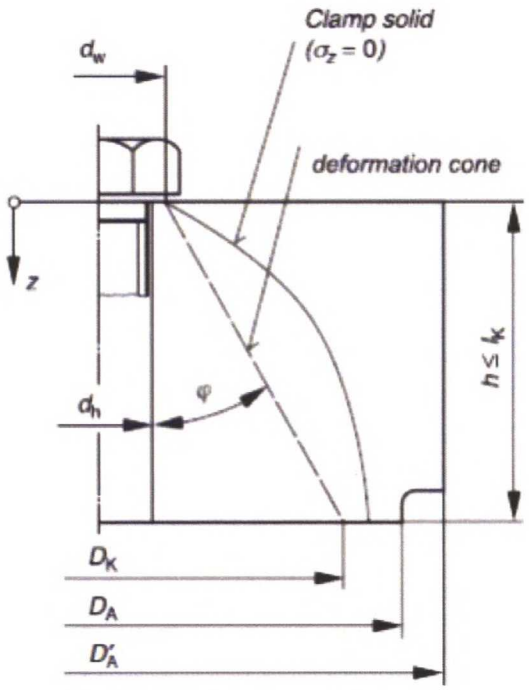

Figure 16. The calculation model according to VDI 2230. [5, p31]

For calculating the elastic resilience of clamped parts, there is needed an auxiliary variable limiting diameter $D_{A,Gr}$. It can be calculated for through bolted joints with equation [5, p33]

$$D_{A,Gr} = d_w + l_k \cdot \tan(\varphi) \tag{19}$$

where l_k is the clamping length and φ is the angle between the screw axis and the deformation cone.

For through bolted joints, the term $tan(\varphi)$ can be expressed [5, p35]

$$\tan(\varphi) = 0.362 + 0.032 \cdot \ln\left(\frac{\beta_L}{2}\right) + 0.153 \cdot \ln(y) \tag{20}$$

where $\beta_L = l_k/d_w$ and $y = D'_A/d_w$. In busbar joints D'_A can be treated as the outside diameter of the basic solid at the interface. That means, the variables D'_A and D_A in figure 16 are equal.

Depending on the value of limiting diameter $D_{A,Gr}$, the right equation for elastic resilience of clamped parts is chosen. If the joint is wide, there is only the imaginary deformation cone in the joint, it is $D_A \geq D_{A,Gr}$, and the elastic resilience of clamped parts is [5, p34]

$$\delta_P = \frac{2 \cdot ln\left[\frac{(d_w+d_h)\cdot(d_w+l_k\cdot\tan(\varphi)-d_h)}{(d_w-d_h)\cdot(d_w+l_k\cdot\tan(\varphi)+d_h)}\right]}{E_p \cdot \pi \cdot d_h \cdot \tan(\varphi)} \tag{21}$$

where d_h is the hole diameter of clamped parts and E_P is the Young's modulus of clamped parts.

If the joint is narrow, there is also an imaginary sleeve with the deformation cone in the joint, it is $d_w < D_A < D_{A,Gr}$, and the equation forms to [5, p34]

$$\delta_P = \frac{\frac{2}{d_h \cdot \tan(\varphi)} \cdot ln\left[\frac{(d_w+d_h)\cdot(D_A-d_h)}{(d_w-d_h)\cdot(D_A+d_h)}\right] + \frac{4}{D_A^2-d_h^2}\left[l_k - \frac{D_A-d_w}{\tan(\varphi)}\right]}{E_p \cdot \pi} \tag{22}$$

When the elastic resiliences are calculated, the preload losses can be calculated. First is calculated preload loss due to embedding and relaxation. This calculation takes into account the local plastic deformations in the joint. Plastic flattening of surface roughness at the bearing areas and contact surface is designated as embedding. The time-dependent preload loss due to creep is designated as relaxation. The preload loss due to embedding and relaxation is [5, p63-64]

$$F_Z = \frac{f_Z}{\delta_S + \delta_P} \tag{23}$$

Where f_Z is the amount of embedding from table 2. The amount of embedding depends on the surface roughness of clamped parts and f_Z is calculated by adding the values on right row. For example, if R_Z is 8 µm, f_Z is 3 (thread) + 3*2 (nut and screw bearing areas) + 2 (contact surface between parts) = 11 µm. The values of table 2 are not appropriated if the limiting surface pressures are exceeded.

Table 2. Guide values for joint embedding. [5, p64]

Average roughness height R_z according to DIN 4768	Loading	Guide values for amounts of embedding in µm		
		in the thread	per head or nut bearing area	per inner interface
< 10 µm	tension/compression	3	2,5	1,5
	shear	3	3	2
10 µm up to < 40 µm	tension/compression	3	3	2
	shear	3	4,5	2,5
40 µm up to < 160 µm	tension/compression	3	4	3
	shear	3	6,5	3,5

There is also another method to determine f_Z according to Airila et al. There is introduced an equation which gives the amount of embedding. The equation is [2, p238]

$$f_Z = 3.29\left(\frac{l_k}{d}\right)^{0.34} \cdot 10^{-6} \tag{24}$$

This method seems better to determine the amount of embedding, because it takes the joint thickness and screw diameter into account. The VDI 2230 values are well suitable, when the clamped parts are made of steel and the screw is tightened to 90 % of its yield strength. In this case, neither of above-mentioned things are fulfilled so the method of Airila et al. is used.

The operating temperature affects to the joint preload significantly. In low temperatures occurs preload loss due to thermal contraction, which can loosen the joint and cause increase of joint resistance and lead to complete failure of the joint. Due to thermal expansion in high temperatures, the preload increases, which lead to the increase of the contact pressure and the stresses of the screw. In other words, the temperature changes during operation can cause the joint is either loose or too tight. This shall be taken into account in the calculations.

The preload change due to temperature change can be calculated according to VDI 2230: [5, p65]

$$\Delta F_{Vth} = F_{VRT}\left(1 - \frac{\delta_S + \delta_P}{\delta_S \frac{E_{SRT}}{E_{ST}} + \delta_P \frac{E_{PRT}}{E_{PT}}}\right) + \frac{l_k(\alpha_S \cdot \Delta T_S - \alpha_P \cdot \Delta T_P)}{\delta_S \frac{E_{SRT}}{E_{ST}} + \delta_P \frac{E_{PRT}}{E_{PT}}} \tag{25}$$

where

F_{VRT} is the preload in room temperature which is in this work the same as the assembly preload F_M.

E_{SRT} is the Young's modulus of the screw material at room temperature

E_{ST} is the Young's modulus of the screw material at temperature different from room temperature

E_{PRT} is the Young's modulus of the clamped parts at the room temperature

E_{PT}	is the Young's modulus of the clamped parts at temperature different from room temperature
α_S	is the coefficient of linear thermal expansion of the screw
α_P	is the coefficient of linear thermal expansion of the clamped parts
ΔT_S	is the temperature difference of the screw from room temperature
ΔT_P	is the temperature difference of the clamped parts from room temperature

The above-mentioned preload changes shall be taken into account when determining the behavior of the joint in operating conditions. The preload loss due to embedding and relaxation F_Z occurs immediately, when the joint is tightened, but the maximum preload loss can be reached not until after a few days. The preload change due to temperature change ΔF_{Vth} occurs every time, when the joint temperature changes. The temperature change can increase or decrease the preload depending on if the joint is cold or hot. [5, p65]

The new assembly preload in certain temperature can be calculated [5, p73]

$$F_V = F_M - F_Z - \Delta F_{Vth} \tag{26}$$

The preload change due to temperature change ΔF_{Vth} can be omitted if it is known that the joint temperature is constant.

If the new assembly preload F_V differs a lot from old assembly preload F_M, the calculations in chapter 2.4.2 shall be checked again.

2.4.4 Surface pressure, loosening of joint and thread length of engagement

It is important to take care that the surface pressures in the joint are on the allowed level. If there are too high surface pressures in the joint, the material of clamped parts yields and cause unexpected preload loss. Hence, the busbars are softer material than the fasteners the highest surface pressure occurs under the screw head or nut. Washers are used in busbar joints to even out the pressure under the screw head or nut. Still the limiting pressure is located between washer and busbar.

The surface pressure under the washer or nut or screw head is [5, p84]

$$p_M = \frac{max\{F_M, F_V\}}{A_{p\,min}} \tag{27}$$

where $A_{p\,min}$ is the minimum bearing area under the screw head, nut or washer. The preload shall be chosen by which is the largest preload.

The minimum bearing area can be calculated [5, p84]

$$A_{P\,min} = \frac{\pi}{4}(d_{wa}^2 - d_h^2) \tag{28}$$

where d_h is the diameter of assembly hole and d_{wa} is the diameter of bearing surface of the screw d_w or if there is used washers $d_{wa} = d_w + 1.6h_s$, h_s is the thickness of the

washer. If there is used self-clinching insert in the joint, d_{wa} is the outer diameter of the insert.

If the surface pressure is larger than the limiting surface pressure of material, the contact area shall be increased or the preload shall be decreased.

The length of engagement shall be checked to ensure the thread of nut or other threaded part will last under loading. Bolted joint shall be designed so the screw breaks earlier than the thread, because it is easier to repair the joint just by replacing the screw. According VDI 2230 the minimum thread length can be calculated with equation [5, p87]

$$m_{eff\_min} = \frac{R_m \cdot A_S \cdot P}{C_1 \cdot C_3 \cdot \tau_{BM}\left(\frac{P}{2} + (d_{min} - D_{2max}) \tan 30°\right) \cdot \pi \cdot d_{min}} \tag{29}$$

where

R_m is the tensile strength of the screw
A_S is the stress cross section of the screw, average of the cross section of pitch diameter d_2 and the minimum cross section of the screw A_0
τ_{BM} is the shearing strength of the nut
d_{min} is the outer diameter of the screw at lower tolerance limit
D_{2max} is the pitch diameter of the nut at upper tolerance limit

The variable C_1 is [5, p86]

$$C_1 = 3.8\frac{s}{d} - \left(\frac{s}{d}\right)^2 - 2.61 \tag{30}$$

where s is the width across flats.

It is needed to calculate strength ratio for calculating variable C_3. The strength ratio is [5, p86]

$$R_S = \frac{\tau_{BM} \cdot \left[\frac{P}{2} + (d - D_2) \cdot \tan 30°\right] \cdot d}{\tau_{BS} \cdot \left[\frac{P}{2} + (d_2 - D_1) \cdot \tan 30°\right] \cdot D_1} \tag{31}$$

where

D_2 is the pitch diameter of the nut
τ_{BS} is the shearing strength of the screw
D_1 is the nut minor diameter

If $0.4 < R_S < 1$, C_3 is [5, p86]

$$C_3 = 0.728 + 1.769R_S - 2.896R_S^2 + 1.296R_S^3 \tag{32}$$

If $R_S \geq 1$, $C_3 = 0.897$.

When substituting C_1 and C_3 to equation 29, the minimum thread length can be calculated. The value received from equation 29 is the minimum thread length of nut or

threaded insert. If the threaded thickness of the nut or insert is smaller than the received value, nut or insert shall be replaced with thicker one. Equation 29 is not suitable for tapped thread joints. [5, p86]

The loosening of bolted joint is caused by slackening and loosening torque of the screw thread. Slackening is a result of relaxation and creep of the screw or the clamped parts. Creep occurs when the joint is in high temperature operating conditions and/or the surface pressures increases over limiting pressure. Slackening shall be avoided by selection of material or using e.g. spring washer in the joint. Spring washer compensates the preload loss caused by slackening. The loosening torque results from the nature of screw thread. The amount of loosening torque depends on the preload and the pitch. Loosening torque can be checked by calculation. Loosening torque is [1, p382][2, p240][5]

$$M_L = \frac{1}{2} F_V \left(-\frac{P}{\pi} + 1.155\mu_G \cdot d_2 + \mu_K \cdot D_{km} \right) \quad (33)$$

If the loosening torque is negative, there is risk to loosening of the joint. Otherwise the loosening torque is not a problem.

3 The busbar joints in a frequency converter

3.1 Mechanical loads

There is always defined an operating life for machines and devices. During that time the device shall operate without failures with or without service actions. Operating conditions determine the requirements of the structure. Mechanical requirements of device or structure depend on loads in structure. Loads are usually static or dynamic loads. Static loads are constant magnitude loads acting on certain point in structure during operation. Dynamic loads are variable magnitude loads, which act on certain frequency on certain point in structure. [2, p9-15]

Static loads can be handled easily, because they are possible to calculate by hand and the strength of the structure depends on the geometry of structure and material properties. Dynamic loads are more difficult to calculate, because they depend also on operating conditions. The dynamic loads shall be simplified for getting results with reasonable effort from calculation. Other option is to use computer simulations for determining weak spots of structure. Fatigue behavior of the structure is the most significant factor under dynamic loading. [2, p9, 23-26]

Normally, the mechanical requirements are strict for bolted joints, because they shall be suitable in various operation conditions. For electrical busbar joints, the mechanical requirements are different and not always so strict than for the regular bolted joints because busbars do not carry structural loads. Busbars are supported to the frame of the device or cabinet and hence normally there are not external loads in the joint. In some cases the joint might carry the weight of busbar, but there are not other loads in the joint. Despite the external structural loads are lacking, the busbar joint shall be designed to withstand loads that may occur during operation.

The most important requirement is the joint preload. The preload shall be high enough to form adequate surface pressure on the contact area of the joint. The higher contact pressure acts on the contact area of the joint the smaller contact resistance is. On the other hand high preload eases the joint to carry possible external loads without slipping and loosening. Adequate preload enables the force transmission by friction, when the joint behavior is foreseeable and previous calculations are valid. The preload shall not be too high, because it causes plastic deformations in the joint. [2, p225]

The device shall withstand vibration and shocks without damages. Every part of structure has a mass and stiffness, which determine the dynamic behavior of the whole structure. Vibration forms when the loading that acts on the structure alternates. The alternating load is caused by moving masses or parts of the structure or vibration from environment of the structure. In the case of frequency converter, all the vibration comes from the environment of the converter, because there are not any significant moving masses in the device. Vibration is harmful to the device operation and it can cause unexpected stresses in the structure of the device. Bolted joints are discontinuities in the structure and these are sensitive for effects of vibration. In bolted joints vibration might cause micro slippages in the joint and during the time loosen the joint. The VDI 2230 do not deal with the vibration accurately. There is calculated the stresses of the joint caused by vibration, but the joint loosening is not dealt with. [18, p2-5]

The frequency converter shall be fulfilled the requirements in the vibration test. ABB's frequency converters are tested according to standard IEC 68-2-6. The standard defines the testing procedure, measuring, test type and guidelines to execute the test. The used vibration in the test is sinusoidal. The test can be carried out with constant vibration amplitude and frequency or by sweeping constant vibration amplitude with different frequencies. ABB uses normally endurance sweep tests in marine devices with 1 mm amplitude in frequencies 2-13.2 Hz and acceleration 7 m/s^2 in frequencies 13.2-100 Hz and in industrial devices with 0.075 mm amplitude in frequencies 10-50 Hz and acceleration 9.81 m/s^2 in frequencies 50-150 Hz. The test sweeps used in ABB are marked in figure 17. There is usually also carried out vibration response test, where smaller amplitude and acceleration are used than in corresponding endurance test. Any component, mechanical or electrical, shall not be damaged after the vibration test. In addition to endurance and response tests, there can be carried out shock tests according to IEC 255-21. [19][20]

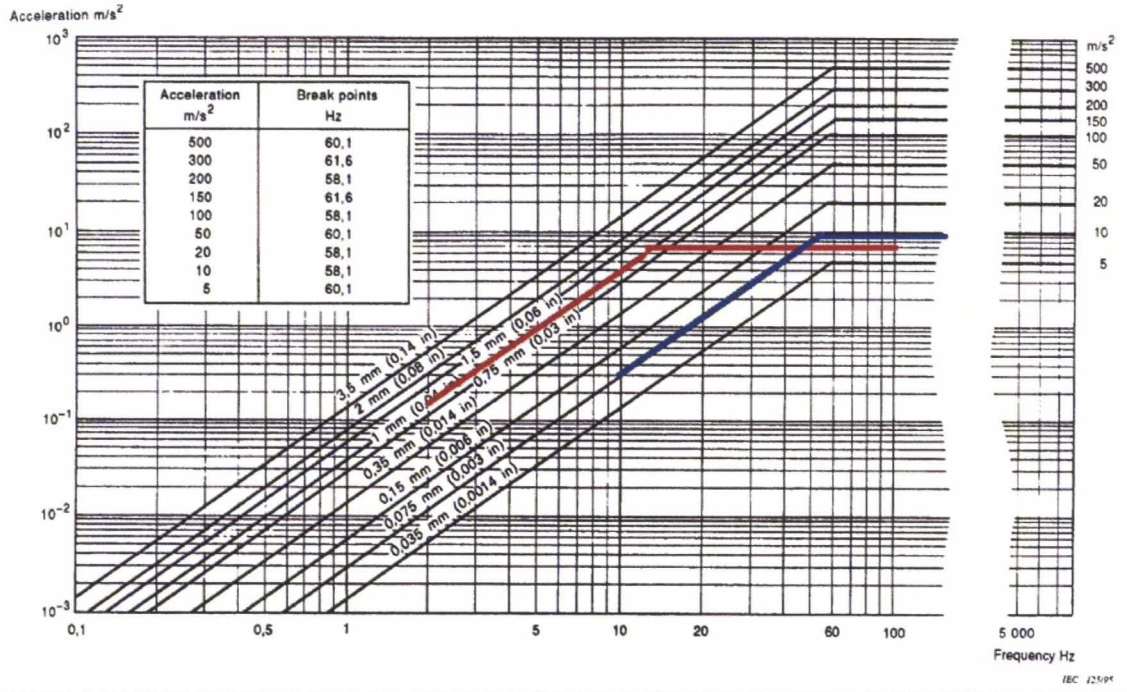

Figure 17. Vibration test sweeps according to IEC 68-2-6. The marine endurance test sweep used in ABB marked with red and the industrial endurance test sweep marked with blue. [19]

In the point of view bolted joints, the only way to handle vibration is to ensure the preload remain high enough in all conditions. There are not external loads in busbar joints, which ease significantly the reliability of the joint under vibration. The transverse movement caused by vibration in the joint is the worst scenario. Adequate preload ensures the friction force between clamped parts prevent the relative movement of the clamped parts. If the amount of relaxation is high, it is recommended to use spring washer in the joint to compensate the relaxation and ensure the preload. The vibration may cause the screw or nut to rotate and loosen the joint. To avoid this kind of loosening, there can be used locking insert in the nut or glue in the threads. [2, p240]

The busbar joints may have mechanical loads caused by electrical and thermal phenomena, but these loads are dealt with in following paragraphs. These loads may be significant and they may have effect to the reliability of the joint.

3.2 Electrical loads

3.2.1 Electromagnetic forces

The electrical requirements of bolted busbar joint are simply used to achieve conduction with low power losses and withstand the electromagnetic forces. The electromagnetic force is formed, when the magnetic fields of two current-carrying conductors are affecting to each other according to Biot-Savard law. Depending on the direction of the current, the conductors are attracting or repelling each other. The effect of electromagnetic force is introduced with two example cases in figure 18. The higher the currents are in the conductors, the higher is the force. The highest electromagnetic force occurs when the device is short-circuited. The short-circuit currents and forces are dealt with in standards IEC 61660-1, IEC 61660-2 and IEC 909. [21][22][23]

According to IEC 61660-2 the electromagnetic force can be calculated with equation [22]

$$F_{EM} = \frac{\mu_0}{2\pi} \cdot i_1 \cdot i_2 \cdot \frac{l}{a} \tag{34}$$

where

μ_0	is the permeability of the medium
i_1	is the current in busbar line 1
i_2	is the current in busbar line 2
l	is the distance between supports of busbar
a	is the distance between busbar center lines

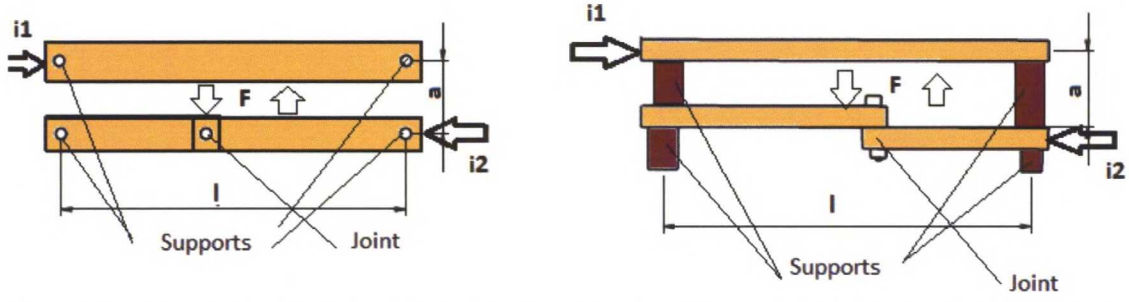

Figure 18. Possible cases of the electromagnetic force, when current is going opposite directions in busbars.

The short-circuit current depends on where it occurs. In DC-circuit the short-circuit current is different than in AC-circuit. The standards deal with time-depending short-circuit currents in different circuits. The placement of the failure in the circuit affects also to the short-circuit current. In this case the most interested current value is the highest value, because it causes the highest electromagnetic force. The highest short-circuit current usually occurs at the beginning moments of short-circuit. The short-circuit current shall be calculated or measured for every circuit. According to Oksanen, the peak value of short-circuit current in frequency converter is 75-175 kA depending on the device. [21][23][24]

In normal use, when the current is less than 1200 A, the electromagnetic force is very small, usually about 1 N, so the effect of the electromagnetic force can be ignored. Instead, during short-circuit the electromagnetic force can be so high, the joint might slip which leads to failure of the joint. The requirement under short-circuit situation is the joint shall not fall apart. The joint is not needed to be functioning after short-circuit.

The actual calculation of the effects of the electromagnetic forces in short-circuit situation is difficult, because the busbars are supported to the frame with slightly flexible supports. This flexibility absorbs energy caused by the work of electromagnetic so the actual forces in the joint are unknown. The loads can be found out for example with FEM simulations. In practice the electromagnetic force shall be handled with the support structure thus the busbar joint shall not be loaded by the electromagnetic force. [24]

3.2.2 Contact resistance

The more significant requirement for busbar joint is low contact resistance of the joint. The contact resistance describes the electrical resistivity of the joint. The contact resistance determines the power losses and the heating of the joint. If the contact resistance is large in the joint, the resistance causes voltage drop in the joint which leads to power loss. In practice, the power loss is observed as temperature rise of the joint. Large power loss may distract the operation of the device and high joint temperature may weaken the joint. [25, p2]

The surfaces of busbar are not smooth, when observing on the microscale. When this kind of two rough surfaces are set against each other, the contact area forms from spots, where the highest peaks of the surface are in contact to the other surface. That means the whole apparent contact surface of the joint is not in contact, but only partially. The joint is electrically conductive only on these contact spots, where metal to metal contacts are. When the actual current conducting area is smaller than the apparent contact surface, the resistivity of the joint is higher. [25, p1-2]

Contact resistance calculation is used to understand mechanics of the contact surfaces. The rough surfaces are simplified to ease the calculation. The roughness of the surface is simplified to consist of semispherical peaks as seen in figure 19. After the simplification the case can be handled with tribological contact theory of rough surfaces. The theory divides in two sections: elastic contact and plastic contact. The contact type is plastic in bolted busbar joints, because the plastic flattening of the roughness peak increases the contact area and conductivity. The plastic contact type is valid also for other types of bolted joint, because, as in chapter of designing theory mentioned, there are some local plastic deformations in contact surfaces, which are taken into account in the preload loss calculation. The plastic contact is now observed accurately to calculate the contact resistance. [25, p2][26, p52-53]

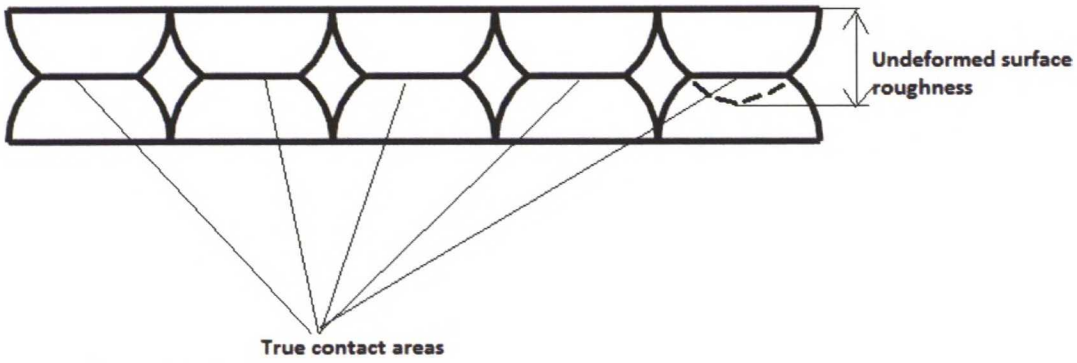

Figure 19. The idealized model of two rough surfaces after plastic deformation.

The contact resistance calculation bases on the theory of plastic contact of rough surfaces. The calculation is not valid if the contact is elastic. In this case the preload in bolted busbar joint is adequate to cause plastic deformations on contact surfaces. First is calculated the actual contact area of the joint. It is [26, p55]

$$A_c = \frac{F_M}{H} \tag{35}$$

where H is the hardness of busbar material in Brinell scale. If the busbar is plated, hardness H is the hardness of softer material.

This is the actual contact area where the current can pass the joint. With the actual contact area can be calculated the contact resistance. Contact resistance can be expressed according to Slade et al. [25, p12]

$$R_c = \frac{\rho}{2}\sqrt{\frac{\pi\eta}{A_c}} \tag{36}$$

where ρ is the resistivity of busbar material and η is an empirical coefficient of order unity for clean interfaces.

The empirical coefficient is a problem, when calculating contact resistance, because there is not a way to calculate it. It shall be determined by an experiment for every case to get reliable results. In this work is used a coefficient that is determined in earlier tests. According to Luoma et al. the empirical coefficient is $1/\pi$. This coefficient is determined for uncoated busbars, but now the busbars are tin plated. The coefficient with tin plated busbars is presumably different, but that coefficient is not determined in this work. The contact with plated busbars is better than busbars without plating that means the coefficient is smaller. Therefore, the calculation is on safer side. [27]

The plating of busbar shall be taken into account in calculations, because the plating changes contact resistance. The resistivity difference between plating and busbar causes there is an extra interface in the contact where the current shall go through. The current distribution changes in this interface between plating and busbar and the contact resistance increases. In figure 20 is shown the current distribution with different resistivity platings.

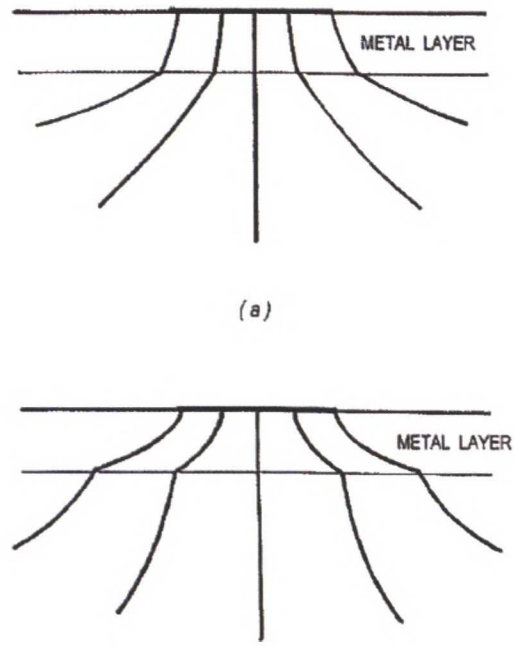

Figure 20. Current distribution in busbar and its plating layer. Distribution is like in upper figure, when the resistivity of plating is larger than busbar material, and like in lower figure when resistivity of plating is smaller. [25, p17]

The effect of plating can be taken into account by modifying equation 36. According to Slade et al. the contact resistance for plated busbars is [25, p18]

$$R_c = \frac{\rho_p + \rho \cdot P_f}{4} \sqrt{\frac{1}{A_c}} \tag{37}$$

where ρ_p is the resistivity of plating and P_f is the plating factor from figure 21 and there is noticed that $\eta = 1/\pi$.

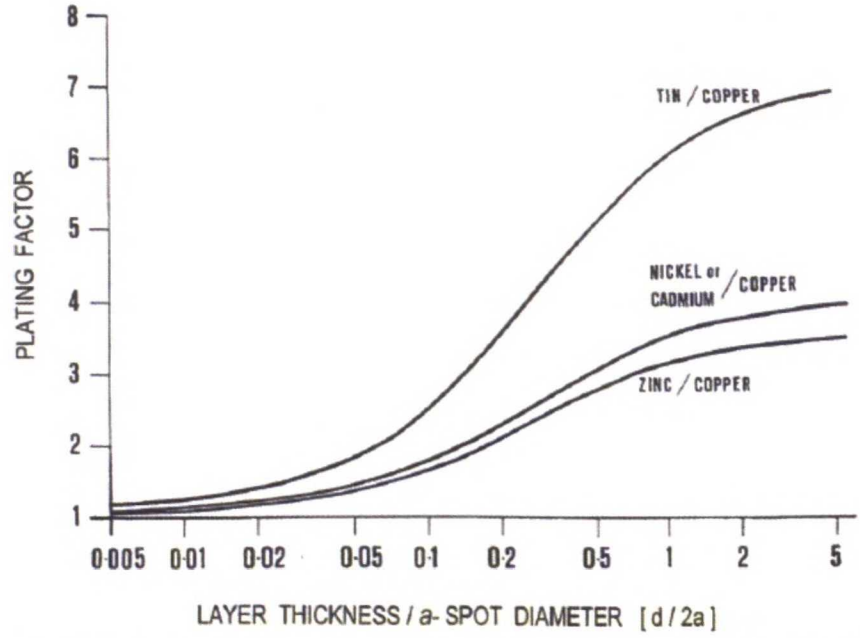

Figure 21. Plating factors for different plating-base material pairs. [25, p18]

There shall be calculated the proportion of coating layer thickness d and contact spot diameter $2a$ to get the plating factor. The contact spot radius a is a bit difficult to calculate accurately. When using the idealized theory the contact spot area can be expressed [26, p53]

$$A_i = \frac{A_c}{n} \tag{38}$$

where n is the number of contact spots.

If it is assumed the preload divides equally to the whole contact area, all the surface roughness peaks are in contact. The number of contact spots can be calculated by calculating how many surface roughness peaks there are in the contact surface

$$n = \frac{b \cdot l}{4\sigma'^2} - \frac{\frac{\pi}{4}d_h^2}{4\sigma'^2} \tag{39}$$

where b is the width of the joint, l is the overlapping length of the joint and σ' is the combined surface roughness of the contact surfaces.

The combined surface roughness can be calculated with equation [26, p129]

$$\sigma' = \sqrt{Rq_1^2 + Rq_2^2} \tag{40}$$

where Rq_1 and Rq_2 are the root mean square values of surfaces roughness of contact surfaces.

Finally, the contact spot radius can be calculated [25, p11]

$$a_c = \sqrt{\frac{A_i}{\pi}} \tag{41}$$

When the contact spot radius is calculated, it is possible to determine plating factor from the figure 21 and calculate the contact resistance. From the equations 35 and 37 can be seen that resistivity of busbar material and plating, joint preload and hardness of busbar or plating are the significant parameters in the calculation of contact resistance. Joint preload is the easiest parameter to affect by design. By increasing joint preload, the contact resistance can be reduced. The basic target is to get the contact resistance as close as the resistance of busbar. This kind of design ensures the temperature of joint does not rise too much and the power loss of joint is not significant.

3.3 Thermal loads

The busbar joint shall withstand temperature changes of the operating environment. There are different reasons for temperature change. The most usual reasons are the temperature change due to change in operating conditions and due to heat generation of the frequency converter. If the resistance of the busbar line is large, the busbars and joints generate heat by themselves. Temperature changes cause length changes of busbar. In low temperatures busbar shrinks and causes preload loss in the joint. Respectively in high temperatures busbar expands and causes an extra load in the joint.

The linear deformation of part due to thermal expansion can be calculated with equation [5, p65]

$$f_T = \alpha_T \cdot l \cdot \Delta T \tag{42}$$

where α_T is the coefficient of thermal expansion, l is the length of part and ΔT is the temperature difference.

The most stressful load caused by temperature is transverse loading. The transverse loading causes fatigue loads in the contact surface or slipping, if the friction force is not adequate. During the time both things cause sliding on the contact surface and wearing of the contact surfaces. Wearing forms abrasive particle layer between contact surfaces, which increases joint resistance. The phases of wearing are shown in figure 22. [25][26]

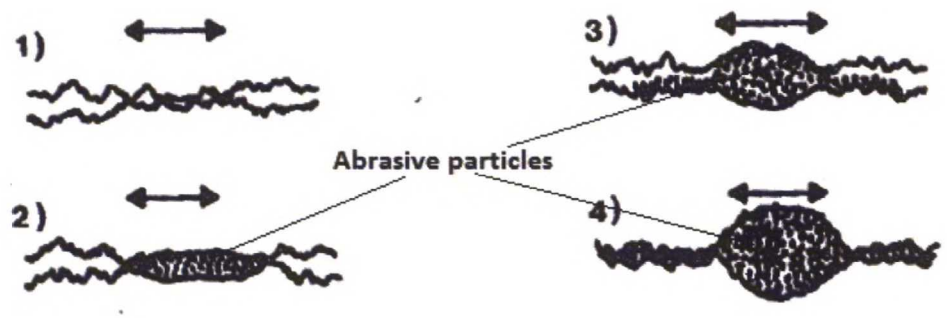

Figure 22. Forming of abrasive particle layer when contact surfaces slide under transverse loading. [26, p117]

The force caused by the length thermal expansion of busbar is mostly lead to the supports of busbar. The rest of the thermal expansion force falls on the joint. To avoid the sliding of contact surfaces the friction force between contact surfaces shall be adequate to prevent sliding. The length thermal expansion shall be taken into account in whole busbar line design.

The more significant load, in point of view the busbar joint, is the load change caused by thickness thermal expansion of the joint members. This joint preload change has been taken into account when calculated temperature-dependent preload changes in the joint in the equation 25. The busbar joints are quite sensitive to temperature changes, because the coefficient of thermal expansion of busbar is different than the coefficient of screw and nut. Copper and aluminum have larger coefficient of thermal expansion than steel. That means the preload may increase rapidly, when temperature rises and decrease, when temperature drops. It is also noticeable that copper and aluminum are good thermal conductors, which helps the heat transfer away from the joint. If only one section of busbar with the joint is in high temperature, the heat tries to spread evenly in the busbar, which cools the joint. [5, p65, 119]

One way to manage heating of busbar is to cool it for example blowing air past busbar. The heat is transferred to the air and carried out of the device. There are three ways to transfer heat out of the busbar; conduction, convection and radiation. Usually these phenomena act at the same time if the busbar line is on hand. Every heat transfer mechanism act differently and their heat transfer power is different. [28, p7]

Conduction occurs in stationary medium which can be gas, liquid or solid. Heat transfers through part via electrons or thermal vibration. Conduction occurs until the heat has spread evenly in the part. The elapsed time, when heat is spread evenly, depends on the conductivity of material. The heat transfer power by conducting can be calculated with equation [28, p19]

$$\Phi_{cond} = \lambda \cdot A \frac{\Delta T}{l} \tag{43}$$

where λ is the conductivity of material, A is cross section area of part.

In convection heat transfer, heat transfers via moving medium, which can be gas or liquid. The heat transfer occurs in boundary layer between cooled part and medium. Convection heat transfer can be divided in natural convection and forced convection. Natural convection is caused by density differences in medium. Warmer substance has smaller density than cooler substance, which cause substance flow, when warmer substance rises up. Forced convection is brought about by external device like fan or pump, which causes substance flow. Convection contains usually two types of flow, laminar and turbulent flow. Laminar flow consists of parallel stream lines, which follow accurately the surface of part. Turbulent flow contains vortexes, which move perpendicularly to the flow direction. Turbulent flow is more efficient way to transfer heat than laminar flow. The most efficient way to transfer heat is to use forced convection, where is turbulent flow. The heat transfer power by convection can be expressed [28, p22, 68-70]

$$\Phi_{conv} = \alpha_{conv} \cdot A_{surf}(T_s - T_\infty) \tag{44}$$

where α_{conv} is the convective heat transfer coefficient, A_{surf} is the surface area of part, T_s is the surface temperature and T_∞ is the temperature of environment.

In radiation heat transfer, heat transfers via electromagnetic radiation. Radiation do not need medium so it works also in vacuum, where radiation is most efficient. The medium reduce the efficiency of radiation, because the atoms of medium absorb part of the radiation energy. The heat transfer power by radiation can be calculated with equation [28, p8, 116-118]

$$\Phi_{rad} = \varepsilon \cdot \sigma \cdot A_{surf}(T_s^4 - T_\infty^4) \tag{45}$$

where ε is the emissivity of material, σ is the Stefan-Boltzmann's coefficient.

Previous calculations help to manage the temperature of busbar line and joint. If the heat source is the busbar line and the heating power is known, the natural cooling can be calculated and with that information design possible additional cooling. Normally the additional cooling is not needed.

The most critical thermal phenomenon for bolted joint is the thermal expansion of joint. The easiest way to affect the thermal behavior of the joint is to increase flexibility of the joint for example by spring washer. When the joint expands in high temperature, the spring washer is elastic and it allows the joint expand without increasing the preload

significantly. In lower temperatures the spring load of the spring washer maintains the preload, when the joint is shrinking.

3.4 Manufacturing requirements

Busbars are made of copper or aluminum and the material is sheet or bar. Usually bar is used as blank, because it needs only a few working phases to get finished. If the busbar is formed complicatedly or it is wide and thin, it is easier to make it of sheet material.

The copper and aluminum busbars can be used as they are, but there is used tin plating for minimizing the contact resistance. The surface hardness of busbar can be decreased by plating it with softer material like tin. When the surface hardness is lower, the true contact area increases and the contact resistance decreases. Plating also protects the busbar against corrosion and wear. The number of working phases in assembly decrease, because the contact surfaces need not cleaning before assembly. At the same time the assembly errors due to sloppy cleaning of contact surfaces decrease. [25, p16]

The tin plating process is an electroplating method. Busbar is dipped in electrolyte solution that contains tin ions. Busbar is joined to power supply as cathode. When the current is switched on, the positive tin ions gather on the surface of busbar forming a coating layer. The tin ions gather on the cathode surface on positions, where the easiest access is. Usually the tin ions seek on the edges of the busbar, which leads to uneven coating layer. With additives in the electrolyte, the coating layer spread evenly on the surface of busbar. The principle of electroplating is seen in figure 23. [29, p395-396]

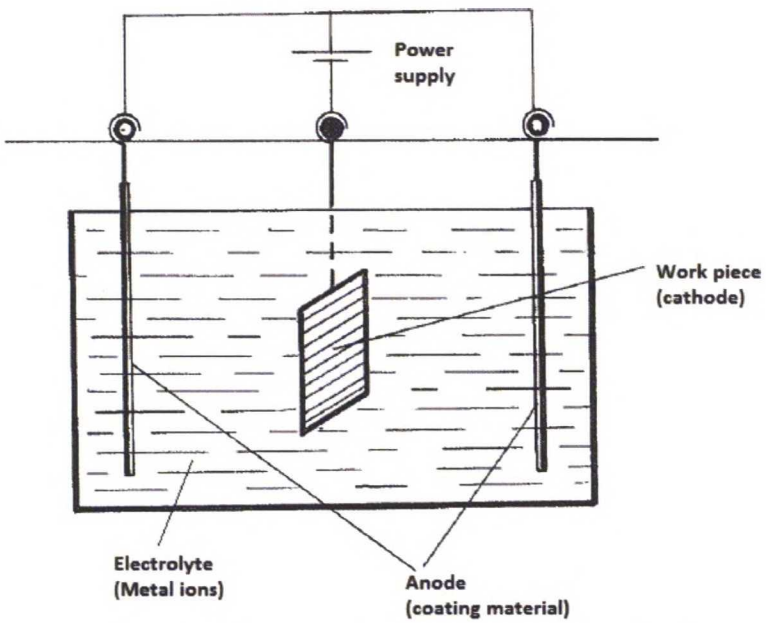

Figure 23. Electroplating of a work piece. [29, p396]

There are different shapes in the busbar. There can be bends in the busbar to get the route of busbar line as wanted. There are also needed holes in the busbar for bolted joints to attach busbars together. Holes and grooves can be made by machining, laser cutting or punching. Usually the punching is the used method, because it is the cheapest way to make simple shapes. By machining and laser cutting is possible to make

accurately very complicated shapes. Now, it is dealt with basic busbars so the punching is the used method.

The choice of manufacturing method is not significant in normal use, but it is noticeable that punching set some restrictions in further design. The most significant restriction is caused by inaccurate sizes of shapes. This inaccuracy restricts especially the use of self-clinching inserts, which usually demands accurate size of hole. The inaccuracy is caused by the cutting process. The hole diameter on punch side can be made accurately, when is noticed the hole diameter is a bit larger than the punch diameter. The accuracy can be affected with the choosing and the tolerances of a tool. The typical punch tool is introduced in figure 24. The problem is the rupture of material on die side. The rupture is caused, when the punch does not cut completely the material, but it shreds the material. Result is the hole diameter on the die side is larger than on the punch side. The form of punched shape can be seen from figure 25. The rupture depends on the material, tool and the thickness of work piece. [29, p233-234]

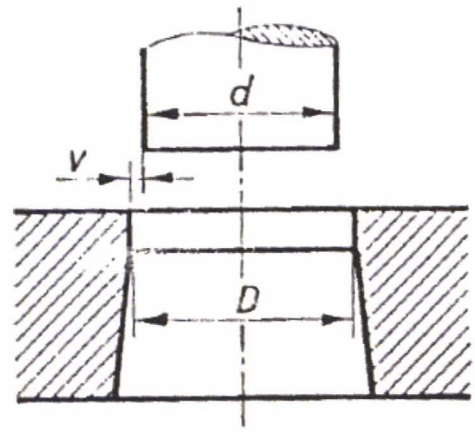

Figure 24. The punch and die. The punch diameter is smaller than the die diameter to ease cutting. [29, p233]

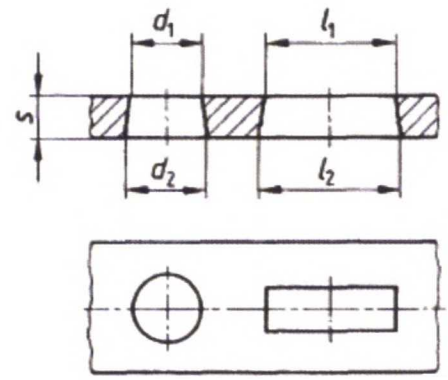

Figure 25. The rupture on the die side can be seen as larger diameter or length of the shape. [30]

There is standard for sheet metal punching on steel sheets, but not for copper and aluminum sheets. The standard SFS 5803 defines allowable tolerances for punched shapes. The maximum tolerance on the die side is also defined, which eases the design to exploit the die side of work piece. The SFS 5803 announce that for copper and aluminum sheet these tolerances shall be agreed with supplier. Copper and aluminum

have lower shearing strength than steel, which cause larger rupture on the die side. The thickness of sheet defines the minimum hole diameter that can be punched according to SFS 5803. For steel sheets, the recommendation is the hole diameter shall be larger than the thickness of the sheet. [31]

The inaccuracies of hole shape are a problem when attaching a self-clinching insert into a busbar. The self-clinching insert requires accurate hole, where it can fasten on. If the hole is too large or the wall of hole is slanted, the grooves of self-clinching insert may not be filled completely with sheet material. The incomplete inflation of grooves weakens the joint between self-clinching insert and the busbar. Despite the problem, it is possible to use punched busbars with self-clinching inserts. There is the restriction that the insert shall be fastened on the punch side, which is accurate. If the collar of self-clinching insert is long enough, the fastening can be made also on die side, but the loading of the insert shall be reduced.

One working phase in busbar manufacturing is bending, when the busbar is bended to follow the wanted busbar line path. Normally, the bends are simple and there are not many bends in one busbar, because of simple manufacturing. Numerous bends and other shapes increase the costs significantly. Bending shall be done accurately for getting the joint surfaces in right place. The bending tolerances shall also be taken into account in design to ensure the fastening holes meet each other. Tolerances can be taken into account by designing the clearance hole to oval. The work phases of bending are introduced in figure 26. [29, p268-269]

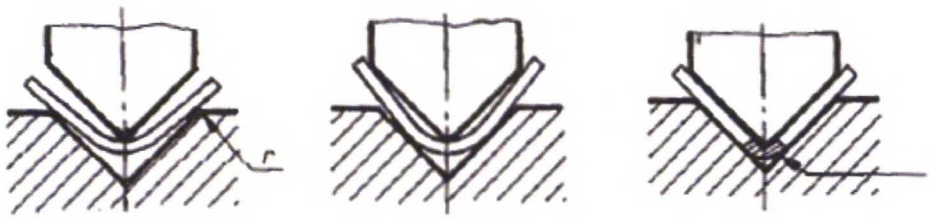

Figure 26. Phases of bending. [29, p269]

There are also some other issues that shall be taken into account, when bending busbar. There shall be notice the elastic recovery of busbar after bending. Because of elasticity of material, the angle after bending is smaller than in the last phase of bending. The bending radius shall be chosen so the material or the possible coating does not fracture. [29, p237]

4 Experimental tests

This chapter introduces the experimental part of this thesis. The purpose is to introduce test equipment, test samples, testing plan and the analysis of the results of the test.

4.1 Purpose of tests

The purpose of test setup was to find out the suitability of self-clinching nut in busbar joint. To find out the most of joint properties with one measuring, the test method was to assemble the busbar joint and measure the preload force and tightening torque during tightening. The other method was the torque out test like the self-clinching insert manufacturers does their products. The torque out test describes the properties of self-clinching insert and the clinching performance of the nut, which are important to know for designing the joint. The selected methods gave extensive information about the joint properties and also the performance of self-clinching nut.

4.2 Equipment

The test equipment is a special screw tightening device, which was built for testing breaking moments of tapping screw joints. The device was designed to multi-purpose device by modular design and component choices. The used torques in tapping screw tests were under 50 Nm, but the frame and servomotor were designed to carry load as far as 230 Nm. The modular design eases the use in other tests, because the device is convertible with the test requirements. There are certain interfaces in the frame, where is possible to build the fasteners for the components that the test needs. [32, p58-59]

The main components of the test device are servomotor, gearbox, flexible coupling, force and torque sensors, linear unit and test piece holder. These components are assembled to the frame plate so the components are accurately placed. The assembly of the test device is introduced in figure 27.

This device was used as the basis in the tests. The torque sensor was needed to replace the sensor with larger scale and the holder of test pieces had to rebuild for the tests. Also force sensor was added to the device.

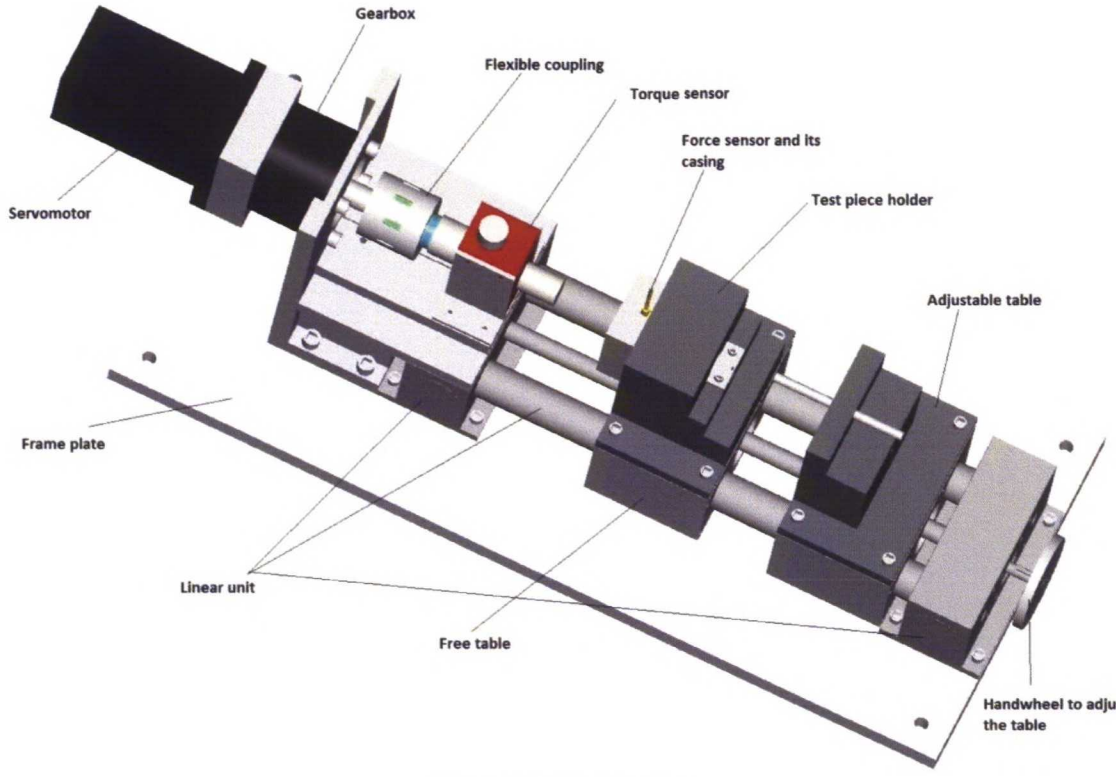

Figure 27. Test device.

The working principle of the device is simple. The torque produced by the servomotor is lead to the gearbox, which increases the torque to wanted level. The servomotor is controlled by frequency converter, which adjusts the speed of motor. The torque sensor is attached to gearbox output shaft with a flexible coupling to compensate possible angle errors of the shafts. There is a square drive socket attached in the output shaft of the torque sensor. The test joint is tightened with the torque that the socket transmits. The test joint is in the test piece holder and the force sensor is assembled in the test joint. The test piece holder is assembled on the free table, which can move freely along the linear guide. The adjustable table shall be adjusted next to free table thus the test joint is in correct placement. The function of the adjustable table is to prevent the movement of the free table during tightening.

The servomotor and the controlling drive are ABB's manufacturing. The servomotor is needed to produce the torque for the screw tightening. The drive controls the motor thus the rotating speed is constant and the motor stops in fault. The servomotor is from ABB's MS-series and the drive is from ABB's ACSM1-series. The specific model number of the servomotor is MS4815N4008E43C10 and the model number of the drive is ACSM1-04AS-09A5-4. The servomotor has an encoder feedback, where the drive gets the speed and torque signal to the motor controlling. The planetary gear is attached at the end of the motor to multiply the torque of the motor. The torque at the gearbox output is the used testing torque. In figure 28 can be seen the continuous torque (zone A) and the intermittent torque (zone B) of the servomotor at different rotating speeds. The rated rotating speed is 3000 rpm and the torque above that value decreases. The continuous torque is 4.8 Nm and the intermittent torque is 14.3 Nm. The test procedure is so short that it can be considered as intermittent and hence the intermittent values are used. The gear ratio of the gearbox is 20 thus the maximum achievable torque is 286 Nm. The needed maximum test torques were estimated to be between 100-150 Nm. [33]

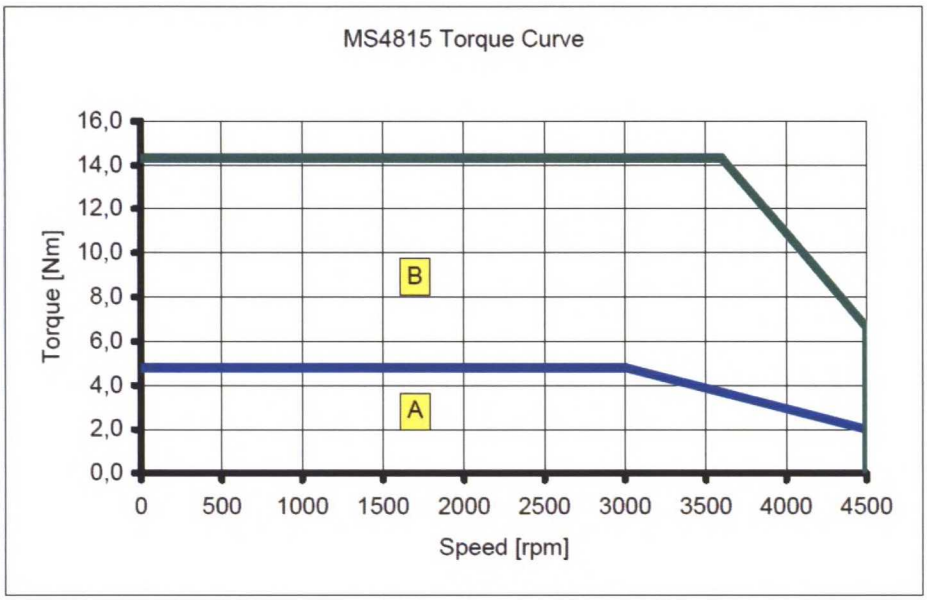

Figure 28. The produced torque of the servomotor at different rotating speeds. [33]

The drive was controlled by Drivestudio 1.5 -program. Drivestudio is ABB's control software for drives, when the drive is wanted to control by computer. The basic controls can be made with Drivestudio and the monitoring of the drive is real-time. Complex and automated drive maneuvers can't be done with Drivestudio so the control is always manual. [34]

There is assembled a flexible coupling on the output shaft of the gearbox. The purpose of coupling is to allow small assembly errors between the gearbox and the torque sensor. If the connection between the gearbox and the torque sensor is rigid, the misalignment in shaft lines causes extra loads to the shafts. Especially, the torque sensor shall not be loaded heavily with extra shaft loads.

The torque and force sensors are made by Futek. The torque sensor is Futek TRD605 non-contact square drive rotary torque sensor. The specific model number is FSH02031. With this sensor is possible to measure torques up to 250 Nm. The sensor has square drive connectors in the input and output so it is easy to attach with the help of square drive compatible accessories. A square drive socket was used directly in the output shaft to tighten the screw. [35]

Figure 29. Torque sensor. [35]

The torque sensor has an internal amplifier and connector to data logger. For this test was ordered Futek's own shielded cable and an USB data logging device. The data logging device model is Futek USB320. With the USB data logging device the data is possible to transfer easily to computer. When ordered the sensor and data logging device together, Futek calibrates the sensor, cable and data logging device as a one unit. This means that the announced errors are the total errors of the system. The data logging device is also compatible only with the calibrated sensor. [35]

The loading on the shafts of the sensor is limited as previous mentioned. The maximum axial load on the shaft is 2000 N and respectively the maximum radial load is 150 N. Because there is a flexible coupling on the input shaft, the loads are low and allowable. On the output shaft, the loads may occur during tightening because of placement errors. In this test, the axial movement was free so the only load was radial load caused by axial misalignment. The shaft lines were aligned in design and the placement of test piece is adjustable so the radial load is small. [35]

The force sensor is Futek LTH500 donut load cell with capacity to measure loads up to 66000 N. The sensor is supposed to assemble as a part of the joint, which is wanted to measure. In this test, the sensor was assembled between the plain washer and busbar. To avoid possible high surface pressures on the busbar surfaces, there were assembled a steel plate between the sensor and busbar. [36]

Figure 30. Force sensor. [36]

The force sensor was also ordered with USB data logging device. The sensor has the shielded signal cable assembled in the sensor so it is not needed to order separately. The data logging device model is Futek USB220 for the force sensor. The sensor and data logging device are calibrated together like the torque sensor. [36]

The sensors were controlled by computer with Futek's measurement software "Sensit Test and Measurement software 2.2". The software controls the sensor settings and collects the data. The data is possible to export to Excel for further processing.

The linear unit was not needed in this test, but it was already in device so it needed to taken into account in design. The linear unit was made by Rose-Krieger and it has two tables: free table and adjustable table. The free table is used for the test piece holder, because it is closer to the torque sensor. The problem is the table moves freely along the linear guide and it can slip away during tightening. For that reason, the adjustable table, which is on screw guide, is adjusted next to the free table thus the free table can't move away in the measuring. The adjustment of the table can be done by the hand wheel at other end of the unit. The linear unit has a torque limit of 230 Nm so the expected moments of the tests were lower and the use of the unit was safe. [36]

4.3 Test samples

The purpose of experimental tests was to understand the behavior of the self-clinching nut, when the joint is tightened and therefore the joint test was made. The most significant feature is how the self-clinching nut clamps with the busbar. If the nut is partially clamped, the nut may come loose during tightening. There was also performed torque out test for ABB self-clinching nut to define the torque out values for different manufacturing variations. The common failure type and the tightening torque level at failure were tried to find out with the torque out tests. Usually, the most common failure types have been screw failure, clamping failure of self-clinching nut or total failure of self-clinching nut. When the sample size is high enough, the most common failure type is possible to define. Also, it can be concluded the reasons to certain failure type from the results. In addition to previous matters, one target was also checking the suitability of VDI 2230 designing theory for self-clinching nut joints with the help of joint test.

The test samples were defined according to above-mentioned matters. The most interesting nut type to tests was ABB's own self-clinching nut, but also information about KALEI®- and PEM®-nuts were interesting. The ABB self-clinching nut had not been in extensive tests so it needed to test thoroughly. KALEI®- and PEM®-nuts had been tested by their manufacturers and there were some data about them so the test for these nuts was to examine the special requirements of busbar application.

There was needed to test many features from the ABB self-clinching nut to understand the clamping of the nut. The most significant features of the self-clinching nut in the point of view the clamping of the nut are the outside diameter of the nut collar, the hole diameter, where the nut is pressed, busbar material, screw size and the thickness of busbar. Also, the side where the nut is pressed to busbar is significant, because the busbars are punched and hence the die side has larger hole than the punch side. The chosen features for the test are introduced in table 3.

Table 3. Test variations for ABB self-clinching nut.

Busbar material	Copper	Aluminum
Screw size	M10	M12
Outside diameter of the nut	Upper tolerance level	Lower tolerance level
Assembly hole diameter	Nominal value + 0.1 mm	Nominal value - 0.1 mm
Material thickness	6 mm	10 mm
Assembly side	Punch side	Die side

The reasons to choose the above-mentioned features to the test were these features had been noticed in production to have an effect. The busbar materials were tin plated copper and tin plated aluminum as used in production. The screw sizes were chosen to match the most common sizes in busbar joints. The outside diameters of the collar of the self-clinching nut were divided in upper and lower tolerance level groups to describe the deviation of the production. The nominal diameters of the collar are 13.2 mm for M10 and 15.3 for M12 and the allowed tolerance for the diameter of collar is ±0.1 mm according to detail drawings. The hole diameters in busbar were chosen to show the effect of the hole diameter change near current instructed nominal value. The nominal assembly hole diameters are 13.1 mm for M10 and 15.2 for M12 according to the detail drawings. Busbar thicknesses were chosen to match the most common busbar thicknesses. Assembly sides were supposed to show the effect of assembly hole quality. When the nut is punched on die side in inaccurate hole, the torque out torque should be lower. Because of variation of the assembly hole and the collar diameter, there was needed for measurements before assembly of the nut.

The number of samples should be high, when wanted accurate data. The available amount of money, the accuracy of the test and available amount of time are the most restrictive factors. In this case the number of variables is 6, every variable has two levels and if the number of samples is 10, the total number of samples is $10*2^6 = 640$ pieces. This amount of samples is expensive to produce and time-consuming to test. For that reason it is sensible to use methods of design of experiments (DoE). There can be

made ½-factorial tests instead of full factorial tests to decrease the total number of samples. The introduction to DoE and the actual test matrix for ABB self-clinching nut is presented later.

KALEI®- and PEM®-nuts were not tested so deeply. The assembly of nuts was made during the nut manufacturer's guidelines thus the variable factors were busbar material, screw size and material thickness. The DoE-analysis was not performed for KALEI®- and PEM®-nuts, because of low number of variables. The quality of KALEI®- and PEM®-nuts was estimated high so the measurements of the nuts were not performed.

The number of samples in the tests was chosen to be 10 per test for ABB self-clinching nuts in torque out test and 5 per test in joint test. The KALEI®- and PEM®-nuts were better known so 10 samples per test was decided to be adequate number of samples, because only the joint test was carried out.

The outside geometry of test pieces was defined by the requirements of the equipment. The outside diameter of force sensor was about 75 mm and hence the dimensions of the test piece were good to be larger than that value. The dimensions of test pieces 80 mm x 80 mm were selected, because 80 mm is one standard busbar width and easy to manufacture. On the other hand, larger test piece would have been difficult to fasten in the test device. Only exception about test pieces was test pieces of 6 mm aluminum. There was not available aluminum 80 mm x 6 mm busbar so the aluminum 60 mm x 6 mm busbar was estimated to be adequate for these test pieces. Some test pieces are introduced in figure 31.

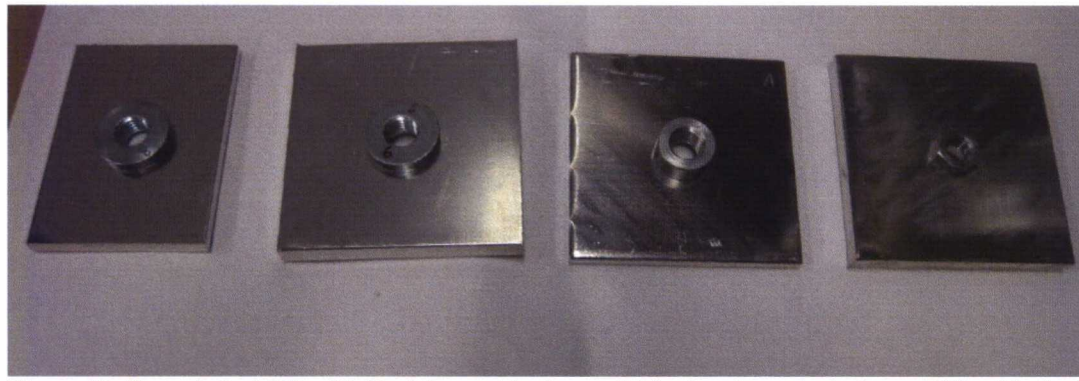

Figure 31. From left: ABB self-clinching nut in 6 mm thick aluminum test piece, ABB self-clinching nut in 10 mm thick test piece, PEM®-nut in 6 mm thick test piece and KALEI®-nut in 10 mm thick test piece.

The samples are manufactured by one supplier with normal production quality. The quality of punched hole was supervised by measuring the first and last of the batch and randomly three pieces in the batch. The outside diameter of ABB self-clinching nut was ordered to measure from every nut that was assembled. The measurements were performed with slide gage by measuring the feature in three spots and calculating the average value.

4.4 Design of experiments

Design of experiments contains a range of experimental techniques, which help to measure a certain process in a controlled manner and to analyze the results. The purposes of techniques are to identify the critical inputs and to understand their affect on

the process. There are several special methods as Response surface and Taguchi to handle the results. [38, p191]

This case corresponds well 2^k-factor experiments. It is a special case of variance analysis, where is many factors, which have only two levels: high (+) and low (-). The values of the factors affect on the average values of the output. The statistical model of 2^k-factor experiment contains k pcs main effects, $\binom{k}{2}$ pcs interaction effects of two factors, $\binom{k}{3}$ pcs interaction effects of three factors etc. Usually the main effects are the most significant factors, but sometimes the interaction effects of two factors can be significant. The interaction effects of three or more factors are normally not significant, because the significance decreases the more factors there are in the interaction effect. In table 4 is introduced an example from 2^3-factor experiment. There is marked all main factors and one interaction effect of two factors. The rows describe one test run and there is marked an example output value from the test. The interaction factor gets its value by multiplying the values of interactive factors. [39, p234-235]

Table 4. Example from 2^3-factor experiment.

	Factors				
	A	B	C	A*B	Output
1	-1	-1	-1	1	12.85
a	1	-1	-1	-1	13.01
b	-1	1	-1	-1	14.52
ab	1	1	-1	1	14.71
c	-1	-1	1	1	12.93
ac	1	-1	1	-1	13.09
bc	-1	1	1	-1	14.61
abc	1	1	1	1	14.81

The certain main and interactive effect of the factors in 2^k-factor experiment can be estimated by equation [39, p235]

$$X = \frac{(a\pm1)(b\pm1)\cdots(k\pm1)}{n\cdot 2^{k-1}} \tag{45}$$

Where a, b…k are the sum of observation values of the factor that act in the certain effect. If the factor act in the run, the factor the sign is (-), otherwise (+). In equation 45 n is the number of the iterations and k under the division sign is the number of factors.

Because the main and interactive effects are orthogonal contrasts, the corresponding sums of squares can be calculated with equation [39, p236]

$$SSX = n \cdot 2^{k-2} \cdot X^2 \tag{46}$$

The sum of squares for all observations is [39, p237]

$$SST = \sum_{i=1}^{2}\sum_{j=1}^{2}\cdots\sum_{k=1}^{2}\sum_{l=1}^{n} y_{lij\cdots k}^2 - \frac{1}{n\cdot 2^k}T^2 \tag{47}$$

Where $y_{lij..k}$ is the observation value of the certain run and T is the sum of all observation values.

The residual sum of squares describes the internal deviation in the group. It can be considered as the error of the analysis. The residual sum of squares can be expressed [39, p237]

$$SSE = \sum_{i=1}^{2}\sum_{j=2}^{2}\cdots\sum_{k=1}^{2}\sum_{l=1}^{n}\left(y_{lij\cdots k} - \frac{1}{n}\sum_{l=1}^{n} y_{lij\cdots k}\right)^2 \quad (48)$$

It is also noticeable that all the sums of squares satisfy variance analysis composition so [39, p237]

$$SST = SSA + SSB + \cdots + SSAB + SSAC + \cdots + SSABC + \cdots + SSAB \ldots K + SSE \quad (49)$$

The null hypothesis shall be formed to see, if the certain factor has an effect on the process. For factor X, the null hypothesis is form: H_X: No X effect. For testing the null hypothesis, shall be calculated the test variable [39, p248]

$$F_X = 2^k(n-1)\frac{SSX}{SSE} \quad (50)$$

Which follow the F-deviation with degrees of freedom (1, 2^k(n-1)). If the test variable is large, the null hypothesis shall be rejected and the effect of the factor is large.

A response surface model can be formed from the data to represent results in graph. The response surface model is polynomial function either linear or higher degree. The linear model is assumed to be adequate in this case. The linear response surface model can be expressed [39, p247]

$$\hat{y} = \bar{y} + \left(\frac{a_+ + a_-}{2}\right)A + \left(\frac{b_+ + b_-}{2}\right)B + \left(\frac{ab_+ + ab_-}{2}\right)AB + \cdots + \varepsilon_e \quad (51)$$

Where $\bar{y}$ is arithmetic average of observation values and ε_e is the random error, which can contain also insignificant multifactor interaction effects. The variables a, b…k are the sum of observation values of the factor, when the factor is high with subscript (+) and with subscript (-), when the factor is low.

Fractional factorial experiments can be done to reduce the number of test runs. The ½-fractional or 2^{k-1} factor test is used in this case to halve the needed number of runs. When doing fractional factor experiments, the resolution of test decreases, because some higher degree multifactor interaction effects are confounded with main effects or other multifactor interaction effects. Because of confounding the results do not give exact effect of a certain factor. The higher degree multifactor interaction effects are not significant so the results give the effects of the main factors with adequate accuracy. If the more accurate results are needed, the most significant factors shall be examined with a new full factorial experiment. [39, p321-323]

The experiment matrix for ½-fractional experiments can be formed from corresponding full factorial experiment matrix. When the full factorial experiment matrix is formed, the sign of the interaction effect of all (ABC…K) factors is defined. The sign of the interaction effect is (+) for half of the runs and (-) for other half. The ½-factorial experiment matrix is the matrix, where the sign of the interaction effect ABC…K is either (+) or (-). When defining the experiment matrix with this method, the interaction

effect ABC…K is excluded from the results. The matrix shall be formed with extra factor, which equals the interaction effect ABC…K, if that interaction effect is significant and results are needed. [39, p324-325]

The test matrix in this experiment for ABB self-clinching nut is described in table 5. The coded factors are: A is busbar material, B is busbar thickness, C is assembly hole diameter, D is assembly side, E is tolerance level and F is screw size.

Table 5. The test matrix for 6 factor 1/2-fractional experiment.

	A	B	C	D	E	F	ABCDEF
1	1	1	1	1	1	1	1
2	1	1	1	1	-1	-1	1
3	1	1	1	-1	1	-1	1
4	1	1	-1	1	1	-1	1
5	1	-1	1	1	1	-1	1
6	-1	1	1	1	1	-1	1
7	1	1	1	-1	-1	1	1
8	1	1	-1	1	-1	1	1
9	1	-1	1	1	-1	1	1
10	-1	1	1	1	-1	1	1
11	1	1	-1	-1	1	1	1
12	1	-1	1	-1	1	1	1
13	-1	1	1	-1	1	1	1
14	1	-1	-1	1	1	1	1
15	-1	1	-1	1	1	1	1
16	-1	-1	1	1	1	1	1
17	-1	-1	-1	-1	-1	-1	1
18	-1	-1	-1	-1	1	1	1
19	-1	-1	-1	1	-1	1	1
20	-1	-1	1	-1	-1	1	1
21	-1	1	-1	-1	-1	1	1
22	1	-1	-1	-1	-1	1	1
23	-1	-1	-1	1	1	-1	1
24	-1	-1	1	-1	1	-1	1
25	-1	1	-1	-1	1	-1	1
26	1	-1	-1	-1	1	-1	1
27	-1	-1	1	1	-1	-1	1
28	-1	1	-1	1	-1	-1	1
29	1	-1	-1	1	-1	-1	1
30	-1	1	1	-1	-1	-1	1
31	1	-1	1	-1	-1	-1	1
32	1	1	-1	-1	-1	-1	1

The final analyze of the results was done with Minitab 16. Minitab is computer software for analyzing the DoE data. The results were collected in Excel-file, which was used input to Minitab. Minitab calculated the effects of factors and formed the graphs about them.

The DoE calculation was set by starting the Minitab DoE-tool from path Stat -> DOE -> Factorial -> Create Factorial Design. The design settings were set as described in figure 32. There was set 6 factor 2-level factorial design in the first window, then ½-fraction

design with 10 replications in the second window. Next, the factors were named and the upper and lower levels were announced.

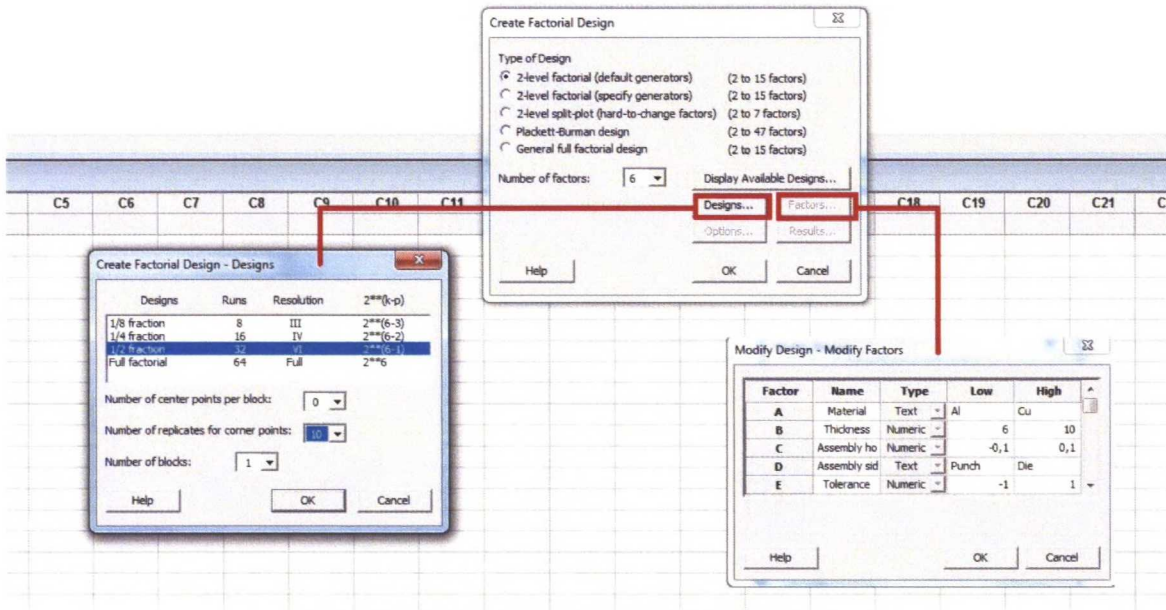

Figure 32. Setting the design setup of analysis.

When the measurements were done, there was added a column, where were the results of the samples. Then the analysis settings were set from path Stat -> DOE -> Factorial -> Analyze Factorial Design. The settings were added as presented in figure 33. The factors to analysis and to prediction calculation were set and wanted graphs for results were chosen. After the settings were set, the design was ready to run.

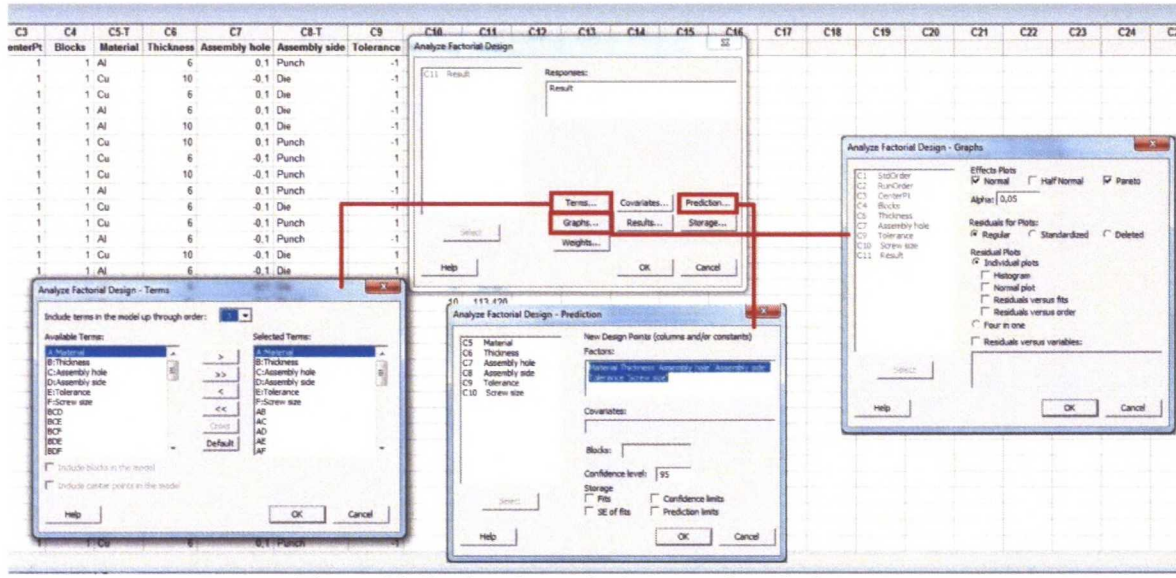

Figure 33. Setting the analysis setup of analysis.

4.5 Testing plan

The purpose of experiments was to determine the torque out values and the preload force during tightening in the joint test. The failure type was also observed to find out

possible systematic failure types in both tests. The effects of variable factors can be estimated from the breaking torque values and the failure type. The preload force was measured to see the amount of preload with different tightening torques.

The torque out test for ABB self-clinching nut was performed according to the PennEngineering's test method. There were used two plain washers between nut and screw head to prevent the neck of screw touching the nut thread. The tightening torque was measured during tightening.

The driving speed of the test was determined to be 25 rpm, because the tightening was wanted to be smooth. The joints of this size are tightened in production by hands with torque wrench and by bolt driving gun. Bolt guns may have high rotation speeds, over 1000 rpm, and the test doesn't describe this kind of tightening well. To get more accurate results, the determined driving speed is better, because the tightening is better under control. The determined driving speed was set in the drive before the tests. Torque limit was also set in the drive to avoid overloading of the tester.

The settings of force and torque sensors were set before the tests in the controlling software Sensit. Most of the settings were left as default, but the measuring mode, units, sampling rate and reading type were adjusted. The measuring mode was selected to Trakcing mode and the sampling rate to 60 SPS. The sampling rate means, that with driving speed 25 rpm, there is taken 60 samples in about 120 degree of turning. The units were selected to N for force sensor and Nm for torque sensor. The reading types of both sensors were set to Tare from selection Tare/Gross to minimize the possible systematic error of sensor.

Before starting the measuring, the test joint is assembled in the test piece holder in the joint test. For the test joint is needed busbar, where is assembled self-clinching nut, busbar with clearance hole, screw, plain washer and spring washer. The force sensor was also assembled in the joint. In figure 34 is showed the test piece assembly. The screw was lightly tightened by fingers thus there were not any gaps between the parts.

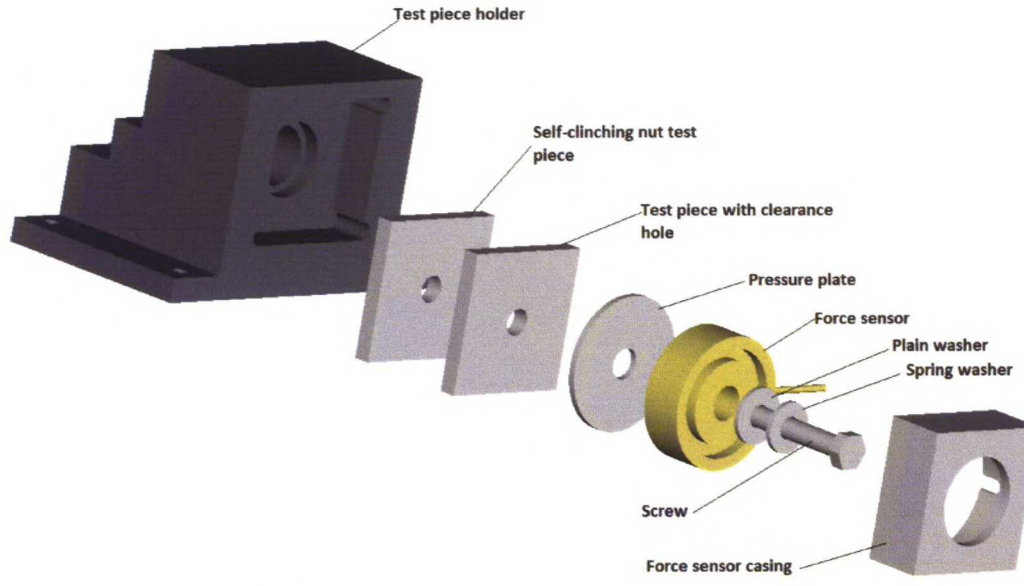

Figure 34. Test piece assembly in joint test.

When the test assembly was assembled in test piece holder and the settings of the drive and the sensors were set, the tables of the linear unit were adjusted thus the socket of torque sensor met the screw. The free table was adjusted so it was not able to slide away, but it allowed a little translation. After these actions, the joint was ready to measuring. The drive was started and the joint was tightened until joint failed.

In torque out test, the setup was similar, but there was not used force sensor and only self-clinching nut test piece was put in the test piece holder. The test method was similar to the method described in chapter 2.3.2.

The test procedure was planned to have constant steps. The steps for one test sample were following:

1. Assemble the test piece/joint and place it to the test piece holder.
2. Adjust the tables of the linear unit in right positions.
3. Create the new data logging file and check the settings of the sensors.
4. Start the logging in Sensit Test and Measurement Software.
5. Start the servomotor in the Drive Studio software.
6. Stop the motor when the test piece/joint is broken.
7. Remove the test piece/joint from the test piece holder.
8. Observe and record the failure type of the test piece/joint.
9. Check the measured values are recorded in the data logging file and save file.

Above-mentioned steps were repeated until the test series was finished. The collected data from ABB self-clinching nut was analyzed with DoE-methods and the data from PEM®- and KALEI®-nuts as it were.

4.6 Error analysis

Every measuring result is an approximation from the true value, because measuring devices are not always accurate enough. The test setup or operating conditions may also cause errors in the results. Sometimes the cause of error may be unknown. The error of measurement shall be taken into account when evaluating the results. The error can be expressed simply by subtracting the true value from the measured value. [40, p93-94]

The error may be unpredictable, but nevertheless the uncertainty of measurement is possible to estimate. The uncertainty of measurement is an estimate of the limits of the error in the measurement with certain level of confidence. The appeared errors can generally be divided in two categories: systematic errors and random errors. Systematic errors appear always the same way, when the test is repeated with the same test setup. The systematic error is caused by calibration error of measuring device, non-linearity of measuring device or other consistent error of test setup. The systematic error is not possible to detect with statistical analysis, because it repeats similarly every time. That is why the systematic error shall be estimated or measured before measurements. The systematic error can be calculated by subtracting the average value of measuring results from the true value. [40, p93-94]

Random errors appear randomly during the measurement and they can't be repeated reliably. The random error is usually caused by temporary change in the operating conditions or error of the experimenter. Random errors are possible to analyze with

statistical analysis. Random error for certain measuring result can be calculated by subtracting the average value of measuring results from the certain measuring result. [40, p94]

In figure 35 is presented the effects of systematic and random errors to the results. There is known the true value in the case that is presented in the figure. When the true value is unknown as usual in the research, the interpretation of the results is more difficult and the errors of the measurement shall be estimated correctly.

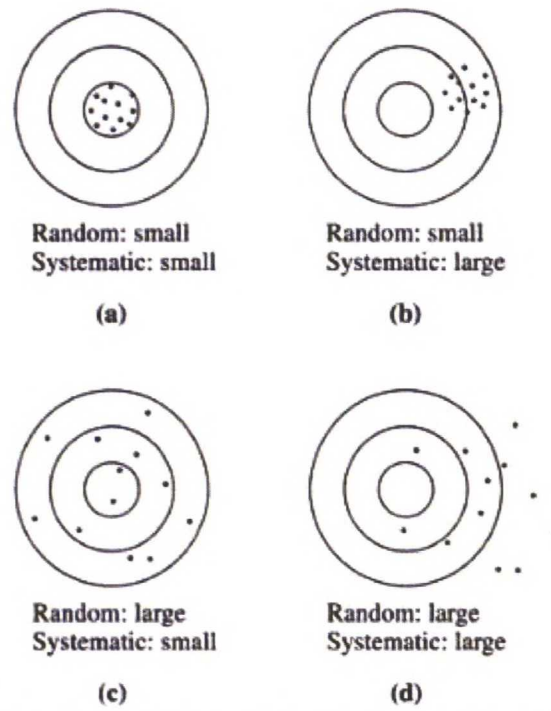

Figure 35. Effects of systematic and random errors to the results. [40, p95]

The systematic error and the random error shall be calculated to calculate the uncertainty of measuring. The uncertainty of measuring can be expressed [39]

$$W_{\bar{y}} = \sqrt{B_{\bar{y}}^2 + P_{\bar{y}}^2} \tag{52}$$

where B_y is the systematic error and P_y is the random error.

The systematic error can be estimated from the calibration sertificates of sensors and other error sources. The random error can be estimated from the results with the help of Student's t-distribution. The random error can be calculated at certain confidence level, when the variable y is measured n times with equation [39, p35][41, p259]

$$P_{\bar{y}} = \pm t \frac{S}{\sqrt{n}} \tag{53}$$

where t is t-variable at certain confidence level with degrees of freedom (n-1) and n is the number of samples. T-variables are tabulated and they can be found e.g. from reference 41. S is the sample standard deviation and it is [39, p31][41, p259]

$$S = \sqrt{\frac{\sum_{i=1}^{n}(y_i - \bar{y})^2}{n-1}} = \sqrt{\frac{\sum_{i=1}^{n}\left(y_i - \frac{\sum_{i=1}^{n} y_i}{n}\right)^2}{n-1}} \quad (54)$$

where y_i is the measured value.

The number of error sources was low, because the measuring setup was simple. The most probable error sources were the sensors. The other error source was misalignment between the joint axis and the axis of torque sensor. The misalignment causes more friction resistance between the socket of torque sensor and the washers. This misalignment was eliminated by designing the fastening of test pieces thus the test piece holder provided adequate support. Also the misalignment of the force sensor was eliminated with the casing of sensor. With these actions, the misalignment of axes was small. The fastening of the socket had a little clearance, which compensated small misalignments.

The error from the sensors contains a few categories. The nonlinearity error describes the nonlinear function of the sensor. The torque sensor TRD605 has nonlinearity error ±0.2 % of rated output value. Correspondingly the force sensor LTH500 has nonlinearity error ±0.5 % of rated output value. Also the used data logger has a nonlinearity error and for USB220 and USB320 data loggers the nonlinearity error is 0.001 % of full scale range. As previously mentioned the sensor, cable and data logger are calibrated together. According to Futek's calibration certificate, the nonlinearity errors of sensor, cable and data logger are included in max system error value. The max system error value is largest error occurred during calibration. The max system error of the torque sensor is ±0.12 % of rated output value depending on the rotation direction and the error of force sensor is -0.027 % of rated output value. The calibration certificate announces also max system error tolerance value, which is the maximum allowed system error. For torque sensor the max system error tolerance is ±0.4 % and for force sensor it is ±1 %.

The sensors have a hysteresis error, which is not included to the max system error. The hysteresis causes different output from the same measurement depending on if the measurand is increasing or decreasing, when the output value is reached. The hysteresis can be caused by friction, flexibility of the structure of the sensor or electrical capacitance. The hysteresis error of the torque sensor is ±0.1 % of rated output value. For the force sensor the hysteresis error is ±0.5 % of rated output value. The hysteresis error is systematic error if the test setup is constant and the hysteresis is repeatable. There may randomly occur temporary peak values due to inconstant thread quality or material during the measuring in this test setup. Hence, the hysteresis error was considered as random error.

The resolution of sensor is one error source. Resolution with analogue displays is half of the gauge length in the scale. With digital displays the resolution is the value of 1 in the least significant digit, which is the last digit of the value. If the display rounds the value, the resolution is ±0.5 in the least significant digit. In this test setup the resolution depended on the resolution of the data logger. USB220 and USB320 data loggers can record the measured value with 16 decimal places. The resolution is so accurate compared to other error sources the error from the resolution is insignificant and it is not taken into account.

The temperature can affect to measuring results, if the temperature changes during measuring or the measuring temperature is higher than specified temperature of the sensor. Both sensors have compensated temperature limits wherein the affects of temperature are compensated. The limits of compensated temperature are for torque sensor from +5°C to +50°C and for force sensor from +15°C to +72°C. The measurements were performed in temperature between above-mentioned limits so the error from temperature is ignored.

In summary, the used error values for systematic error of sensors are for torque sensor ±0.4 %, which means 1 Nm and for force sensor ±1 %, which means 660 N. When sensors are working normally, the above-mentioned values are the maximum errors.

5 Results

5.1 Calculations according to VDI 2230

One aim of this work was to check the suitability of VDI 2230 design guidelines for joints with self-clinching insert. Next is introduced the results of calculations according to VDI 2230. The calculation was carried out for corresponding joints that were tested joints. The self-clinching insert do not change a lot the calculation compared to regular through bolted joint. The only significant change is in the surface pressure calculation, where the smaller bearing area of self-clinching insert shall be taken into account.

The material properties and thread dimensions of screw and nut were needed for calculations. Screw data is easy to get because standard screws were used. The screw and nut data is from standard ISO 4017 and screw manufacturer. The used fastener data in calculations is introduced in table 6.

Table 6. Dimensions of fastener elements. Reference announced in brackets.

Busbar		
lxb (mm)	80x80 (except 6mm Al 60x80)	
t (mm)	6 or 10	
d_h (mm)	11 (M10)	13.5 (M12)
Screw	**M10**	**M12**
P (mm)	1.5 [6]	1.75 [6]
d_w (mm)	14.63 [6]	16.63 [6]
S (mm)	17 [6]	19 [6]
d_{min} (mm)	9.732 [42]	11.701 [42]
d_2 (mm)	8.994 [42]	10.829 [42]
d_0 (mm)	8.16 [5]	9.855 [5]
Nut		
D_1 (mm)	8.376 [42]	10.106 [42]
D_2 (mm)	9.026 [42]	10.863 [42]
D_{2max} (mm)	9.206 [42]	11.063 [42]
Plain washer		
h_s (mm)	2.5 [43]	3 [43]
Spring washer		
h_{sw} (mm)	2.5 [43]	3 [43]
D_{sw} (mm)	10.5 [43]	13 [43]
ABB-nut		
d_{wa} (mm)	26	26
d_{ha} (mm)	13	15.1
PEM		
d_{wa} (mm)	17.35 [11]	20.55 [11]
d_{ha} (mm)	14 [11]	17 [11]
KALEI		
d_{wa} (mm)	15 [13]	17 [13]
d_{ha} (mm)	12.5 [13]	14.5 [13]

Material data is needed for busbar material and plating to calculate the joint properties. Busbar material used in power electronics is copper Cu-OF or Cu-ETP and aluminum EN AW 6101A T6. The material properties of Cu-OF and Cu-ETP are very similar so they are introduced as one. The plating is 8 µm thick tin layer. Aluminum busbar has also 2-3 µm interfacial layer of nickel or copper. The interfacial layer affects to contact resistance, but the effect was estimated to be small so it is ignored in calculation. The material properties of joint elements are introduced in table 7.

Table 7. Material properties of joint elements.

Screw	**Steel**		
R_m (MPa)	800 [42]		
R_{p02} (MPa)	640 [42]		
$T_{BM/BS}$ (MPa)	600 [5]		
E (GPa)	200 [5]		
α_S (1/K)	$11.1*10^{-6}$ [5]		
Busbar and plating	**Copper**	**Aluminum**	**Tin**
α_P (1/K)	$16.8*10^{-6}$ [44]	$23*10^{-6}$ [45]	
p_{max} (MPa)	200 [44]	200 [45]	
E (GPa)	130 [44]	70 [45]	
ρ (Ωm)	$1.7*10^{-8}$ [44]	$3.05*10^{-8}$ [45]	$11.6*10^{-8}$ [25]
H (MPa)			50 [25]

The calculations were performed as described in chapter 2.4. Also the calculation of contact resistance from chapter 3.2.2 was carried out. The tightening torque used in calculations was from ABB's design guideline. There was used tightening torques according to the guideline in calculations. The calculation does not take into account the shape of the self-clinching insert and hence the joint properties are the same for all inserts except for the surface pressure.

The calculated values are in room temperature unless the surface pressure, which is calculated in the highest operating temperature, and the contact resistance, which is calculated in the lowest operating temperature. The reason to use the above-mentioned manner is to calculate the highest values of surface pressure and contact resistance. Surface pressure is the largest in high temperature, when preload is high, and contact resistance is the largest in low temperature, when preload is low. The operating temperature was estimated to be from -40°C to+100°C. The Young's modulus changes due to temperature change. According to Deutsches Kupferinstitut, the Young's modulus of copper is 134 GPa at -40 °C and 125 GPa at +100 °C [44]. For aluminum, there was not available corresponding data so the values were estimated from data of copper. The estimated values were 74 GPa at -40 °C and 65 GPa at +100 °C. The change of Young's modulus is so small between these temperatures that the total error is not significant, although the estimation error can be even 1-2 GPa. The Young's modulus for screw material is according to VDI 2230 205 GPa at -40 °C and 190 GPa at +100 °C [5].

The surface roughness of busbar is needed to know for contact resistance calculation. The used value 0.65 µm is the average value of surface roughnesses of plated busbars from the quality control measurements of production. There is sliding contacts in the joint and friction coefficients were needed. The sliding contacts were assumed to be in thread and between screw head and washer. The friction coefficients were estimated to be the same for thread and between screw head and washer. The friction coefficient can

be from 0.125 to 0.45 according to VDI 2230, because the contacts are dry steel-steel – type [5].

When calculating preload forces by certain tightening torque, the result depends on the friction coefficient. In figure 36 is presented the preload-tightening torque graphs with different friction coefficients for joints with screw size M10 and M12. The preload values are the assembly preloads, which does not take into account the embedding. The curves end in different spots in the figure, because only the points, which are at safe distance from the yield strength of the screw, are drawn in the graph. According to VDI 2230 the maximum allowed utilization factor of yield strength is 0.9 [5]. The actual tightening torques at 90 % of the yield strength of the screw with different friction coefficients are introduced in table 8.

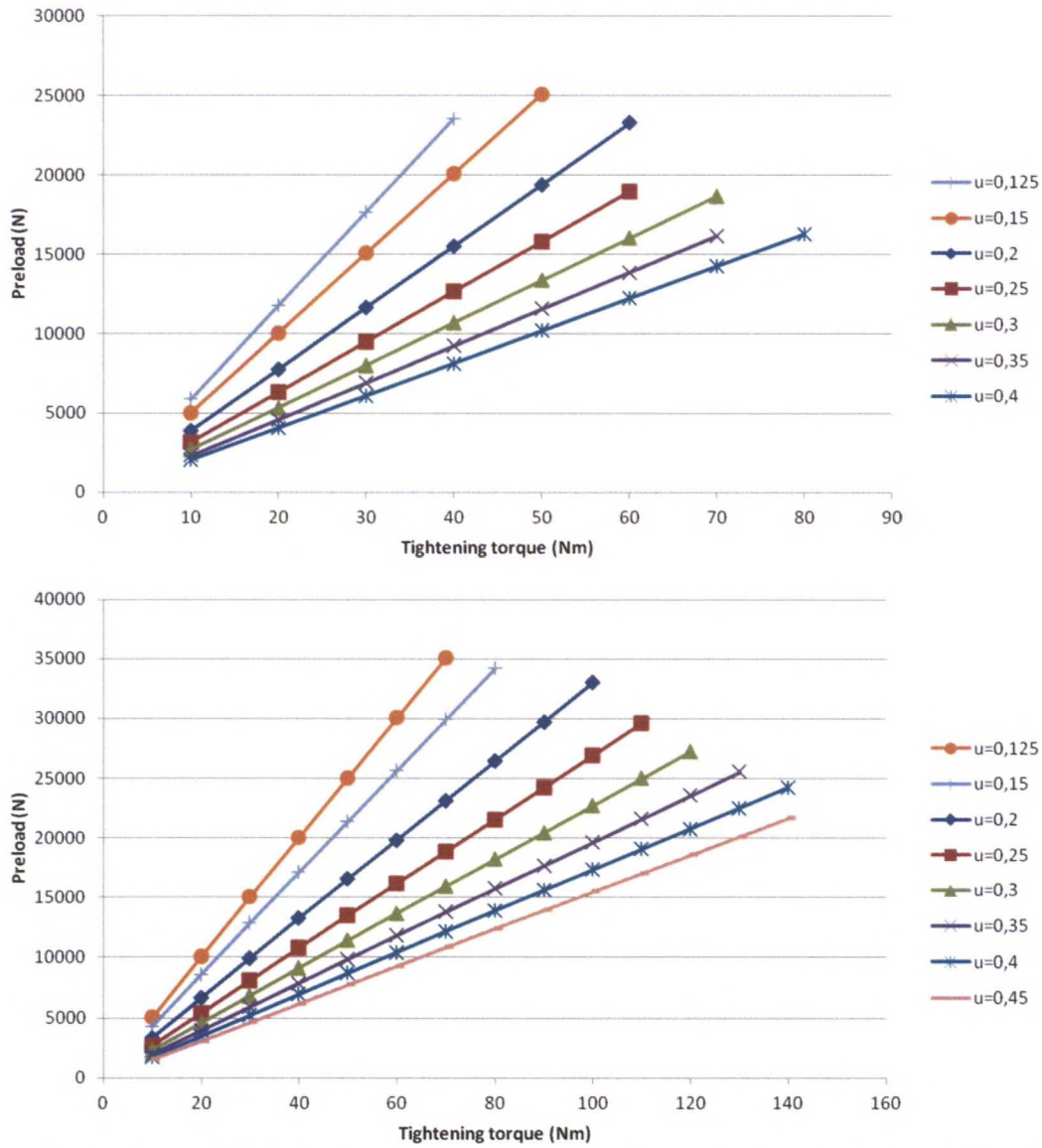

Figure 36. Preload-tightening torque graphs with different friction coefficients according to VDI2230. M10 above graph and M12 below.

Table 8. Tightening torques at 90 % of the yield strength of the screw.

	Tightening torque at $0.9*R_{p0.2}$ (Nm)	
Friction coefficient	**M10**	**M12**
0.125	44	76
0.15	50	86
0.2	59	103
0.25	67	116
0.3	73	127
0.35	78	136
0.4	82	142
0.45	85	148

Next, it is calculated the main joint properties for M10 and M12 joints with different friction coefficients. The used tightening torque is from ABB's production guideline. From tables 9, 10, 11 and 12 can be seen the effect of the friction coefficient to the joint properties.

Table 9. The calculation results for 6 mm copper bar samples.

Cu 6mm	**M10 (μ=0.125)**	**M10 (μ=0.3)**	**M10 (μ=0.45)**	**M12 (μ=0.125)**	**M12 (μ=0.3)**	**M12 (μ=0.45)**
M_V (Nm)	40	40	40	70	70	70
F_M (kN)	23.9	10.9	7.4	35.2	16.0	10.9
Utilization factor	0.82	0.49	0.43	0.83	0.50	0.43
F_Z (N)	1150	1150	1150	1360	1360	1360
Thread torque (Nm)	21.2	19.5	19.1	37.4	34.5	33.7
m_{eff} (mm)	4.2	4.2	4.2	5.3	5.3	5.3
p (MPa) **ABB**	60.0	28.5	20.2	100.2	47.5	33.6
p (MPa) **PEM**	289.8	137.7	97.7	336.6	159.5	113.1
p (MPa) **KALEI**	442.7	210.3	149.2	569.8	270	191.4
R_c (μΩ)	2.8	4.6	6.1	2.3	3.7	4.8

Table 10. The calculation results for 10 mm copper bar samples.

Cu 10mm	**M10 (μ=0.125)**	**M10 (μ=0.3)**	**M10 (μ=0.45)**	**M12 (μ=0.125)**	**M12 (μ=0.3)**	**M12 (μ=0.45)**
M_V (Nm)	40	40	40	70	70	70
F_M (kN)	23.9	10.9	7.4	35.2	16.0	10.9
Utilization factor	0.82	0.49	0.43	0.83	0.50	0.43
F_Z (N)	1050	1050	1050	1230	1230	1230
Thread torque (Nm)	21.2	19.5	19.1	37.4	34.5	33.7
m_{eff} (mm)	4.2	4.2	4.2	5.3	5.3	5.3
p (MPa) **ABB**	60.9	29.7	21.4	101.3	49.2	35.4
p (MPa) **PEM**	293.9	143.4	103.4	340.4	165.2	118.8
p (MPa) **KALEI**	449	219	158	576.2	279.6	201.1
R_c (μΩ)	2.8	4.6	6.2	2.3	3.7	4.9

Table 11. The calculation results for 6 mm aluminum bar samples.

Al 6mm	M10 (μ=0.125)	M10 (μ=0.3)	M10 (μ=0.45)	M12 (μ=0.125)	M12 (μ=0.3)	M12 (μ=0.45)
M_V (Nm)	40	40	40	70	70	70
F_M (kN)	23.9	10.9	7.4	35.2	16.0	10.9
Utilization factor	0.82	0.49	0.43	0.83	0.50	0.43
F_Z (N)	960	960	960	1090	1090	1090
Thread torque (Nm)	21.2	19.5	19.1	37.4	34.5	33.7
m_{eff} (mm)	4.2	4.2	4.2	5.3	5.3	5.3
p (MPa) **ABB**	63.5	32.6	24.4	104.4	52.9	39.3
p (MPa) **PEM**	306.5	157.5	118	350.9	177.8	132
p (MPa) **KALEI**	468.2	240.6	180.2	593.9	301	223.4
R_c (μΩ)	4.0	6.9	9.6	3.3	5.4	7.3

Table 12. The calculation results for 10 mm aluminum bar samples.

Al 10mm	M10 (μ=0.125)	M10 (μ=0.3)	M10 (μ=0.45)	M12 (μ=0.125)	M12 (μ=0.3)	M12 (μ=0.45)
M_V (Nm)	40	40	40	70	70	70
F_M (kN)	23.9	10.9	7.4	35.2	16.0	10.9
Utilization factor	0.82	0.49	0.43	0.83	0.50	0.43
F_Z (N)	893	893	893	1038	1038	1038
Thread torque (Nm)	21.2	19.5	19.1	37.4	34.5	33.7
m_{eff} (mm)	4.2	4.2	4.2	5.3	5.3	5.3
p (MPa) **ABB**	65.6	34.7	26.5	107.5	55.9	42.3
p (MPa) **PEM**	316.6	167.5	127.9	361.1	187.9	142.1
p (MPa) **KALEI**	483.6	255.8	195.4	611.3	318.1	240.5
R_c (μΩ)	4.1	7.1	10.5	3.3	5.6	7.8

5.2 Torque out test

Torque out test was performed with ABB self-clinching nut. The used test method was similar to PennEngineering's method that was introduced in chapter 2.3.2 and the results were handled with the help of DoE-methods.

The assembly hole for self-clinching nut and the collar of self-clinching nut were measured by supplier to supervise the quality and to track deviant measuring results. It turned out that the quality of punched hole was nearly constant. The difference between wanted assembly hole diameter and actual diameter value, which means systematic error, was about ±0.03 mm and the deviation among one set was about ±0.01 mm. The largest measured error among all samples was 0.08 mm. Also the quality of self-clinching nuts was good. The difference between the largest and the smallest measured diameters was 0.07 mm for both screw sizes. It turned out that the self-clinching nuts were very difficult to divide in two tolerance categories. Only single samples of M10 self-clinching nuts had the diameter of collar under the nominal value marked in drawing. Respectively, only a few of the M12 self-clinching nuts had the diameter of collar over the nominal value marked in drawing. Most of the self-clinching nuts had the diameter of collar at the distance of 0.03 mm from the nominal value. Most of the

sample sets had correct tolerance level, but in some sets there was no difference of tolerance level. The lack of tolerance difference causes that the significance of effect of tolerance level is not reliable result, but it describes roughly the direction of effect.

Figure 37 presents the measured torque during the test of one test sample. The blue curve is the tracking value of the torque during the test, the red curve presents the highest measured torque and the green curve is the lowest measured torque. The graph can be divided in three sections according to the phases of measuring. The part 1, marked in figure 37, presents the situation when the data logging is on but the motor has not started yet or the screw can freely rotate a few rounds. The tightening of screw occurs in part 2 of the graph. In part 3 of the graph, the self-clinching nut fails and starts to rotate. The torque out value for the test sample is the highest measured torque during the test.

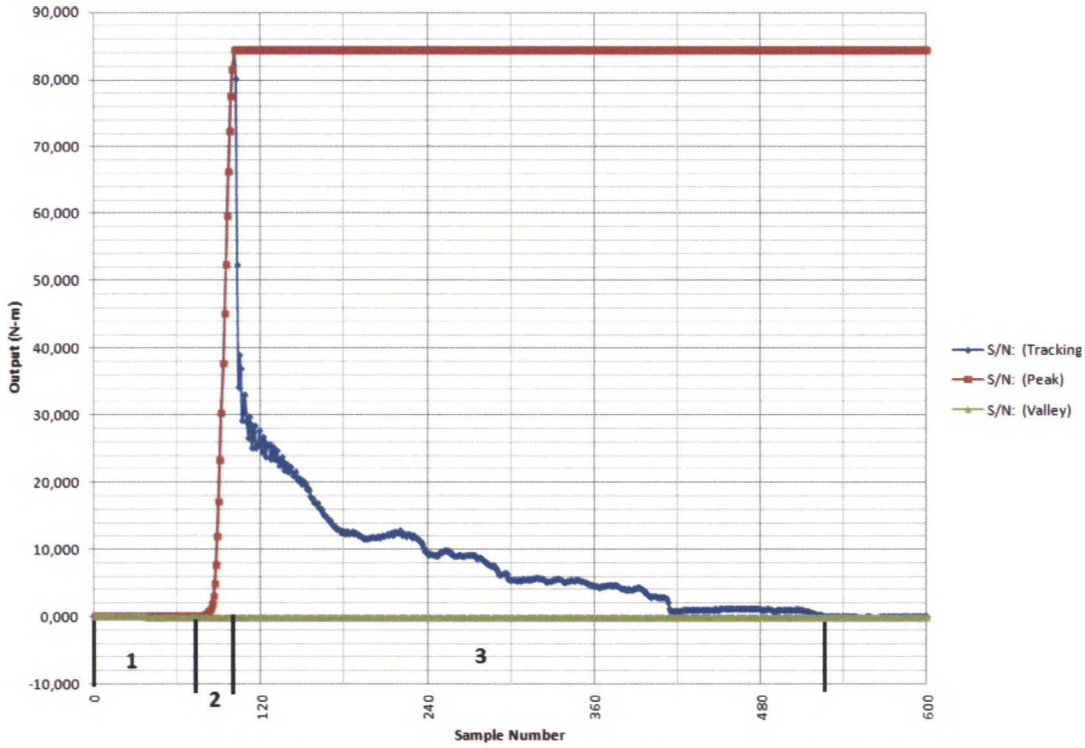

Figure 37. Data logging graph of one test sample in torque out test.

The results of torque out test for 6 mm copper bar with screw size M10 are introduced in table 13. The results of all samples can be found in appendix A. There were many screw failures in these samples. The samples, where the nut was assembled on die side in a large hole, were the only samples, where all self-clinching nuts failed. About half of the samples, where the nut was assembled on punch side in a large hole failed, because the nut started to rotate. Respectively, only one piece of the samples, where the nut was assembled on die side in a small hole failed, because the nut started to rotate. All other samples failed, because the screw failed. In addition, the screw was not able to rotate by fingers in all samples, where the nut was assembled on punch side in a small hole and in some samples, where the nut was assembled on die side in a small hole.

Table 13. Results of torque out test 6 mm copper bar, screw size M10 test samples.

Assembly hole, assembly side and tolerance	12.9 mm, punch side, upper tolerance	12.9 mm, die side, lower tolerance	13.1 mm, punch side, lower tolerance	13.1 mm, die side, upper tolerance
The most probable failure type	Screw failure	Screw failure	Self-clinching nut failure	Self-clinching nut failure
Mean torque (Nm)	93.5	99.4	92.7	91.4
Standard deviation (Nm)	6.1	14.0	8.7	3.6
Systematic error (Nm)	±1	±1	±1	±1
Random error (Nm)	±4.3	±10.0	±6.2	±2.5
Total uncertainty (Nm)	±4.4	±10.0	±6.3	±2.7

The results of 6 mm copper bar with M12 self-clinching nut, introduced in table 14, are same kind of the results with M10 self-clinching nut. There were less screw failures during measuring so the results describe better the torque out properties of nut. The thread was also a problem for the samples that were assembled in small hole and hence the screw did not rotate by fingers.

Table 14. Results of 6 mm copper bar, screw size M12 test samples.

Assembly hole, assembly side and tolerance	15.0 mm, punch side, lower tolerance	15.0 mm, die side, upper tolerance	15.2 mm, punch side, upper tolerance	15.2 mm, die side, lower tolerance
The most probable failure type	Screw failure	Self-clinching nut failure	Self-clinching nut failure	Self-clinching nut failure
Mean torque (Nm)	184.3	176.0	119.7	62.1
Standard deviation (Nm)	17.6	7.5	7.5	14.3
Systematic error (Nm)	±1	±1	±1	±1
Random error (Nm)	±12.6	±5.4	±5.4	±10.2
Total uncertainty (Nm)	±12.6	±5.5	±5.5	±10.3

There were also many screw failures among test samples of 10 mm copper bar with M10 self-clinching nut. The results are in table 15. Like the samples of 6 mm copper with M10 self-clinching nut, the only actual torque out value was able to measure from

the samples, where the self-clinching nut was assembled on die side in a large hole. The threads of the samples, where self-clinching nut was assembled in small hole, were poor.

Table 15. Results of 10 mm copper bar, screw size M10 test samples.

Assembly hole, assembly side and tolerance	12.9 mm, punch side, lower tolerance	12.9 mm, die side, upper tolerance	13.1 mm, punch side, upper tolerance	13.1 mm, die side, lower tolerance
The most probable failure type	Screw failure	Screw failure	Screw failure	Self-clinching nut failure
Mean torque (Nm)	98.7	101.5	95.6	67.7
Standard deviation (Nm)	5.7	7.1	7.6	4.1
Systematic error (Nm)	±1	±1	±1	±1
Random error (Nm)	±4.1	±5.1	±5.5	±2.9
Total uncertainty (Nm)	±4.2	±5.2	±5.6	±3.1

The results for 10 mm copper bar with M12 self-clinching nut are better, because there are a few screw failures. Still the samples, where self-clinching nut was assembled in small hole, are worse than the samples, where nut was assembled in large hole. The threads are poorer among small hole samples than among large hole samples and the screw failures occur among small hole samples. The results can be seen in table 16.

Table 16. Results of 10 mm copper bar, screw size M12 test samples.

Assembly hole, assembly side and tolerance	15.0 mm, punch side, lower tolerance	15.0 mm, die side, upper tolerance	15.2 mm, punch side, upper tolerance	15.2 mm, die side, lower tolerance
The most probable failure type	Screw failure	Self-clinching nut failure	Self-clinching nut failure	Self-clinching nut failure
Mean torque (Nm)	179.6	109.0	135.3	52.3
Standard deviation (Nm)	14.6	9.2	16.2	5.0
Systematic error (Nm)	±1	±1	±1	±1
Random error (Nm)	±10.4	±6.6	±11.6	±3.7
Total uncertainty (Nm)	±10.5	±6.7	±11.7	±3.7

The results of 6 mm aluminum with M10 self-clinching nut are introduced in table 17. There were less screw failures among these samples than corresponding copper samples. Also all threads of the samples were better than in copper samples. Screw failures occurred only in the samples, where self-clinching nut was assembled on punch side in a small hole.

Table 17. Results of 6 mm aluminum bar, screw size M10 test samples.

Assembly hole, assembly side and tolerance	12.9 mm, punch side, lower tolerance	12.9 mm, die side, upper tolerance	13.1 mm, punch side, upper tolerance	13.1 mm, die side, lower tolerance
The most probable failure type	Screw failure	Self-clinching nut failure	Self-clinching nut failure	Self-clinching nut failure
Mean torque (Nm)	94.5	61.4	70.0	15.1
Standard deviation (Nm)	10.6	5.1	10.6	3.1
Systematic error (Nm)	±1	±1	±1	±1
Random error (Nm)	±5.3	±3.7	±7.6	±2.2
Total uncertainty (Nm)	±5.4	±3.8	±7.6	±2.4

The results of 6 mm aluminum with M12 self-clinching nut are presented in table 18. The results describe well the torque out values of different variations, because only one screw failure occurred among these samples. Also all threads were good quality and the screw was possible to turn by fingers.

Table 18. Results of 6 mm aluminum bar, screw size M12 test samples.

Assembly hole, assembly side and tolerance	15.0 mm, punch side, upper tolerance	15.0 mm, die side, lower tolerance	15.2 mm, punch side, lower tolerance	15.2 mm, die side, upper tolerance
The most probable failure type	Self-clinching nut failure	Self-clinching nut failure	Self-clinching nut failure	Self-clinching nut failure
Mean torque (Nm)	169.3	100.8	80.6	47.8
Standard deviation (Nm)	3.7	4.5	9.1	8.2
Systematic error (Nm)	±1	±1	±1	±1
Random error (Nm)	±2.7	±3.2	±6.5	±5.9
Total uncertainty (Nm)	±2.8	±3.4	±6.6	±5.9

The results of 10 mm aluminum with M10 self-clinching nut are similar to the results of corresponding 6 mm aluminum samples. The results are introduced in table 19. Only among the samples, where self-clinching nut was assembled on punch side in small hole occurred screw failures. The threads of all samples were good.

Table 19. Results of 10 mm aluminum bar, screw size M10 test samples.

Assembly hole, assembly side and tolerance	12.9 mm, punch side, upper tolerance	12.9 mm, die side, lower tolerance	13.1 mm, punch side, lower tolerance	13.1 mm, die side, upper tolerance
The most probable failure type	Screw failure	Self-clinching nut failure	Self-clinching nut failure	Self-clinching nut failure
Mean torque (Nm)	108.0	34.0	77.4	14.9
Standard deviation (Nm)	9.4	5.6	13.5	5.3
Systematic error (Nm)	±1	±1	±1	±1
Random error (Nm)	±6.8	±4.0	±9.7	±3.8
Total uncertainty (Nm)	±6.8	±4.1	±9.7	±3.9

The results of 10 mm aluminum with M12 self-clinching nut are presented in table 20. The torque out values were able to get from all samples and screw failures did not occur. The threads of all samples were good.

Table 20. Results of 10 mm aluminum bar, screw size M12 test samples.

Assembly hole, assembly side and tolerance	15.0 mm, punch side, lower tolerance	15.0 mm, die side, upper tolerance	15.2 mm, punch side, upper tolerance	15.2 mm, die side, lower tolerance
The most probable failure type	Self-clinching nut failure	Self-clinching nut failure	Self-clinching nut failure	Self-clinching nut failure
Mean torque (Nm)	156.0	86.7	99.9	10.1
Standard deviation (Nm)	4.2	7.9	9.4	3.4
Systematic error (Nm)	±1	±1	±1	±1
Random error (Nm)	±3.0	±5.7	±6.7	±2.4
Total uncertainty (Nm)	±3.1	±5.7	±6.8	±2.6

All in all, the results are not completely good, because there are so many screw failures and samples, which could not break due to safety limits of the device. These samples distract the results so the confidence of the results is lower than wanted. The confidence affects to the analysis of the most significant variables. However, it can be seen from the results that direction of the effects is possible to see. When analyzing the results as they are, the most significant variables can be found. The low confidence of results affects in this case to the internecine order of the effects of the variables, but it does not affect, if the effect is significant or not.

To determine the most significant effects of the variables, Minitab was used software to calculate the standardized effects of the variables. The results of all samples were entered to Minitab and the significance values of the variables, correspondence of results and prediction of results were calculated. The significances of variables are presented in figure 38. All effects over the value 1.97 are significant. The constructed DoE model explains 96.57 % of the results and the model can predict 95.77 % of the new results in the future. The coverage probability and the prediction probability values are good.

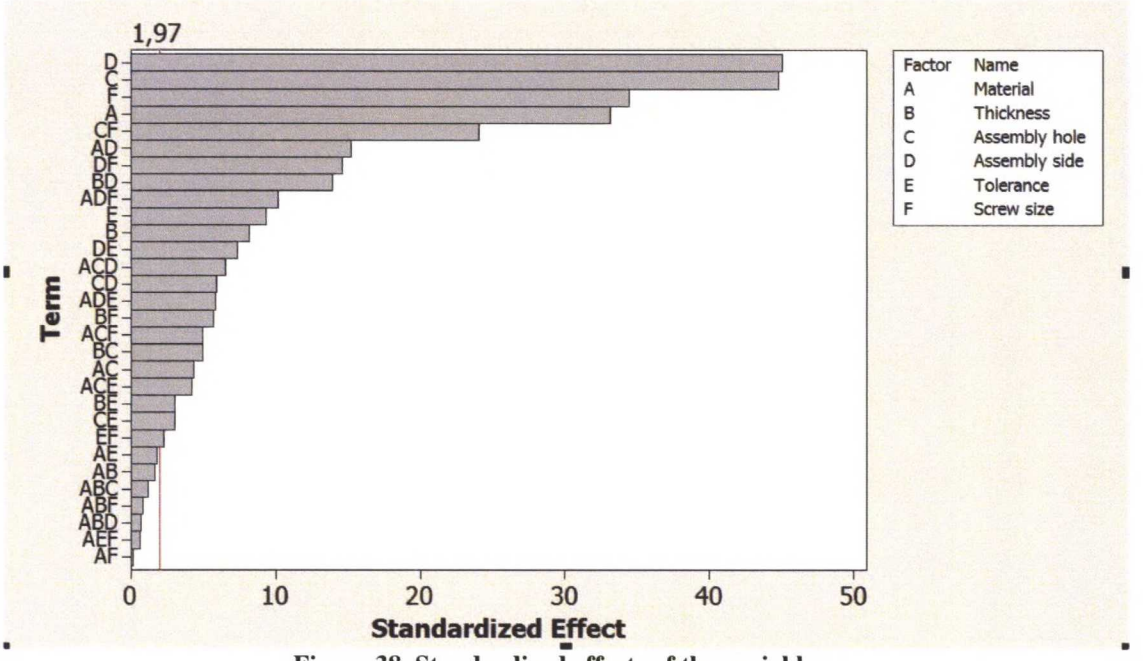

Figure 38. Standardized effects of the variables.

It shall be remembered that there are confounded high degree combined effects in the effects seen in figure 38. The high degree combined effects are not significant, when compared to the main effects, so the significance of high degree combined effect can be ignored, but the results are not exact. To get exact results, the least significant effects shall be removed and a new full factorial test shall be done.

5.3 Joint test

There were made joint tests for screw-nut joints, ABB self-clinching nut with the same variations as in torque out test and KALEI®- and PEM®-nuts. The idea of joint test was to measure preload force during tightening of joint. Torque-force curves were possible

to form for different joint types after the test. These curves are easy to compare against each other and estimate how well they correspond to each other. Also the suitability of VDI 2230 is possible to figure out.

The measuring was similar to torque out measuring apart from the force sensor, which was set on. The data logging graph of torque sensor was similar to the torque out test, but the torque did not drop until the motor was turned off, because the nut rarely failed in this test. The preload force graph is presented in figure 39. The same tightening phases that are in torque graph can be found in the graph.

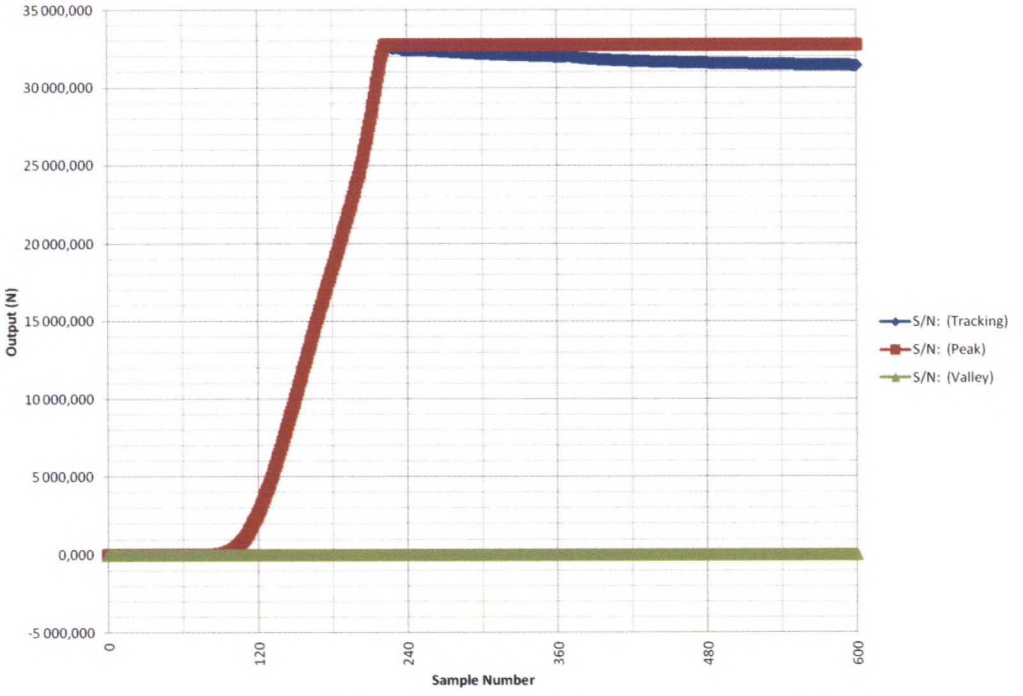

Figure 39. Data logging graph of one sample in joint test.

5.3.1 Regular through bolted joints

The joint test with regular through bolted joints was made with 10 test samples per set. The purpose of this test was to create the benchmark for self-clinching nut joints.

There was calculated in chapter 5.1 the torque-preload curves with different friction coefficients and the result was a straight line for certain friction level. The friction coefficient can change a lot from one sample to another so the results among the set can vary a lot. The variation of friction coefficient can be seen in regular through bolted joints. One set of screw-nut joints, in this case 10 mm copper bar with M12 screw, is presented in figure 40. It can be seen the measured samples follow linear curve quite good. The variation seems to be mainly from the variation of friction coefficient or the resistive forces of thread. All samples are quite well between theory curves of friction coefficients 0.25 and 0.35.

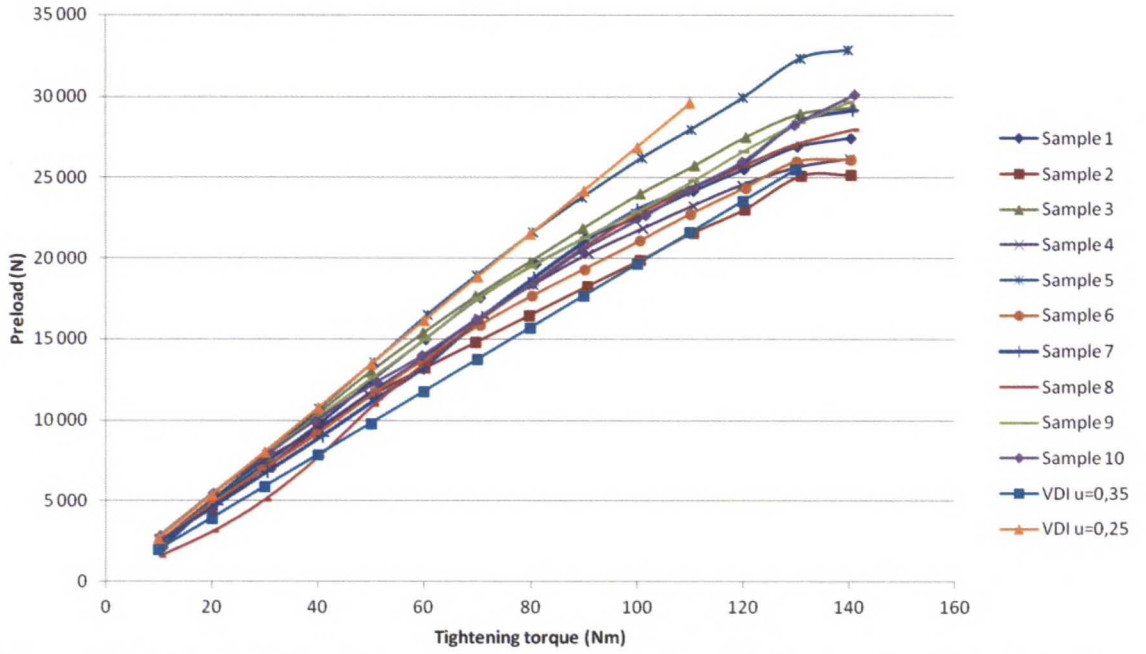

Figure 40. Results of joint test for regular through bolted joint with 10 mm copper bar and screw size M12.

For other samples of screw-nut joints, the graphs are similar as in figure 40. There are presented the extreme values of friction coefficient among the screw-nut samples in table 21. It can be seen from the table that all samples with M12 screw have almost the same variation of friction coefficients. Almost all the curves of samples are between theory curves of friction coefficients 0.2 and 0.4. Instead, the samples with M10 screw divide in two categories. The thin joints with 6 mm busbars are between theory curves of friction coefficients 0.2 and 0.4 and the joints with 10 mm busbars are between theory curves of friction coefficients 0.125 and 0.2. This difference causes the preloads of thin joints are lower than thick joints. The same phenomenon can be seen in figure 41, where is introduced the comparison of the two joint thicknesses for both screw sizes. The comparison curves are from the mean values of all samples of the set.

Table 21. The observed friction coefficients of regular through bolted joints during measuring.

	Friction coefficient	
Joint type	**The lowest observed**	**The highest observed**
Al6 M10	0.2	0.4
Al6 M12	0.25	0.4
Al10 M10	0.125	0.2
Al10 M12	0.25	0.35
Cu6 M10	0.2	0.4
Cu6 M12	0.2	0.4
Cu10 M10	0.125	0.2
Cu10 M12	0.25	0.35

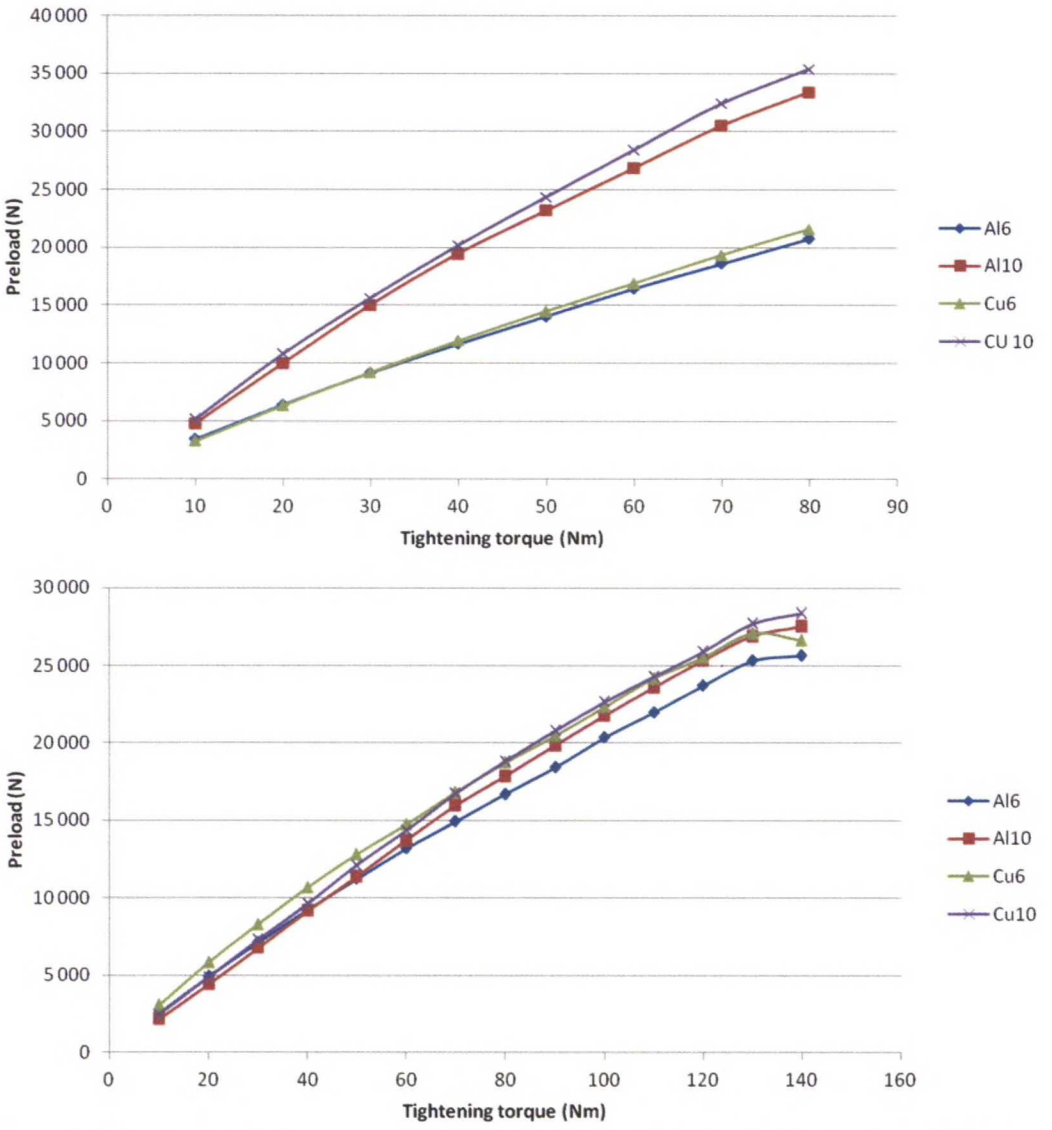

Figure 41 The mean value curves of different thicknesses of busbars. Above graph M10 joints and below M12 joints.

Next, the preloads of the joints are presented at the tightening torques that were in VDI 2230 calculations in chapter 5.1. The observed tightening torques are 40 Nm for M10 joints and 70 for M12 joints. The variation of friction coefficient is included in random error and that way into measuring uncertainty. The preloads for M10 joints are presented in tables 22 and for M12 joints in table 23.

Table 22. Preload of M10 joint at 40 Nm.

M10 joints	Cu6	Cu10	Al6	Al10
Mean preload (kN)	11.9	20.2	11.7	19.5
Standard deviation (N)	2790	1880	1710	2860
Systematic error (N)	±660	±660	±660	±660
Random error (N)	±2000	±1340	±1230	±2040
Total uncertainty (N)	±2100	±1500	±1390	±2150

Table 23. Preload of M12 joint at 70 Nm.

M12 joints	Cu6	Cu10	Al6	Al10
Mean preload (kN)	16.8	16.7	14.9	16.0
Standard deviation (N)	3660	1210	2560	920
Systematic error (N)	±660	±660	±660	±660
Random error (N)	±2620	±860	±1830	±660
Total uncertainty (N)	±2700	±1090	±1940	±930

5.3.2 ABB self-clinching nut

The joint test with ABB self-clinching nut was made with 5 samples and the samples were the same variations that was used in torque out test. The results are same kind as the results of regular through bolted joints. The torque-preload curves follow roughly a straight line and that line is possible to find with VDI 2230 theory by adjusting the friction coefficient. The torque-preload curves of one variation of 10 mm aluminum M12 joint are presented in figure 42.

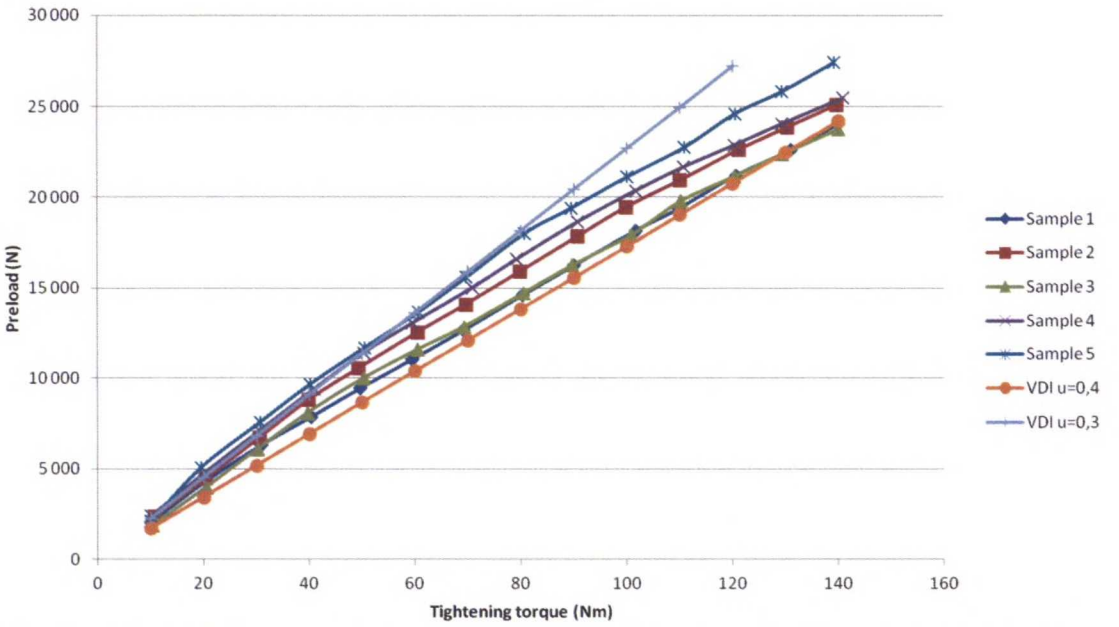

Figure 42 The gained preload with different tightening torques with 10 mm aluminum ABB self-clinching nut joint. Nut assembled in a small hole on die side.

The variation of friction coefficient is similar than among the regular through bolted joints. There is possible to see the large friction coefficient values among the samples, where the nut is assembled in small hole. Especially, among copper bar test samples the phenomenon is clearly observable. The problem with threads of the samples, reported also during torque out test, is causing the high resistance of rotation. The observed extreme values of friction coefficient during measurements are presented in table 24.

Table 24. The observed friction coefficients of ABB self-clinching nut joints during measuring.

Joint type			Friction coefficient	
			The lowest observed	The highest observed
Al6	M10	12.9 punch	0.2	0.4
		12.9 die	0.3	0.4
		13.1 punch	0.4	0.4
		13.1 die	0.2	0.4
	M12	15.0 punch	0.3	0.4
		15.0 die	0.35	0.4
		15.2 punch	0.35	0.4
		15.2 die	0.35	0.4
Al10	M10	12.9 punch	0.15	0.2
		12.9 die	0.15	0.25
		13.1 punch	0.15	0.25
		13.1 die	0.15	0.25
	M12	15.0 punch	0.3	0.4
		15.0 die	0.3	0.4
		15.2 punch	0.35	0.35
		15.2 die	0.3	0.4
Cu6	M10	12.9 punch	0.25	0.4
		12.9 die	0.25	0.4
		13.1 punch	0.3	0.4
		13.1 die	0.25	0.4
	M12	15.0 punch	0.3	0.45
		15.0 die	0.35	0.45
		15.2 punch	0.3	0.4
		15.2 die	0.35	0.45
Cu10	M10	12.9 punch	0.15	0.3
		12.9 die	0.125	0.2
		13.1 punch	0.15	0.2
		13.1 die	0.125	0.2
	M12	15.0 punch	0.3	0.4
		15.0 die	0.3	0.35
		15.2 punch	0.3	0.35
		15.2 die	0.3	0.4

There are compared ABB self-clinching nut variations to regular through bolted joint with screw size M10 and aluminum bar in figure 43. The curves are formed from the mean values of the tested sets. There can be seen the results, especially the samples of 10 mm aluminum bar, are almost identical. There is more deviation in samples of 6 mm aluminum bar. The difference of preload between thick and thin joint is similar to the regular through bolted joint.

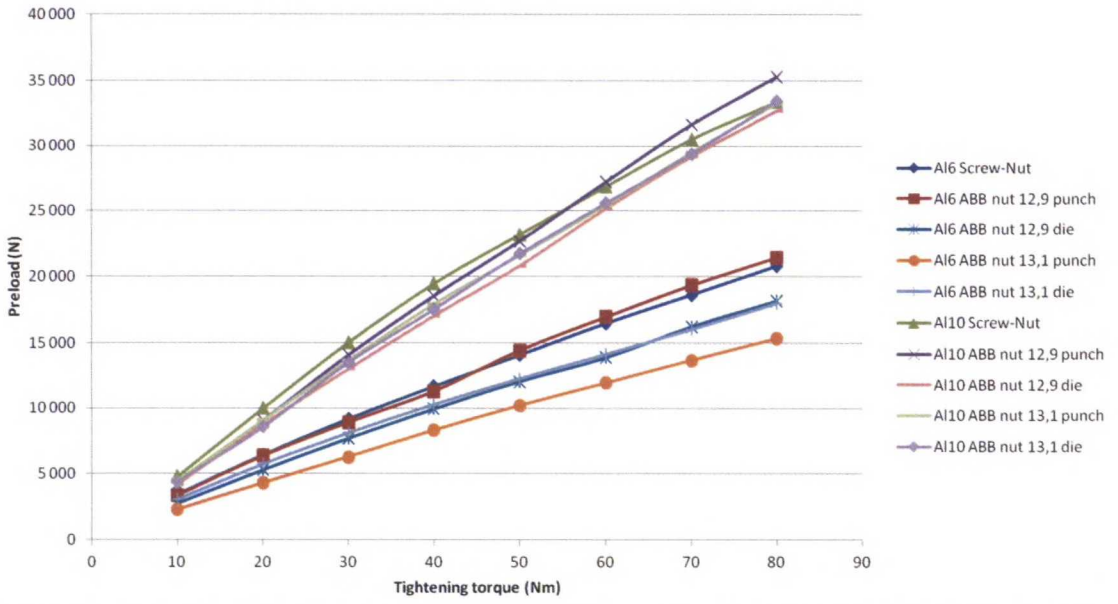

Figure 43. Comparison between ABB self-clinching nut and regular through bolted joint with screw size M10 in aluminum bar.

The results are similar, when comparing the M10 joints of copper. The results are introduced in figure 44. The joint with ABB self-clinching nut corresponds well to the regular through bolted joint. The ABB nut samples, where nut is assembled in small hole, differ most from other sets. Especially, the nut in 10 mm copper bar in small hole on punch side is completely different than other variations. The reason of large difference is poor thread quality. Also for these samples, the joint thickness has an effect to preload.

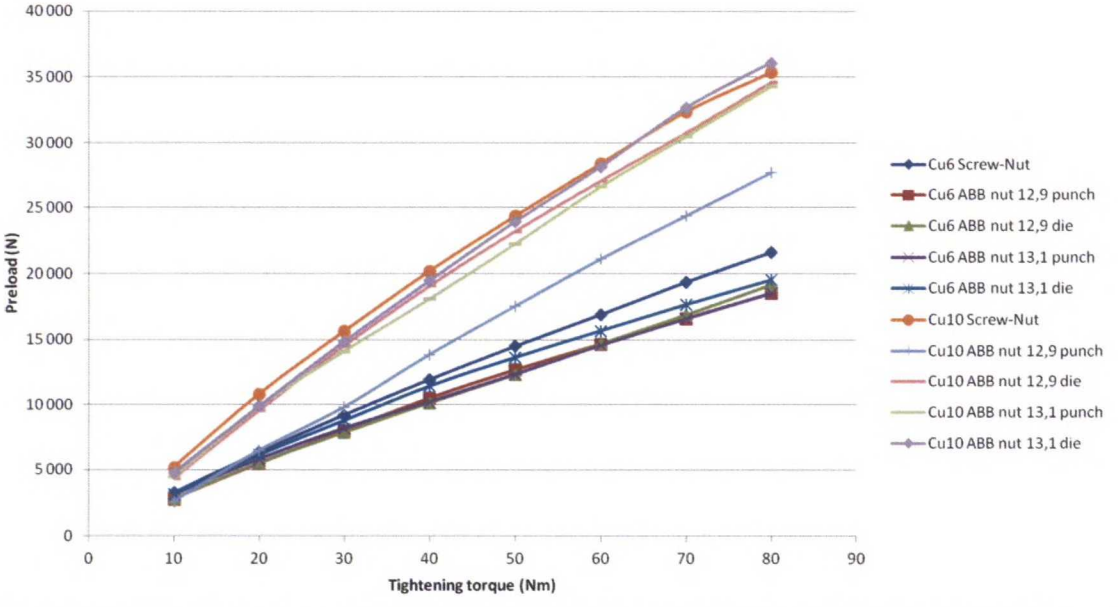

Figure 44. Comparison between ABB self-clinching nut and regular through bolted joint with screw size M10 in copper bar.

The results of M12 aluminum joints are quite consistent as it can be seen in figure 45. The joint thickness does not have an effect to the preload and the assembly variations do not have significant effect to the preload. The regular through bolted joints can reach higher preloads than joints with ABB self-clinching nut.

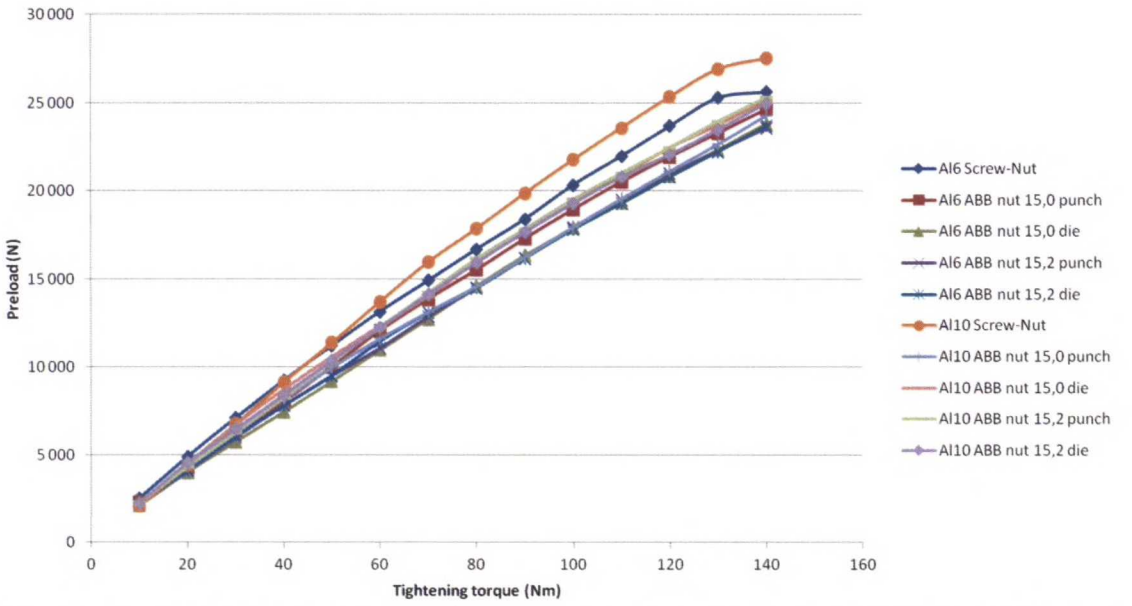

Figure 45. Comparison between ABB self-clinching nut and regular through bolted joint with screw size M12 in aluminum bar.

The results of M12 copper joints are the same kind than M12 aluminum joints, but the difference between regular through bolted joints and self-clinching nut joints is larger. The deviation between assembly variations of ABB self-clinching nut is also larger. The results are presented in figure 46.

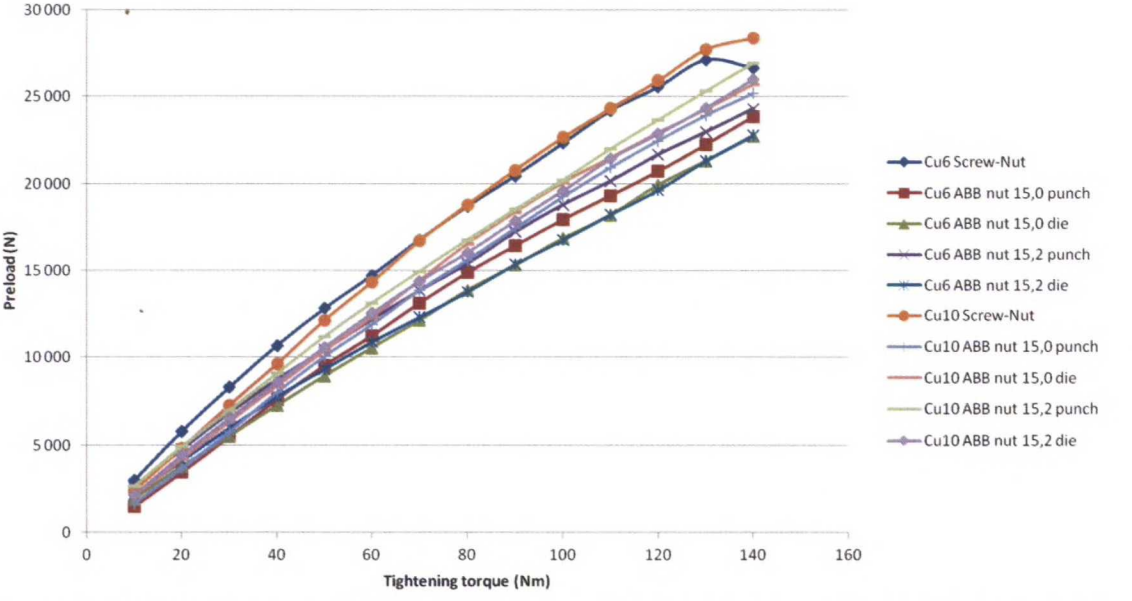

Figure 46. Comparison between ABB self-clinching nut and regular through bolted joint with screw size M12 in copper bar.

The preload at usual tightening torque of joint is presented for different variations in following tables. The error calculations are done similarly as for regular through bolted joints. The variations of friction coefficient and resistive forces of thread are included in total measuring uncertainty.

Table 25. Preload of M10 ABB self-clinching nut in 6 mm aluminum at 40 Nm.

Al6 M10	12.9 punch	12.9 die	13.1 punch	13.1 die
Mean preload (kN)	11.3	9.9	8.3	10.3
Standard deviation (N)	2000	1300	610	2560
Systematic error (N)	±660	±660	±660	±660
Random error (N)	±2490	±1610	±750	±3170
Total uncertainty (N)	±2570	±1740	±1000	±3240

Table 26. Preload of M12 ABB self-clinching nut in 6 mm aluminum at 70 Nm.

Al6 M12	15.0 punch	15.0 die	15.2 punch	15.2 die
Mean preload (kN)	13.9	12.7	12.9	13.1
Standard deviation (N)	2100	690	1540	740
Systematic error (N)	±660	±660	±660	±660
Random error (N)	±2600	±860	±1910	±920
Total uncertainty (N)	±2690	±1080	±2020	±1130

Table 27. Preload of M10 ABB self-clinching nut in 10 mm aluminum at 40 Nm.

Al10 M10	12.9 punch	12.9 die	13.1 punch	13.1 die
Mean preload (kN)	18.5	17.0	17.9	17.5
Standard deviation (N)	1700	3100	2540	2620
Systematic error (N)	±660	±660	±660	±660
Random error (N)	±2110	±3850	±3150	±3260
Total uncertainty (N)	±2210	±3910	±3220	±3320

Table 28. Preload of M12 ABB self-clinching nut in 10 mm aluminum at 70 Nm.

Al10 M12	15.0 punch	15.0 die	15.2 punch	15.2 die
Mean preload (kN)	13.1	14.1	14.2	14.2
Standard deviation (N)	1210	1270	360	850
Systematic error (N)	±660	±660	±660	±660
Random error (N)	±1500	±1580	±440	±1190
Total uncertainty (N)	±1640	±1710	±800	±1360

Table 29. Preload of M10 ABB self-clinching nut in 6 mm copper at 40 Nm.

Cu6 M10	12.9 punch	12.9 die	13.1 punch	13.1 die
Mean preload (kN)	10.5	10.1	10.2	11.4
Standard deviation (N)	890	2160	1000	1430
Systematic error (N)	±660	±660	±660	±660
Random error (N)	±1100	±2680	±1240	±1780
Total uncertainty (N)	±1280	±2760	±1410	±1900

Table 30. Preload of M12 ABB self-clinching nut in 6 mm copper at 70 Nm.

Cu6 M12	15.0 punch	15.0 die	15.2 punch	15.2 die
Mean preload (kN)	13.1	12.1	13.8	12.3
Standard deviation (N)	2420	1430	1410	1290
Systematic error (N)	±660	±660	±660	±660
Random error (N)	±3000	±1770	±1750	±1610
Total uncertainty (N)	±3070	±1890	±1870	±1740

Table 31. Preload of M10 ABB self-clinching nut in 10 mm copper at 40 Nm.

Cu10 M10	12.9 punch	12.9 die	13.1 punch	13.1 die
Mean preload (kN)	13.8	19.1	18.1	19.5
Standard deviation (N)	3340	2300	590	2350
Systematic error (N)	±660	±660	±660	±660
Random error (N)	±4140	±2860	±740	±2920
Total uncertainty (N)	±4190	±2930	±990	±2990

Table 32. Preload of M12 ABB self-clinching nut in 10 mm copper at 70 Nm.

Cu10 M12	15.0 punch	15.0 die	15.2 punch	15.2 die
Mean preload (kN)	13.8	14.4	15.0	14.4
Standard deviation (N)	2090	750	1240	1320
Systematic error (N)	±660	±660	±660	±660
Random error (N)	±2600	±930	±1540	±1640
Total uncertainty (N)	±2680	±1140	±1680	±1770

5.3.3 KALEI®- and PEM®-nuts

The joint test was performed with KALEI®- and PEM®-nut samples with 10 samples per set. The results of joint test are similar to the regular through bolted joint and ABB self-clinching nut joint. The measured curves follow roughly straight lines, which can be found with VDI 2230 calculation by adjusting the friction coefficient. The observed extreme values of friction coefficient among samples are introduced in table 33.

Table 33. The observed friction coefficients of KALEI®- and PEM®-nut joints during measuring.

	Friction coefficient	
Joint type	**The lowest observed**	**The highest observed**
Al6 M10 KALEI	0.2	0.4
Al6 M12 KALEI	0.3	0.45
Al10 M10 KALEI	0.15	0.2
Al10 M12 KALEI	0.3	0.45
Cu6 M10 KALEI	0.2	0.4
Cu6 M12 KALEI	0.4	0.45
Cu10 M10 KALEI	0.125	0.3
Cu10 M12 KALEI	0.25	0.4
Al6 M10 PEM	0.2	0.35
Al6 M12 PEM	0.25	0.35
Al10 M10 PEM	0.125	0.3
Al10 M12 PEM	0.2	0.3
Cu6 M10 PEM	0.15	0.4
Cu6 M12 PEM	0.25	0.35
Cu10 M10 PEM	0.125	0.2
Cu10 M12 PEM	0.15	0.3

There are formed the mean value curves from the measuring data for M10 aluminum test samples in figure 47. The PEM®-nut samples correspond well to regular through bolted joint and the joints with 6 mm busbar are identical. KALEI®-nut samples do not reach as high preloads as through bolted joint.

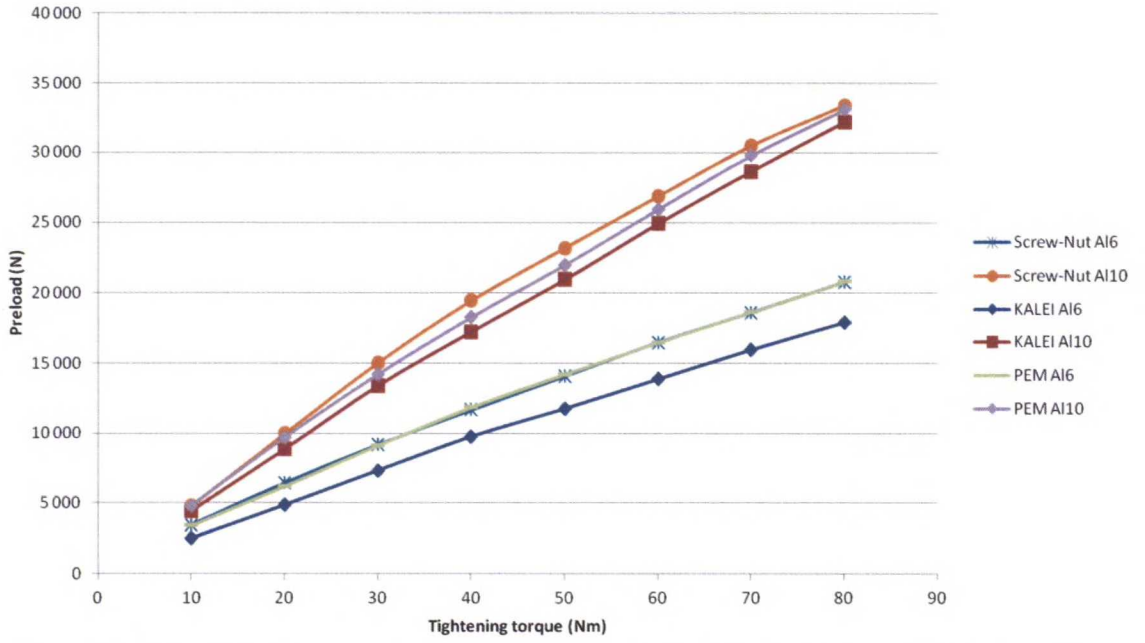

Figure 47. Comparison between KALEI®-nut, PEM®-nut and regular through bolted joint with screw size M10 in aluminum bar.

When the busbar material is switched to copper, the results are similar than with aluminum, but PEM®-nut samples are even better than regular through bolted joint. The graph of results is presented in figure 48.

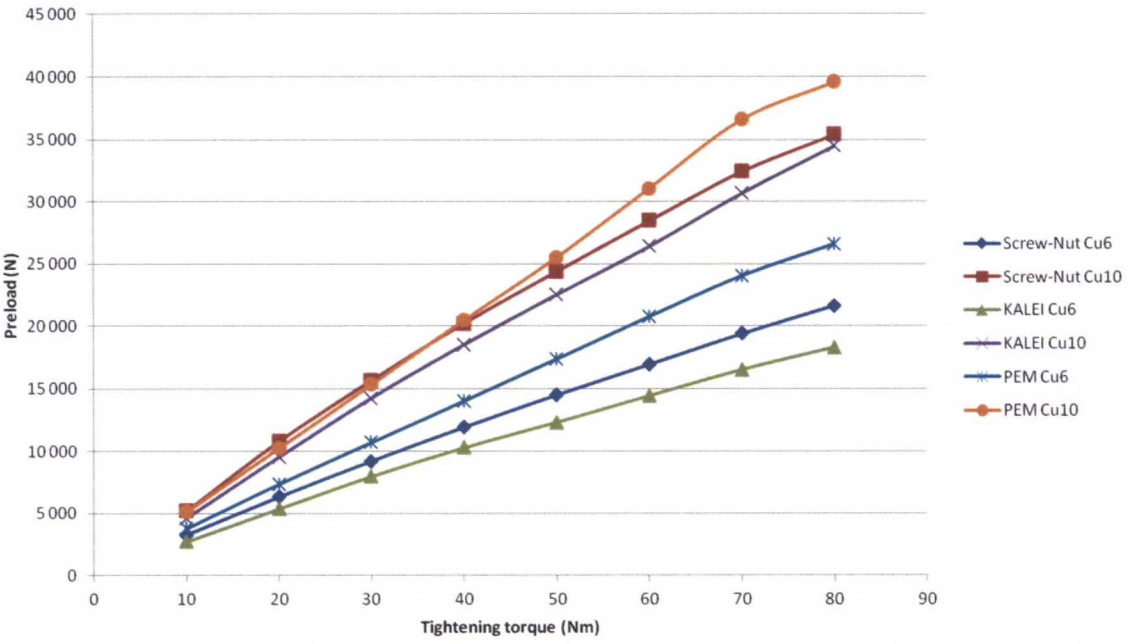

Figure 48. Comparison between KALEI®-nut, PEM®-nut and regular through bolted joint with screw size M10 in copper bar.

The same thing can be seen with M12 aluminum joints in figure 49 that was noticed with M10 copper joints. PEM®-joints reach as high preloads or higher as regular through bolted joint. The preload of KALEI®-joints remain lower.

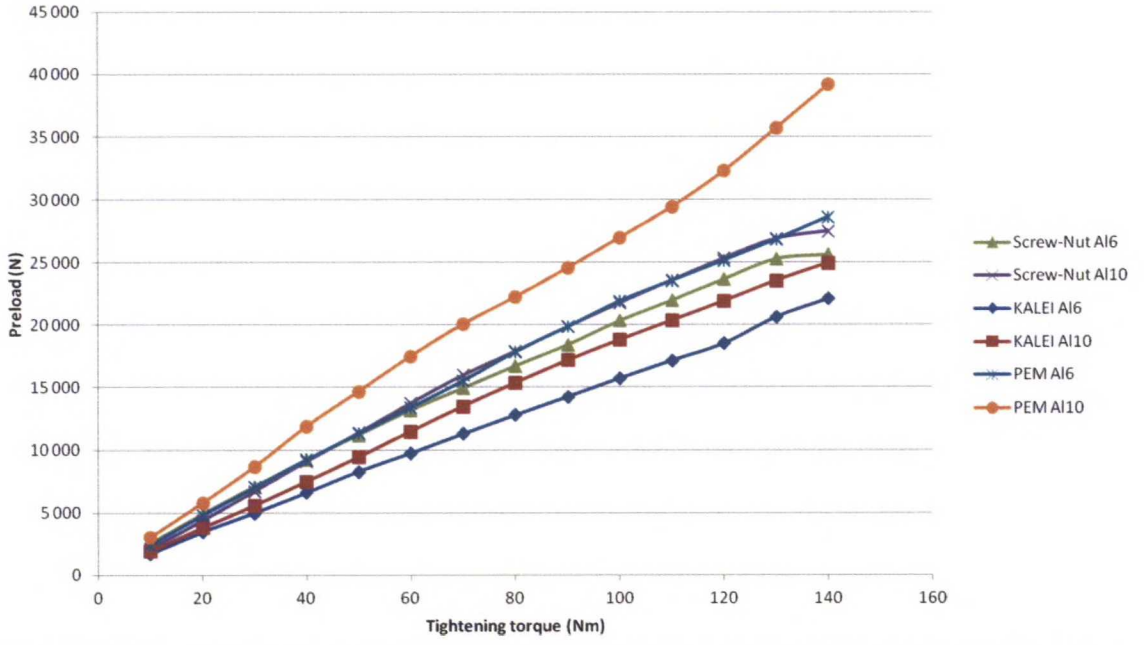

Figure 49. Comparison between KALEI®-nut, PEM®-nut and regular through bolted joint with screw size M12 in aluminum bar.

When the busbar material is switched to copper, the results are similar with M12 aluminum joints. The results are introduced in figure 50.

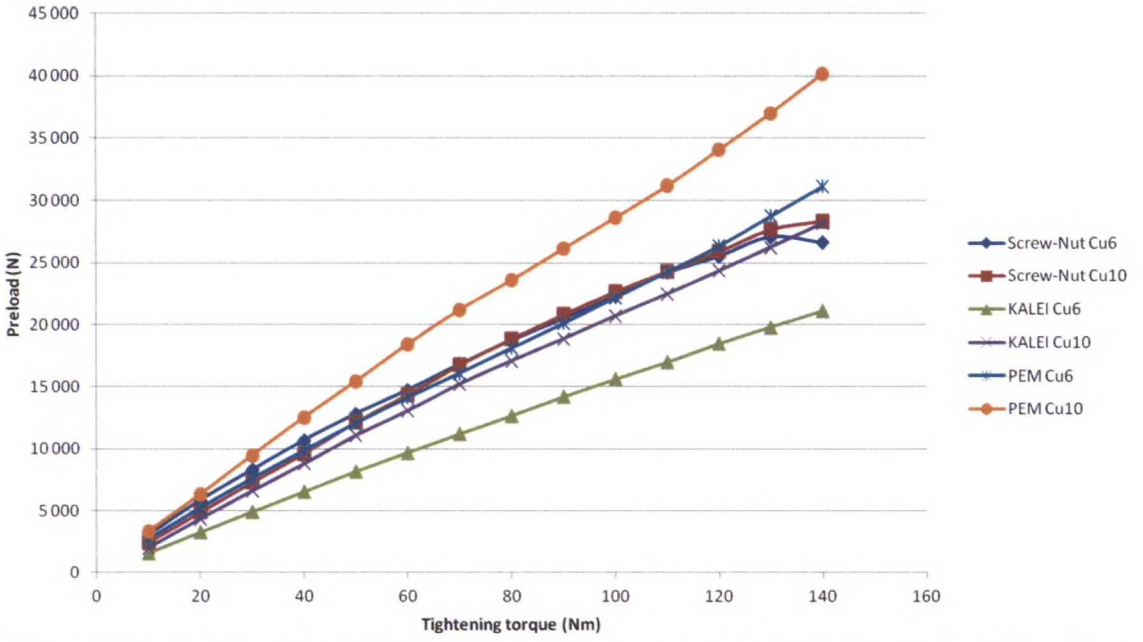

Figure 50. Comparison between KALEI®-nut, PEM®-nut and regular through bolted joint with screw size M12 in copper bar.

The preloads at assembly tightening torques are presented in following tables.

Table 34. Preload of M10 KALEI®- and PEM®-joints at 40 Nm.

KALEI M10	Cu6	Cu10	Al6	Al10
Mean preload (kN)	10.3	18.5	9.8	17.2
Standard deviation (N)	2090	3200	2210	1770
Systematic error (N)	±660	±660	±660	±660
Random error (N)	±1490	±2290	±1580	±1260
Total uncertainty (N)	±1630	±2380	±1710	±1430
PEM M10				
Mean preload (kN)	14.0	20.4	11.9	18.3
Standard deviation (N)	4980	2980	1940	2710
Systematic error (N)	±660	±660	±660	±660
Random error (N)	±3570	±2130	±1390	±1940
Total uncertainty (N)	±3630	±2230	±1540	±2050

Table 35. Preload of M12 KALEI®- and PEM®-joints at 70 Nm.

KALEI M12	Cu6	Cu10	Al6	Al10
Mean preload (kN)	11.2	15.2	11.3	13.5
Standard deviation (N)	940	2980	2310	1440
Systematic error (N)	±660	±660	±660	±660
Random error (N)	±670	±2130	±1650	±1020
Total uncertainty (N)	±940	±2230	±1780	±1230
PEM M12				
Mean preload (kN)	16.1	21.2	15.5	20.1
Standard deviation (N)	1190	3360	1170	2360
Systematic error (N)	±660	±660	±660	±660
Random error (N)	±850	±2400	±840	±1690
Total uncertainty (N)	±1080	±2490	±1070	±1810

6 Discussion

The main benefit of using self-clinching inserts is to reduce the thickness of the joint and that way save the space in device. Also the facilitation of device assembly by reducing the number of joint parts and easing the assembly in tight positions is important benefit. The disadvantage is there are not any general design guidelines for the use of self-clinching insert. The only guidelines come from the insert manufacturers and they cover only one product line at time. VDI 2230 design guideline is the most common guideline used in bolted joints and if that is usable for self-clinching inserts, it improves the design of self-clinching insert joint.

One of the aims of this work was to examine the suitability of self-clinching inserts in busbar joints. According to the literature review in the beginning of this work the self-clinching insert manufacturers have developed inserts that suit in busbar joints. The information from manufacturers announces the joint properties equal the regular through bolted joints. The results of the performed measurements also partially support the promises of manufacturers. The preload that can be reached at certain tightening torque is close to the preload of regular through bolted joint, but usually the preload remains lower.

The other aim of this work was to find out, if the VDI 2230 design guideline is suitable in design of self-clinching insert joints. The measuring results and calculations point out the friction coefficient of threads is important to know. The VDI calculations match quite well the measured values, when the friction coefficient is determined correctly. The measuring results show the VDI calculation is always on safer side in point of view the screw strength. In other words, the calculated preload is the maximum value at certain tightening torque and in reality the preload is a bit lower. The assembly preloads of self-clinching nut joints are possible to calculate with VDI 2230, when the friction coefficient is determined correctly, but the residual preload calculation shall be verified with additional tests. These tests do not describe the long-term behavior of joint.

The joint test results have large deviations among measured sets. The deviation is possible to explain with the variation of friction coefficient. The measuring results are credible, because the different resistive forces of threads could feel when turning the screw by fingers and the friction coefficient get values that are possible. There was not only a large friction coefficient in some of the ABB self-clinching nut sets but also clear deformation of threads. Because the thread of ABB self-clinching nut is partially inside the busbar in assembled position, the thread deforms during assembly, if the assembly hole is too small. The high friction coefficient causes higher tightening torque and lower preload, because the friction force shall be defeated before the joint tightens.

The measuring results point out the geometry of joint affect on the preload. All tested M10 joints showed the thick joint had higher preload than thin. The difference can be explained with friction coefficient, but it is not satisfying explanation, because the screws used in thin joints were the same as with thick joints. On the other hand M12 joints were consistent apart from KALEI®- and PEM®-joints, where difference in preload was observed between thin and thick joints. One explanation can be that embedding has a little effect already during tightening. The elasticity of joint is better with thick joint, which compensates the preload loss due to embedding. The embedding could also explain the non-linearity of measured preload curves.

The VDI 2230 design guideline can be used as a basis of design of self-clinching nut joints. The deviation of measuring results shows the friction coefficient in calculation shall be chosen carefully. The basic rule is to choose the smallest friction coefficient that is expected, because if the real friction coefficient is smaller the screw may be too close the yield strength or over it. The disadvantage of this kind of design is the preload may be much lower, if the real friction coefficient is large.

The low preload may cause joint loosening after the embedding of joint and thermal expansion. Also vibrations and other loads during operation may cause slipping in the joint. The preload has a significant effect on contact resistance, which increases when preload decreases. The behavior can be seen from the results of VDI 2230 calculations in tables 9-12.

The results of joint tests show it is possible to determine limits for friction coefficient within the results fit. According to the results there should be used different friction coefficients for different joints. Based on these results, the recommended friction coefficients for different joints are introduced in table 36. It is possible to calculate the preload with VDI 2230 method with these friction coefficients. There is introduced also the largest friction coefficients that were observed during tests in table 36. These values shall be taken into account, when designing the joint, because they describe the worst case that may occur in the joint.

Table 36. Recommended and the largest measured friction coefficients for VDI 2230 calculations.

	Screw-Nut		**ABB self-clinching nut**		**KALEI**		**PEM**	
Material and screw size	**Recommended friction coefficient**	**The largest measured**	**Recommended friction coefficient**	**The largest measured**	**Recommended friction coefficient**	**The largest measured**	**Recommended friction coefficient**	**The largest measured**
Al6 M10	0.2	0.4	0.2	0.4	0.2	0.4	0.2	0.35
Al6 M12	0.25	0.4	0.3	0.4	0.3	0.45	0.25	0.35
Al10 M10	0.125	0.2	0.15	0.25	0.15	0.2	0.125	0.3
Al10 M12	0.25	0.35	0.3	0.4	0.3	0.45	0.2	0.3
Cu6 M10	0.2	0.4	0.25	0.4	0.2	0.4	0.15	0.4
Cu6 M12	0.2	0.4	0.3	0.45	0.4	0.45	0.25	0.35
Cu10 M10	0.125	0.2	0.125	0.3	0.125	0.3	0.125	0.2
Cu10 M10	0.25	0.35	0.3	0.4	0.25	0.4	0.15	0.3

The joints with self-clinching nut managed well in joint test. The adhesion between nut and busbar was enough to keep self-clinching nut in place. Only a couple of samples failed, because the self-clinching nut came loose. The failed samples were in 10 mm aluminum samples, where the nut was assembled in a large hole on die side. One of the failed samples is presented in figure 51.

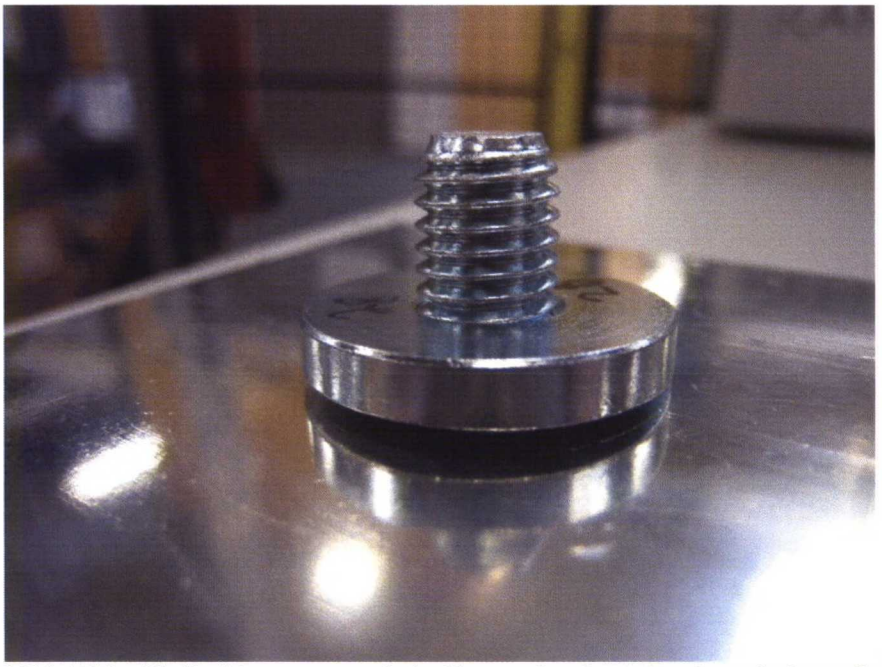

Figure 51. M10 ABB self-clinching nut sample in 10 mm aluminum in a large hole on die side after the joint test.

Despite the good results in joint test, there remains an uncertainty over the long-term properties of KALEI®- and PEM®-nuts. The surface pressure values of KALEI®- and PEM®-nuts are higher than the corresponding value of ABB self-clinching nut, because the bearing area is smaller. The aluminum is more restrictive than copper, because the yield strength of aluminum is a bit lower 170 MPa [45] so the surface pressure shall be below that. ABB self-clinching nut fulfils easily that requirement as can be seen in the tables 9-12. PEM®-nut fulfils the requirement, when the friction coefficient is moderate, but KALEI®-nut does not meet the requirement until the friction coefficient is large. Based on that result KALEI®-nut is not suitable in high power busbar joints. ABB self-clinching nut corresponds regular through bolted joint so there is not any hindrance for using it in busbar joints. PEM®-nut is possible to use in busbar joints, but the suitability shall be verified before using, because PEM®-nut fulfils the requirements only just. The maximum allowed preloads for self-clinching nuts are presented in table 37. These calculations are made for the projection area of the nut bearing area and they do not take the shape of collar of the nut into account. The shape likely decreases the surface pressure so the effect shall be verified with additional tests.

Table 37. Maximum allowed preload for self-clinching nuts.

	Preload (kN)	
Nut type	**M10**	**M12**
ABB-nut	67.7	59.8
PEM	14.0	17.8
KALEI	9.2	10.5

There were also many position errors of the self-clinching nut among KALEI®-samples, which do not support the use of nut in busbar joints. There were none observations of position errors from ABB self-clinching nut and PEM®-nut samples. Some of the KALEI®- nuts were settled a bit in angled position in nut assembly. In figure 52 is presented one of the worst error positions of the KALEI®-nut. The position error causes the screw axis not to coincide with the normal axis of the joint. The angle between screw axis and joint axis was about 3-4 degrees. The samples that had position error were difficult to attach in the test device and the angled position could have caused error in preload. The supplier was asked about the nut assembly and the answer was that all self-clinching inserts are assembled the same way with the same machine. KALEI®-nuts seem to be sensitive to position errors. KALEI®-nut has not a large bearing area like the other self-clinching nuts and that may cause that the nut can't straighten itself if it is angled in the beginning of assembly.

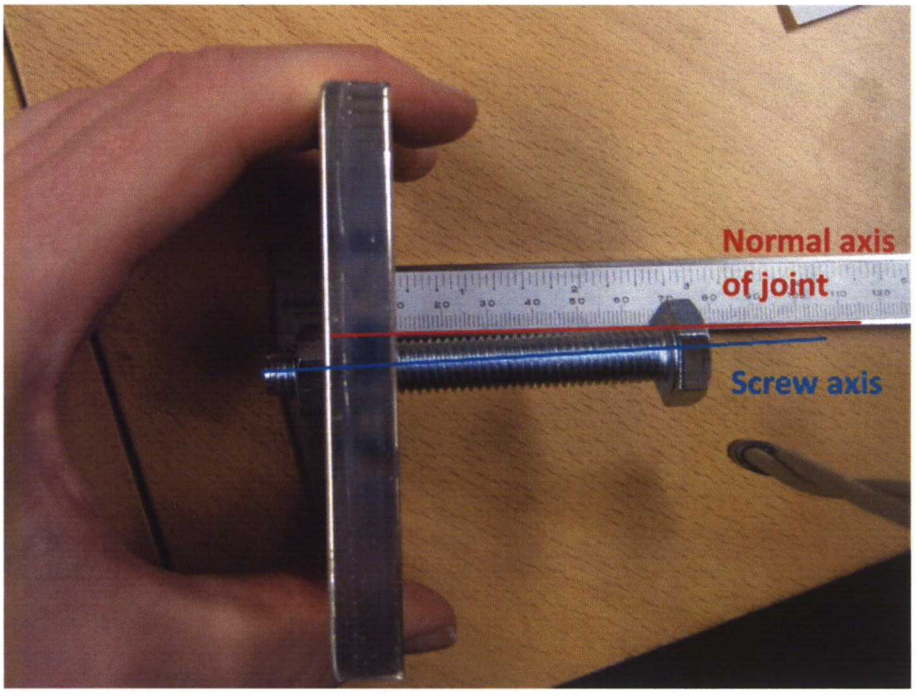

Figure 52. KALEI®-nut assembly error.

Torque out test showed the significant variables in the ABB self-clinching nut joints as presented in figure 38. There are some clear effects of variables like effects of screw size and assembly hole diameter which can be predicted without tests. The main and combined effects of screw size and assembly hole are logical; if the screw size is large, the torque out value is large and if the assembly hole is large, the torque out value is low. The results show that the most significant variable is the assembly side of self-clinching nut. When the nut is assembled on die side, the torque out torque is clearly lower than the nut that is assembled on punch side. The difference of torque out values increases, when the busbar is thick and even more, when the material is switched to aluminum. The previous behavior can be seen in measuring results and in figure 38, where the combined effects of material, assembly side and thickness are highly significant.

The reason for the difference of torque out values between sides of busbar is the rupture of material in the hole on the die side. The self-clinching nut is not attached with the

whole length of the collar of the nut in the busbar. In the worst case the length of the rupture is so long that the nut is barely attached. In figure 53 is presented two samples, where the nut was assembled on die side. There can clearly be seen, where the nut has been connected to busbar.

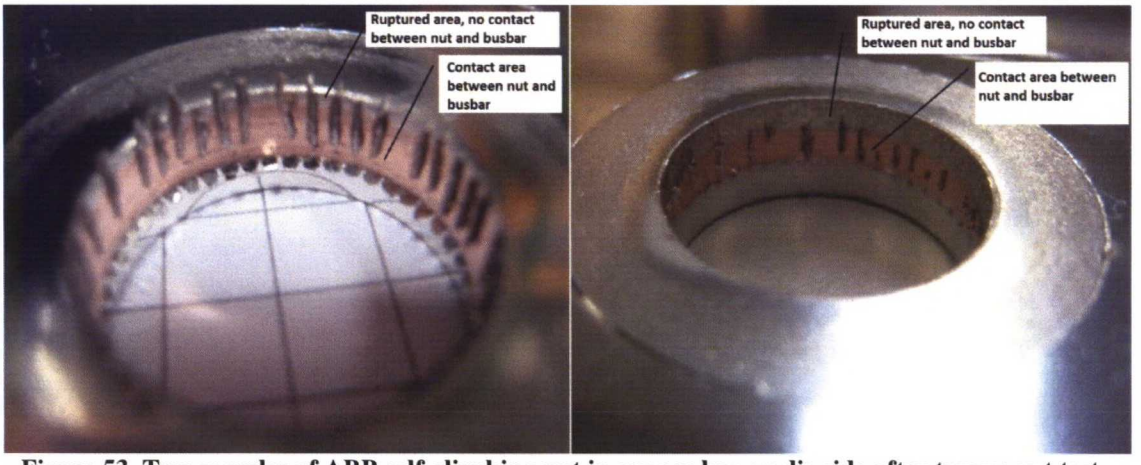

Figure 53. Two samples of ABB self-clinching nut in copper bar on die side after torque out test.

One reason for the deviation among one sample set is the deviations of assembly hole diameter and collar diameter of self-clinching nut. Although, it was announced that the qualities of assembly hole and collar of the nut were good, the difference of a few hundredth of a millimeter in overlapping can affect quite much. The overlapping could have varied about ±0.02 mm among one set.

The problem during torque out test was that the failure type of some samples was screw breakage and the actual torque out value was not able to get. In the DoE analysis, there is not done any preparation of data because of screw failures. The decision was made, because when compared the same kind of joint sets to each other, the direction of effect was clearly on view. In other word, the internecine effects of variables at least on the level showed in figure 38.

The PEM®-nut is well documented by manufacturer and the breaking values are announced in data sheets. The KALEI®-nut has also some data of strength performance, but it is not documented as well as the PEM®-nut. The measuring results can be now exploited in the design of bolted joint. The torque out values can be formed from the data. The torque out values of ABB self-clinching nut are presented in table 35 with the corresponding values of PEM®- and KALEI®-nuts. The torque out values of ABB self-clinching nut are formed from the results of samples, where nut was assembled in a large hole. The values of ABB self-clinching nut that are introduced in table 38 are 80 % of the mean torque values among the samples for getting safety margin to failure. There was not available torque out value for PEM®-nut in copper and hence the value is estimated from data of PEM®-screw, where was torque out value in copper. The torque out values of KALEI®-nut are also estimations, because there were only available the values in steel. There was made a few torque out measuring for PEM®- and KALEI®-nuts after the joint test with the same samples to help the estimation of torque out values. The measured values of PEM® and KALEI® are not completely reliable, because the samples were stressed before the test so the torque out test shall be done with new samples for getting more accurate results.

Table 38. The torque out comparison between different self-clinching nut types.

	Torque out (Nm)							
Nut type	**Cu6 M10**	**Cu6 M12**	**Cu10 M10**	**Cu10 M12**	**Al6 M10**	**Al6 M12**	**Al10 M10**	**Al10 M12**
ABB-nut on punch side	74	95	76	108	55	64	61	79
ABB-nut on die side	73	49	54	41	12	38	11	8
PEM[11][14]	45	50	45	50	32.7	35.2	32.7	35.2
KALEI[13]	30	45	30	45	25	30	25	30

The torque out values can be exploited in joint design by using it as a limit of thread torque. If the thread torque is larger than the torque out value of self-clinching nut, there is a risk the nut may come loose. There was calculated possible thread torque in the tables 9-12 and against those values the ABB self-clinching nut manages well. Only if the ABB self-clinching nut is assembled in aluminum bar on die side, the results are not acceptable. PEM®-nut manages mainly well, but there is risk in M12 aluminum joints that the nut comes loose. KALEI®-nut seems to be the weakest of these nuts so the torque out value shall be verified with test, if it is used.

The torque out performance of ABB self-clinching nut is good, when the nut is assembled on punch side. The performance may be unforeseeable, when the nut is assembled on die side. According to the torque out test results, it seems that with little modifications in instructions, the performance is possible to get more constant. The assembly hole diameter is the most critical factor in the performance of the nut. The copper bar samples showed that the thread of the nut deforms, when the nut is assembled in too small hole in this case 0.1 mm smaller than marked in drawing. On the other hand, the results show that the nut is safe even if the assembly hole diameter is 0.1 mm larger than in drawing. The aluminum samples did not have the same kind of behavior than the copper samples. There were not any thread deformations among the aluminum samples. There were very low torque out values, when the nut was assembled on die side in a large hole in aluminum. The corresponding results, when the nut was assembled in a small hole were better and on acceptable level. According to these observations, it might be sensible to use different assembly hole diameters depending on the assembly side of busbar. There is a proposal of possible changes of assembly hole diameter that improves the performance of the nut in table 39.

Table 39. Proposal to new assembly hole diameters for ABB self-clinching nut.

		Current assembly hole diameter		**Proposed assembly hole diameter**	
Busbar material	**Assembly side**	**M10**	**M12**	**M10**	**M12**
Cu	Punch	13	15.1	13.1	15.2
Cu	Die	13	15.1	13	15.1
Al	Punch	13	15.1	13	15.1
Al	Die	13	15.1	12.9	15

There is also the variation of ABB self-clinching nut, which has longer collar that may improve the torque out resistance in thick busbar. In the future, torque out tests are important to do also for longer ABB self-clinching nut. If the torque out values are better in thick busbar, it is more sensible to use the longer nut in thick busbars and the shorter nut in thin busbars.

7 Summary

The self-clinching inserts seems to be suitable fastening elements for busbar joints, when the possible restrictions are taken into account. The most restrictive feature is the bearing area of the insert. When the bearing area is small, the used preload shall be lower than the preload of regular through bolted joint to avoid too high surface pressure against the busbar. Another restriction is the assembly side, when punched busbars are used. The assembly of self-clinching nut shall be made on punch side to ensure the strength of the nut is adequate. ABB self-clinching nut is the only self-clinching nut that is possible to use on die side. Most of the self-clinching inserts have good torque out values so they should not easily fail during tightening of joint.

The ABB self-clinching nut performed mainly well in the tests. The torque out values were good except the samples in thick aluminum in a large hole on die side. The joint test results were close to the results of regular through bolted joint so the performance was good. The most significant factors to the performance of ABB self-clinching nut were found out with the torque out test and presented in figure 38. Based on the test results and observations during measurements, there were proposed small design changes to the self-clinching nut assembly in table 39. The longer version of ABB self-clinching nut shall be tested in the future to see if the longer nut is more sensible to use in thick joints.

PEM®-nuts were tested with joint test and it performed well. The performance of PEM®-nut matches the regular through bolted joint or is even better. Torque out values are adequate in busbar joint use. Only disadvantage in busbar joint use is a bit too small bearing area. The quality of the nuts was good and the nuts are common on the markets. PEM®-nut is worth to consider using in busbar joints, but it needs more tests before extensive use.

KALEI®-nuts were also tested with joint test and the results pointed out it is not suitable in high power joints. The overall joint performance was worse than the performance of regular through bolted joint. The very small bearing area do not allow high preloads in joint and hence the joint with KALEI®-nut is more sensitive to loosening and the maximum allowed current through joint is smaller. The torque out values are also a bit smaller than the values of other nuts. In addition, there were observed assembly errors among KALEI®-samples, which caused the angled position of the nut. Nonetheless, KALEI®-nuts are possible to use in small busbar joints, where through going current is smaller.

According to the literature review, there are some self-clinching screws on the markets, which may be suitable in busbar joints. PennEngineering has HFE- and HFH-series and Würth Elektronik and PSM International have corresponding design of the self-clinching screw, which have suitable geometry for busbar joint use. The actual suitability shall be verified with tests.

According to the measuring results, the VDI 2230 design guideline for bolted joints is reliable calculation method also for joints with self-clinching inserts. The assembly preload of the joint is possible to calculate with VDI 2230 and predict the joint behavior during the operation. The most crucial factor in calculation is the friction coefficient. The measuring results point out the calculation corresponds to the measurements, when

the friction coefficient is estimated correctly. The friction coefficient shall be chosen by the lowest possible friction level to avoid screw failure during tightening. This choosing method produce some joints may have a lot higher friction coefficient, which causes the preload remain lower. There are recommended friction coefficients for measured joint types in table 36.

The used methods to measure and calculate joint properties can be used in additional tests for other interesting self-clinching inserts. Torque out and joint tests give the performance of insert that is required in joint design.

Bibliography

1. Wiegand H, et al. Schraubenverbindungen. 5. Edition. Germany: Springer. 2007. ISBN 978-3-540-21282-9

2. Airila M, et al. Koneenosien suunnittelu. 4. Edition. Finland: WSOY. 2003. ISBN 951-0-20172-3

3. SFS-ISO 68-1. ISO general purpose screw threads. Basic profile. Part 1: Metric screw threads. Finland: Finnish Standard Association. 1998.

4. EN 1993-1-3. Eurocode 3 - Design of steel structures - Part 1-3: General rules - Supplementary rules for cold-formed members and sheeting. European Committee for standardization. 2006.

5. VDI 2230. Part 1: Systematic calculation of high duty bolted joints. Joints with one cylindrical bolt. Germany: Verein Deutscher Ingenieure. 2003.

6. ISO 4017. Hexagon head screws — Product grades A and B. 4. Edition. Switzerland: International Organization for Standardization. 2011.

7. ISO 4032. Hexagon nuts, style 1 - Product grades A and B. 3. Edition. Switzerland: International Organization for Standardization. 1999.

8. DIN 9021. Plain washers with large outside diameter. Germany: Deutsches Institut für Normung.

9. SFS 3737. Electrical connections. Conical spring washer. 2. Edition. Finland: Finnish Standard Association. 1988.

10. PEM® The self-clinching fastener handbook. PennEngineering. [Referred at 15.11.2012]. Available at: http://www.pemnet.com/fastening_products/pdf/Handbook.pdf

11. PEM® Self-clinching nuts. PennEngineering. [Referred at 15.11.2012]. Available at: http://www.pemnet.com/fastening_products/pdf/cldata.pdf

12. PSM Self-clinching nut catalogue. PSM International. [Referred at 15.11.2012]. Available at: http://www.hweckhardt.com/threadedins/PSM/pdfs/Selfclinchingnuts.pdf

13. Würth Sheet metal fasteners. Würth Elektronik. [Referred at 15.11.2012]. Available at: http://www.wurthelektronik.fi/site/media/pdf/we/kuvasto/Puristetuoteluettelo_ohut levyille.pdf

14. PEM® Self-clinching studs and pins. PennEngineering. [Referred at 15.11.2012] Available at: http://www.pemnet.com/fastening_products/pdf/fhdata.pdf

15. DIN 603. Mushroom head square neck bolts. Germany: Deutsches Institut für Normung.

16. Lock nut data. Bossard. [Referred at 21.11.2012] Available at: https://eu.shop.bossard.com/ch/index.cfm?app_page=0:31001:30002:9554:1

17. Horelli, J. Virtakiskoliitosten luotettavuuden analysointi. Master's Thesis. Helsinki University of Technology, Department of Mechanical Engineering. Finland. 2004.

18. Inman, D. Engineering Vibrations. 3. Edition. USA: Pearson Education Inc. 2009. ISBN 978-0-13-136311-3

19. SS-EN 60068-2-6. Environmental testing, Part 2-6: Tests, Test Fc: Vibration (sinusoidal). 2. Edition. Belgium: European Committee for Electrotechnical Standardization. 2008.

20. IEC 255-21. Electrical relays. Part 21: Vibration, shock, bump and seismic tests on measuring relays and protection equipment Section One - Vibration tests (sinusoidal). 1. Edition. Switzerland: International Electrotechnical Commission. 1988.

21. IEC 61660-1. Short-circuit currents in d.c. auxiliary installations in power plants and substations - Part 1: Calculation of short-circuit currents. 1. Edition. Switzerland: International Electrotechnical Commission. 1997.

22. IEC 61660-2. Short-circuit currents in d.c. auxiliary installations in power plants and substations - Part 2: Calculation of effects. 1. Edition. Switzerland: International Electrotechnical Commission. 1997.

23. IEC 909. Short-circuit currents in three-phase a.c. systems - Part 0: Calculation of currents. 1. Edition. Switzerland: International Electrotechnical Commission. 2001.

24. Oksanen T. Taajuusmuuttajakojeistojen kiskotusten optimointi. Master's Thesis. Helsinki University of Technology, Department of Mechanical Engineering. 1998.

25. Slade P, et al. Electrical contacts. USA: Marcel Dekker Inc. 1999. ISBN 0-8247-1934-4

26. Kivioja S. et al. Tribologia - Kitka, kuluminen ja voitelu. 6. Edition. Finland: Otatieto Oy. 2010. ISBN 978-951-672-355-9

27. Luoma, K. et al. Experiment documentation X 81-386: Sähköisten liitosten mitoitus ja materiaalinvalinta. Vaasa 1981, Oy Strömberg Ab. Unpublished research report

28. Lampinen, M. et al. Lämmönsiirto-oppi. Report 155. Helsinki University of Technology, Department of Energy Engineering. Finland. 2008.

29. Ihalainen, E. et al. Valmistustekniikka. 9. Edition. Finland: Otatieto Oy. 2002. ISBN 978-672-205-9

30. SFS 5804. Design rules for stamped steel parts. Finland: Finnish Standard Association. 1996.

31. SFS 5803. Stamped steel parts. General tolerances. Finland: Finnish Standard Association. 1996.

32. Järvinen, S. Development of test device for sheet metal screw joints. Master's Thesis. Aalto University School of Engineering, Department of Engineering Design and Production. Finland. 2012.

33. MS-series - hardware manual. ABB Oy. [Referred 4.12.2012]. Available at: http://www05.abb.com/global/scot/scot201.nsf/veritydisplay/55f1f2226fb125d5c125739b0038373b/$file/en_ms_series_hwman_b.pdf

34. Drivestudio user manual. ABB Oy. [Referred 4.12.2012]. Available at: http://www05.abb.com/global/scot/scot201.nsf/veritydisplay/1ad3a23c4a3cc7d3c1257a0200465eec/$file/User_Manual.pdf

35. Futek model TRD605. Futek Advanced Sensor Technology Inc. [Referred at 10.12.2012]. Available at : http://www.futek.com/files/pdf/Product%20Drawings/trd605.pdf

36. Futek model LTH500. Futek Advanced Sensor Technology Inc. [Referred at 10.12.2012]. Available at : http://www.futek.com/files/pdf/Product%20Drawings/lth500.pdf

37. Linear components catalog. Rose+Krieger. 03/2010. [Referred 4.9.2012]. Available at: http://www.rk-rose-krieger.com/fileadmin/catalogue/lineareinheiten/le_lineareinheiten_dgb.pdf

38. Brook, Q. Lean Six Sigma & Minitab – The Complete Toolbox Guide for all Lean Six Sigma Practitioners. 3. Edition. United Kingdom: Opex Resources Ltd. 2010. ISBN 978-0-954-6813-6-4

39. Montgomery, D. Design and Analysis of Experiments. 8. Edition. Singapore: John Wiley & Sons Inc. 2013. ISBN 978-1-118-09793-9

40. Taylor, J. An Introduction to Error Analysis: The Study of Uncertainties in Physical Measurements. 2. Edition. USA: University Science Books. 1997. ISBN 978-0-935702-75-0

41. Laininen, P. Todennäköisyys ja sen tilastollinen soveltaminen. 5. Edition. Finland: Otatieto Oy. 2001.ISBN 951-672-312-8

42. Ferrometal technical data. Ferrometal Oy. [Referred 15.1.2013]. Available at: http://www.ferrometal.fi/tuotteet/tuotetietoa.html

43. Ruuviliitosten suunnittelu. Würth Elektronik. [Referred at 15.1.2013]. Available at: http://www.wurthelektronik.fi/site/media/pdf/we/kuvasto/suunnitteluopas06.pdf

44. Material data of Cu-OF and Cu-ETP. Deutsches Kupferinstitut. [Referred at 15.1.2013]. Available at: http://www.kupferinstitut.de/front_frame/frameset.php3?client=1&lang=1&idcat=232&parent=13

45. Material data of EN AW 6101A T6. Ruukki Oy. [Referred at 15.1.2013]. Available at: http://www.ruukki.com/Products-and-solutions/Stainless-steel-and-aluminium-products/Aluminium-bars/Aluminium-AW-6101A-T6-busbar-flat

Breaking torques in torque out test Copper bar 6 mm, Screw size M10 Tightening speed 25 rpm 10 samples Values Nm				
Test piece n:o	**12.9 mm, punch side, upper tolerance**	**12.9 mm, die side, lower tolerance**	**13.1 mm, punch side, lower tolerance**	**13.1 mm, die side, upper tolerance**
1	88.37	80.23	90.83	96.60
2	95.72	115.81	89.16	91.95
3	94.61	109.01	95.94	94.96
4	94.49	107.60	107.16	90.33
5	104.41	98.82	77.72	91.52
6	83.56	96.80	88.56	85.22
7	97.40	73.57	100.52	92.18
8	98.23	97.08	91.34	93.68
9	89.71	98.95	101.38	91.73
10	88.36	116.12	84.44	86.12
Mean	93.48	99.40	92.70	91.43
Standard deviation	6.05	13.97	8.72	3.55
Notices:	12.9 mm, punch side, upper tolerance: Screw failure n:o 1-10 12.9 mm, die side, lower tolerance: Screw failure n:o 1-9 13.1 mm, punch side, lower tolerance: Screw failure n:o 2, 3, 7, 9			

Breaking torques in torque out test Copper bar 6 mm, Screw size M12 Tightening speed 25 rpm 10 samples Values Nm				
Test piece n:o	**15.0 mm, punch side, lower tolerance**	**15.0 mm, die side, upper tolerance**	**15.2 mm, punch side, upper tolerance**	**15.2 mm, die side, lower tolerance**
1	172.07	164.47	126.09	53.66
2	163.71	173.10	126.37	45.70
3	161.45	177.04	125.48	65.56
4	196.52	168.67	126.40	65.07
5	205.52	180.17	115.44	50.82
6	178.92	169.62	103.16	64.94
7	183.93	172.12	122.34	55.60
8	178.50	183.95	121.19	92.75
9	185.56	186.49	114.86	76.63
10	216.38	184.29	115.71	50.03
Mean	184.26	175.99	119.70	62.08
Standard deviation	17.60	7.54	7.48	14.28
Notices:	15.0 mm, punch side, lower tolerance: Screw failure n:o 1-3, 6, 8, 9, Motor safety mode n:o 7			

The results of torque out test **(2/4)**

Breaking torques in torque out test Copper bar 10 mm, Screw size M10 Tightening speed 25 rpm 10 samples Values Nm				
Test piece n:o	**12.9 mm, punch side, lower tolerance**	**12.9 mm, die side, upper tolerance**	**13.1 mm, punch side, upper tolerance**	**13.1 mm, die side, lower tolerance**
1	92.98	107.06	96.52	61.56
2	89.40	96.43	88.45	67.46
3	105.58	104.23	100.26	66.66
4	99.65	91.01	81.31	67.11
5	97.02	111.37	103.69	76.62
6	99.00	103.48	97.07	70.56
7	96.50	108.34	100.35	69.95
8	106.51	99.66	95.35	66.95
9	95.34	90.37	87.80	66.13
10	105.23	103.37	105.33	63.81
Mean	98.72	101.53	95.61	67.68
Standard deviation	5.69	7.09	7.63	4.08
Notices:	12.9 mm, punch side, lower tolerance: Data logging error in n:o 6, reading from display, Screw failure n:o 1, 3-10 12.9 mm, die side, upper tolerance: Screw failure n:o 2-10 13.1 mm, punch side, upper tolerance: Screw failure n:o 1-10			

Breaking torques in torque out test Copper bar 10 mm, Screw size M12 Tightening speed 25 rpm 10 samples Values Nm				
Test piece n:o	**15.0 mm, punch side, lower tolerance**	**15.0 mm, die side, upper tolerance**	**15.2 mm, punch side, upper tolerance**	**15.2 mm, die side, lower tolerance**
1	183.98	97.20	97.80	62.22
2	189.97	110.06	143.09	56.62
3	184.65	109.43	123.84	49.94
4	190.28	115.14	125.64	50.25
5	153.10	113.47	135.00	45.20
6	190.17	119.32	140.11	51.67
7	193.18	119.46	140.80	56.17
8	157.46	113.17	156.02	53.04
9	185.15	99.58	145.19	51.11
10	168.41	93.30	145.39	47.00
Mean	179.63	109.01	135.29	52.32
Standard deviation	14.57	9.23	16.24	4.97
Notices:	15.0 mm, punch side, lower tolerance: Screw failure n:o 5,10, Motor safety mode n:o 1-4, 6, 7, 9			

The results of torque out test (3/4)

Breaking torques in torque out test Aluminum bar 6 mm, Screw size M10 Tightening speed 25 rpm 10 samples Values Nm				
Test piece n:o	**12.9 mm, punch side, lower tolerance**	**12.9 mm, die side, upper tolerance**	**13.1 mm, punch side, upper tolerance**	**13.1 mm, die side, lower tolerance**
1	88.89	57.05	80.03	16.57
2	93.01	65.82	82.53	11.71
3	102.02	63.09	60.80	13.71
4	89.81	58.43	70.17	15.95
5	94.94	69.29	75.29	14.46
6	104.05	51.60	77.26	12.80
7	81.69	60.10	78.16	13.28
8	94.09	64.41	58.52	16.30
9	91.06	59.11	50.79	22.60
10	105.48	65.01	66.01	13.76
Mean	94.51	61.39	69.96	15.11
Standard deviation	7.46	5.14	10.57	3.07
Notices:	12.9 mm, punch side, lower tolerance: Screw failure n:o 1-10			

Breaking torques in torque out test Aluminum bar 6 mm, Screw size M12 Tightening speed 25 rpm 10 samples Values Nm				
Test piece n:o	**15.0 mm, punch side, upper tolerance**	**15.0 mm, die side, lower tolerance**	**15.2 mm, punch side, lower tolerance**	**15.2 mm, die side, upper tolerance**
1	172.10	99.06	78.51	54.92
2	162.45	104.02	84.47	40.11
3	172.01	95.92	89.80	38.49
4	167.18	109.90	90.56	41.47
5	171.13	100.46	92.08	49.24
6	163.32	95.00	73.60	60.71
7	169.79	100.43	84.63	41.66
8	172.44	103.58	76.59	40.96
9	171.76	96.69	67.44	53.71
10	170.97	102.84	68.31	56.55
Mean	169.31	100.79	80.60	47.78
Standard deviation	3.72	4.51	9.07	8.17
Notices:	15.0 mm, punch side, upper tolerance: Screw failure n:o 6			

The results of torque out test (4/4)

Breaking torques in torque out test Aluminum bar 10 mm, Screw size M10 Tightening speed 25 rpm 10 samples Values Nm				
Test piece n:o	**12.9 mm, punch side, upper tolerance**	**12.9 mm, die side, lower tolerance**	**13.1 mm, punch side, lower tolerance**	**13.1 mm, die side, upper tolerance**
1	113.42	32.46	94.58	9.94
2	98.90	36.05	73.40	14.89
3	122.15	31.65	44.62	19.38
4	111.26	38.82	84.44	14.46
5	111.89	37.32	77.73	2.67
6	100.55	29.66	80.47	19.28
7	113.08	25.13	72.58	17.60
8	90.53	29.41	79.82	13.83
9	103.29	34.55	75.65	20.16
10	115.35	44.61	90.45	16.71
Mean	108.04	33.96	77.37	14.89
Standard deviation	9.43	5.55	13.53	5.30
Notices:	12.9 mm, punch side, upper tolerance: Screw failure n:o 1-7, 9, 10 13.1 mm, punch side, lower tolerance: Screw failure n:o 4, Nut assembled wrong side n:o 3			

Breaking torques in torque out test Aluminum bar 10 mm, Screw size M12 Tightening speed 25 rpm 10 samples Values Nm				
Test piece n:o	**15.0 mm, punch side, lower tolerance**	**15.0 mm, die side, upper tolerance**	**15.2 mm, punch side, upper tolerance**	**15.2 mm, die side, lower tolerance**
1	156.92	104.22	107.52	13.56
2	159.83	78.34	94.59	11.93
3	154.89	95.68	111.73	9.12
4	151.85	83.95	99.7	7.83
5	151.21	85.05	108.54	6.64
6	161.47	86.85	110.19	16.31
7	155.37	86.10	91.56	8.93
8	156.35	77.65	87.26	9.24
9	150.06	85.66	87.63	5.01
10	161.80	83.48	100.43	12.26
Mean	155.97	86.70	99.92	10.08
Standard deviation	4.17	7.90	9.35	3.41
Notices:				